1997

The effects of amyloid precursor protein C-105 expression and ganglioside GM1 on PC12 cell vulnerability to the calcium ionophore A23 187 and hydrogen peroxide

BOSTON UNIVERSITY

SCHOOL OF MEDICINE

Dissertation

THE EFFECTS OF AMYLOID PRECURSOR PROTEIN C-105 EXPRESSION AND GANGLIOSIDE GM1 ON PC12 CELL VULNERABILITY TO THE CALCIUM IONOPHORE A23187 AND HYDROGEN PEROXIDE

by

CATHERINE MCKEON O'MALLEY

M.S., Northeastern University, 1984

B.A., College of the Holy Cross, 1978

Submitted in partial fulfillment of

the requirements for the degree of

Doctor of Philosophy

1997

Approved by

First Reader [redacted]

Ladislav Volicer, M.D., Ph.D.

Professor of Pharmacology and Psychiatry

Second Reader [redacted]

L. Bruce Pearce, Ph.D.

Adjunct Assistant Professor of Pharmacology

ACKNOWLEDGMENTS

I thank the following individuals for their

guidance and encouragement during my graduate study:

Anil Amaratunga

Richard Fine

Omanand Koul

L. Bruce Pearce

Joseph Squicciarini

Abdul Traish

David Ullman

Ladislav Volicer

Carol Walsh

John Wells

THE EFFECTS OF AMYLOID PRECURSOR PROTEIN C-105 EXPRESSION AND GM1 ON PC12 CELL VULNERABILITY TO THE CALCIUM IONOPHORE A23187 AND HYDROGEN PEROXIDE

(Order No.)

CATHERINE MCKEON O'MALLEY

Boston University School of Medicine, 1997

Major Professor: Ladislav Volicer, M.D., Ph.D., Professor of Pharmacology and Psychiatry

Abstract

Specific mutations in the gene for the beta amyloid precursor protein (APP) cause Alzheimer's disease (AD). A key neuropathological hallmark of AD is extracellular neuritic plaques. The core component of plaques is Aß, a 39-43 amino acid peptide derived from APP. APP C-100 and APP C-105 are C-terminal fragments of APP, 100 and 105 amino acids long, respectively. APP C-100 is a normal metabolite of APP. Aß is located at the N-terminus of the APP C-100 sequence.

To determine whether APP C-105 expression alters cellular vulnerability to calcium and hydrogen peroxide, rat PC12 cells were modified to overexpress APP C-105.

Permanent transfectants (clones) were selected, then characterized by standard molecular biological techniques. DNA and mRNA corresponding to APP C-105 were detected in APP C-105 transfectants, but not in wild type controls. Aggregated APP C-105 was detected in cell lysates and conditioned media from APP C-105 transfectants, but was absent or detected at lower concentrations in vector-transfected and wild type controls.

Cell survival as a function of concentration was determined for A23187, a Ca^{2+} ionophore, and hydrogen peroxide in APP C-105 transfectants and vector-transfected controls. Cells were exposed to A23187 or hydrogen peroxide for 24 hours in RPMI media containing 3 μM insulin, and survival was quantitated using the tetrazolium dye, MTT. APP C-105 expression significantly increased PC12 cell vulnerability to A23187, and significantly decreased vulnerability to hydrogen peroxide.

Other experiments were performed with GM1 ganglioside, which is known to protect cells against numerous insults. When wild type PC12 cells or APP C-105 transfectants were exposed to a toxin and GM1 concurrently for 24 hours, GM1 produced concentration-dependent inhibition of A23187 toxicity in wild type PC12 cells but was ineffective against hydrogen peroxide in both wild type PC12 and APP C-105-transfected clones.

The current study has demonstrated that expression of APP C-105 protects PC12 cells against hydrogen peroxide, but exacerbates the effect of calcium influx. In conjunction with other reports, this study indicates that APP C-105 is an

important regulator of cellular homeostasis. Therefore, the pattern of APP processing may alter vulnerability to neurotoxic insults.

TABLE OF CONTENTS

LIST OF FIGURES

LIST OF TABLES

LIST OF ABBREVIATIONS AND DEFINITIONS

AD

Alzheimer's disease

ApoE

Apolipoprotein E

APP

Amyloid Precursor Protein

APP C-100

A general term describing an amyloid precursor protein fragment extending from the beginning of the Aß region to the carboxyl terminus, containing approximately 100 amino acids. The exact number of amino acids expressed varies among laboratories.

APP C-105

An APP fragment consisting of 105 amino acids, used in the present study to overexpress the C-terminus of the protein. The C-terminus of APP is known as APP C-100.

Aß

A 39-43 amino acid fragment of the amyloid precursor protein, found in neuritic plaques. Neuritic plaques are one of the hallmarks of Alzheimer's disease.

bFGF

Basic fibroblast growth factor

BSA

Bovine serum albumin

dNTPs

Deoxyribonucleotides

EAA

Excitatory amino acids

EPR

Electron paramagnetic resonance

HCHWA-Dutch

Hereditary cerebral hemorrhage with amyloidosis-Dutch type

LDH

Lactate dehydrogenase

IL-1

Interleukin 1

MPTP

1-methyl-4-phenyl 1,2,3,6 tetrahydropyridine

MTT

3-(4,5-dimethylthiazole-2-yl)-2-5,-diphenyl tetrazolium bromide

NGF

Nerve growth factor

NFT

Neurofibrillary tangles

NOS

Nitric oxide synthase

PARS

poly(ADP-ribose) synthetase

PBN

α-phenyl-t-butyl nitrone

PBS

Phosphate buffered saline

PKC

Protein kinase C

PAGE

Polyacrylamide gel electrophoresis

PCR

Polymerase chain reaction

PNII

Protein Nexin II

RADAs

Receptor abuse-dependent antagonists

ROS

Reactive oxygen species

SDS

Sodium dodecyl sulfate

TK

Thymidine kinase

I. INTRODUCTION

A. Alzheimer's Disease

Alzheimer's disease (AD) is a devastating neurodegenerative disease of the elderly, which robs its victims of cognition and memory. It has been estimated that AD afflicted 1.35 million individuals age 65 and over in the United States during 1991 (Ernst and Hay, 1994). For the same year, the direct cost to the nation was estimated at $20.6 billion. Obviously, Alzheimer's disease is a major public health problem, both in terms of dollars and human suffering.

Both familial and sporadic forms of Alzheimer's disease are recognized. Familial Alzheimer's disease can be divided into early-onset (before age 65) and late onset (age 65 and older) pedigrees. Early-onset pedigrees exhibit autosomal dominant inheritance. The diagnosis of probable AD is made clinically, based on the existence of a progressive dementia which can not be attributed to a known cause. Definitive diagnosis can not be made until the presence of AD neuropathology is confirmed in autopsy-derived materials. The neuropathological hallmarks of the disease are extracellular neuritic plaques, intracellular tangles, neuronal cell loss (especially of cholinergic neurons in the basal forebrain), loss of synapses, and reduced levels of neurotransmitters. Alzheimer's pathology is observed in cerebral blood vessels and the brain. The brain areas affected primarily are the hippocampus, amygdala, entorrhinal cortex, and cerebral association cortex (Selkoe, 1994).

The formation of neurofibrillary tangles (NFT) and plaques has been explored extensively, to determine which, if either, entity causes neurodegeneration. The alternative hypothesis is that NFT and plaques are the endproducts of a neurodegenerative process. Tangles appear as paired helical filaments (PHF). These filaments are composed largely of ubiquitin and tau, a microtubule-associated protein. The tau protein in tangles is hyperphosphorylated (Grundke-Iqbal, Iqbal et al. , 1986). Tangles are present in many neurodegenerative disorders. In contrast, abundant neuritic plaque formation is observed only during normal aging, Down's syndrome, and Alzheimer's disease (Selkoe, 1991).

Neuritic (senile) plaques consist of an amyloid protein core, surrounded by dystrophic neurites, activated microglia cells, and astrocytes. [Amyloid is a general term denoting a protein in ß-pleated sheet conformation. Amyloid proteins can be stained by Congo Red or Thioflavin S.] Neurons with various neurotransmitter specificities are represented among dystrophic neurites (Struble, Powers et al. , 1987). The core protein of neuritic plaques is Aß, a 39-43 amino acid length polypeptide derived from the amyloid precursor protein (APP) (Kang, Lemaire and Unterbeck, 1987). Within neuritic plaques, Aß is assembled into approximately 8 nm filaments (Selkoe, 1994). Other neuritic plaque components include apolipoprotein E (ApoE) (Namba, Tomonaga et al. , 1991), α1 antichymotrypsin (Abraham, Selkoe and Potter, 1988), serum amyloid P (Coria, Castano et al. , 1988), heparan sulfate (Snow, Nochlin et al. , 1988), interleukin-1 (Griffin, Stanley et al. , 1989) and basic fibroblast growth factor (bFGF) (Gomez-Pinilla, Cummings and Cotman, 1990). "Diffuse" plaques contain Aß that has not undergone assembly into

fibrils. They occur in much larger numbers than do neuritic plaques, and contain few dystrophic neurites, microglia or astrocytes. It is unknown whether diffuse plaques are precursors to neuritic plaques (but see Mackenzie, 1994).

The primary risk factor for development of Alzheimer's disease is aging. Other risk factors for the disease include Down's syndrome (Katzmann, 1986), head trauma (Roberts, Gentleman et al. , 1994), and mutations in several disease-associated genes. Genes in which mutations have been linked to Alzheimer's disease include the APP gene (Hendricks, van Duijn et al. , 1992; Mullan, Crawford et al. , 1992; Chartier-Harlin, Crawford and Houlden, 1991; Murrell, Farlow and Ghetti, 1991; Goate, Chartier-Harlin et al. , 1991), the ApoE gene (Corder, Saunders and Strittmatter, 1993), the Presenilin 1 (S182) gene on chromosome 14q24.3 (St.George-Hyslop, Haines et al. , 1992; Schellenberg, Bird et al. , 1992; Mullan, Houlden et al. , 1992; van Broeckhoven, Backhovens et al. , 1992; Sherrington, Rogaev et al. , 1995), and the Presenilin 2 (STM2) gene on chromosome 1q31-42 (Levy-Lahad, Wasco et al. , 1995; Levy-Lahad, Wijsman et al. , 1995). APP mutations, and mutations in the Presenilin 1 gene product account for 3% and 70%, respectively, of early-onset familial disease. The Presenilin 2 gene is expected to account for only a small percentage of familial AD cases.

The Presenilin 1 gene encodes a protein 467 amino acids long, with 7 transmembrane regions. A large hydrophilic domain is found between the sixth and the seventh transmembrane domains. The latter region includes two putative N-glycosylation sites. Over fifty mutations in Presenilin 1 have been identified, four of which are positioned near,

or within, transmembrane domains. The protein encoded by the Presenilin 1 gene has a mouse counterpart. It is also homologous to two *Caenorhabditis elegans*' genes, SEL-12 and SPE-4, and to the Presenilin 2 gene product (van Broeckhoven, 1995). Disease-associated mutations occur at conserved residues.

The Presenilin 2 gene was identified in seven Volga German kindreds in which a single missense mutation occurred. In these families, the mean age of onset of AD ranges from 50.2 - 64.8 years. The Presenilin 2 gene product, like the Presenilin 1 gene product, is a transmembrane protein. It contains 7 transmembrane domains, each of which is capped by a lysine residue located at, or near, the carboxyl terminus of the domain. The missense mutation identified within Volga German kindreds occurs immediately N-terminal to the second transmembrane domain, resulting in the substitution of a hydrophobic isoleucine for a hydrophilic asparagine (Rogaev, Sherrington et al. , 1995; Levy-Lahad, Wasco et al., 1995). A second missense mutation in Presenilin 2 has been identified in an Italian kindred (Rogaev, Sherrington et al. , 1995).

The normal functions of the proteins encoded by the Presenilin 1 and Presenilin 2 genes are unknown. Linkage of mutations in Presenilin 1 and Presenilin 2 to AD, and the homology existing between the two genes, suggests that the respective proteins are involved in fundumental processes related to the etiology of AD.

A subset of late-onset familial Alzheimer's disease cases is linked to chromosome 19 (Pericak-Vance, Bebout and Gaskell, 1991). The locus accounting for this linkage is the gene for ApoE, located at 19q13.2 (Mahley, 1988). In a group of Alzheimer patients with

a family history of late-onset AD, the frequency of the ε4 allele was 0.5, compared to a frequency of 0.16 in age-matched controls (Strittmatter, Saunders et al. , 1993). The ε4 allele is also associated with sporadic AD (Saunders, Strittmatter et al. , 1993). Three ApoE alleles are commonly found in the general population, namely, ε2, ε3 and ε4. The ε2, ε3 and ε4 alleles occur with frequencies of 8, 75 and 15%, respectively. ApoE3 contains a single cysteine at position 112; in ApoE4 this residue is replaced by arginine. In ApoE2, the arginine found in ApoE3 at position 158 is replaced by cysteine. ApoE4 is a risk factor for Alzheimer's disease.

The evidence that APP mutations are responsible for the development of AD in a few families with early-onset disease will be discussed below.

B. The Role of the Amyloid Precursor Protein and Aß in Alzheimer's Disease

1. Messenger RNA Splicing, Functional Domains and Post-translational Modifications

A schematic diagram of APP is shown in Figure 1. APP has a large extracellular domain, one transmembrane spanning domain, and a small cytoplasmic domain. It is widely expressed in human tissues including brain, spleen, liver, kidney, lung and heart (Tanzi, McClatchey et al. , 1988). A single copy of the APP gene is located on chromosome 21 at the boundary of 21.q21.3 and 21.q22.1 (Kang, Lemaire and Unterbeck, 1987). The gene contains 19 exons and at least 10 different mRNA species are generated

by alternative splicing (Wisniewski, Ghiso and Frangione, 1994). Of these, three major mRNA species, coding for proteins 695, 751, and 770 amino acids long (APP_{695}, APP_{751}, APP_{770}), include the Aß region. Since the mRNA sequence for Aß spans exons 16 and 17 (APP_{770} numbering), Aß can not be generated by aberrant mRNA splicing (Lemaire, Salbaum et al. , 1989). The 695 mRNA species is confined to the brain (Sola, Mengod et al. , 1993). The 751 and 770 mRNA's include a region which has 50% homology to a Kunitz (serine protease) inhibitor domain (Tanzi, McClatchey et al. , 1988; Ponte, Gonzalez-DeWhitt and Schilling, 1988; Kitaguchi, Takahashi and Tokushima, 1988). Except for the lack of the Kunitz protease inhibitor domain in APP_{695}, APP_{695} and APP_{751} are identical. APP_{770} contains an OX-2 insert (19 residues), located adjacent to the Kunitz protease inhibitor domain, whose function is unknown.

The following domains for APP_{695} have been described (Kang, Lemaire and Unterbeck, 1987): At its N-terminus, APP has a 17 residue signal peptide for transport into endoplasmic reticulum. This is followed by a region rich in cysteine residues. The next one hundred amino acids include many glutamic and aspartic acid residues (negatively charged), as well as a stretch of seven uninterrupted threonine residues. Two consensus sequences for N-linked glycosylation exist at positions 467-469 and 496-498.

Aß occupies a region spanning the extracellular and transmembrane domains of APP; 28 residues are found in the extracellular domain and 11 - 14 residues are located within the membrane. Three lysine residues are located immediately C-terminal to the putative membrane spanning region; the latter feature is commonly found at the membrane-

cytoplasm junction of cell surface receptors (Kang, Lemaire and Unterbeck, 1987). Aß is contained within APP C-100, a C-terminal fragment of APP containing approximately 100 amino acids. In this document, the term APP C-100 will be used to refer to the C-terminus of APP in a general fashion; the term APP C-105 will be used when discussing the clones constructed in this laboratory.

Additional work has resulted in the recognition of other APP domains, in addition to those first described by Kang. For example, a metalloproteinase inhibitor domain is found in the C-terminal glycosylated region of secreted APP (Miyazaki, Hasegawa et al. , 1993). This domain inhibits the action of gelatinase A, a matrix-degrading metalloproteinase. Gelatinase A is able to cleave a synthetic peptide at a site corresponding to Aß lys 16-lys 17 (Miyazaki, Hasegawa et al. , 1993). A potential heparin binding site (APP 96-110) at the N-terminus of APP has been identified on the basis of secondary structure predictions and molecular modeling (Small, 1994). APP also has a zinc II binding site, located at APP 179-208, between the cysteine-rich and the negatively-charged domains (Bush, Multhaup et al. , 1993). Other APP domains are discussed later in relation to the normal functions of APP.

APP undergoes extensive post-translational modifications including N- and O-glycosylation (Weidemann, Konig et al. , 1989; Pahlsson, Shakin-Eshleman and Spitalnik, 1992), sulfation of tyrosine residues (Weidemann, Konig et al. , 1989), and phosphorylation (Oltersdorf, Ward and Henriksson, 1990).

Figure 1. Schematic Diagram of the Amyloid Precursor Protein

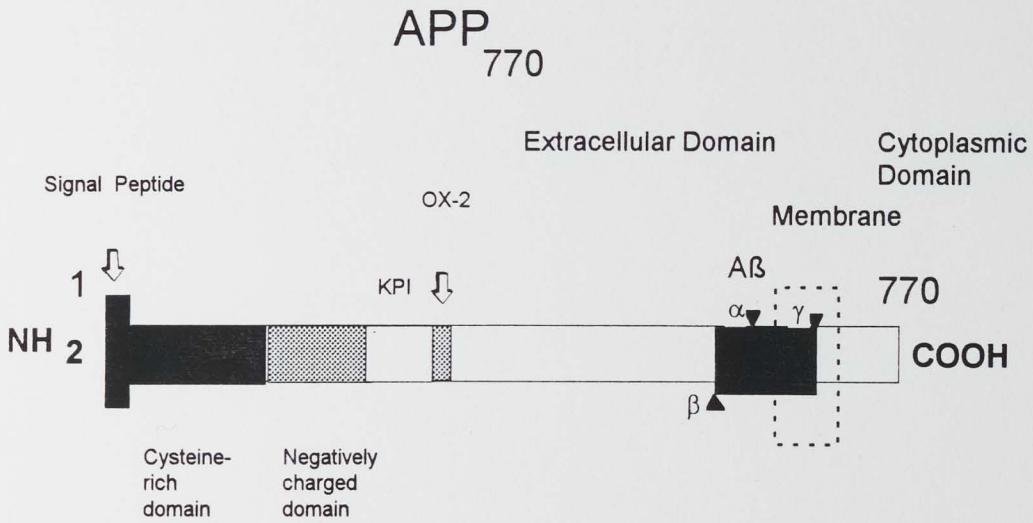

Diagram is not drawn to scale. Arrowheads indicate the cleavage sites of α, β and γ secretase. The APP C-100 fragment of APP extends from the amino terminus of Aß to the carboxyl terminus of APP. The p3 fragment of APP extends from the α secretase site at its amino end to the γ secretase site at its carboxyl end. The APP fragment called Protein Nexin II arises from APP_{751} or APP_{770} and extends from the amino terminus of APP to the α secretase cleavage site.

2. Evidence for a Causal Role of Aß in Alzheimer's Disease

As noted previously, the gene for APP is located on chromosome 21. The discovery of APP's chromosomal location suggested that APP overexpression could lead to Aß deposition, since young adults with trisomy 21 were known to develop dementia and plaques (Katzmann, 1986). In 1990, Levy et al. showed that an APP mutation was responsible for hereditary cerebral hemorrhage with amyloidosis Dutch type (HCHWA-Dutch) (Levy, Carman et al. , 1990). In this condition, susceptibility to cerebral hemorrhage is caused by the deposition of amyloid in cerebral blood vessels. This finding linked amyloid deposition to a mutation in APP for the first time. The HCHWA-Dutch mutation is a substitution of glutamine for glutamic acid at position 22 within Aß. In 1991, a 717 valine to isoleucine mutation (3 residues C-terminal to Aß) was shown unequivocally to cause early-onset Alzheimer's disease, albeit in a small number of pedigrees (Goate, Chartier-Harlin et al. , 1991). Additional mutations (valine to glycine and valine to phenylalanine) have now been identified at the same site (Chartier-Harlin, Crawford and Houlden, 1991; Murrell, Farlow and Ghetti, 1991). A mutation (alanine to glycine) at position 21 within Aß (Hendricks, van Duijn et al. , 1992) has also been observed. In addition, a double mutation located immediately N-terminal to Aß (lysine-methionine to asparagine-leucine) has been implicated in two Swedish pedigrees (Mullan, Crawford et al. , 1992). Transfected cells expressing the Swedish mutation (Cai, Golde and Younkin, 1993; Citron, Oltersdorf et al. , 1992) or overexpressing the C-terminal 100 amino acids of APP (Shoji, Golde et al. , 1992), cause increased release of Aß. The

clustering of mutations causing amyloid deposition within, or near the Aß coding region, suggests that such mutations may alter the way Aß is processed, leading to its accumulation in plaques.

3. Proteolytic Processing of APP

a. Established Pathways of APP Processing

Three APP proteolytic processing pathways have been identified and are described below. The identities of the proteases known as α, ß and γ secretase have not been established. Pathways (2) and (3), are potentially amyloidogenic:

1.) Mature APP is cleaved in the middle of the Aß region (at lys 16 - lys 17 of Aß; i.e., position 687 of APP_{770}) by an unidentified enzyme referred to as α secretase (Esch, Keim et al. , 1990). This cleavage releases a large soluble amino terminal APP fragment (denoted APPs ; also known as Protein Nexin II (PNII) if generated from APP_{751} or APP_{770}) into the extracellular space and leaves a carboxyl terminal fragment (molecular weight approximately 10 kD) in the membrane. This is the so-called "secretory" pathway, which precludes Aß generation. About 30% of all full length, mature APP molecules are cleaved in this manner (Weidemann, Konig et al. , 1989). Preliminary characterization of α-secretase indicates that this enzyme cleaves APP at a predefined distance from the membrane (Sisodia, 1992). The metalloproteinase, gelatinase A, is a potential candidate for α-secretase, based on its ability to cleave a synthetic peptide at a site corresponding to Aß lys 16-lys 17 (Miyazaki, Hasegawa et al. , 1993).

2.) APP is also degraded by an endosomal/lysosomal pathway which produces multiple C-terminal fragments (Golde, Estus et al. , 1992). APP contains a consensus sequence near its carboxyl terminus for reinternalization by clathrin coated pits and targeting to endosomes/lysosomes (Chen, Goldstein and Brown, 1990). Radiosequencing has shown that several C-terminal fragments (10-12 kD) isolated from cell lysates are generated by cleavage at, or near, the N-terminus of Aß. 3.) An APP processing pathway has been identified in platelets (Ghiso, Gardella et al. , 1994). APP is cleaved at amino acid 642 (APP_{770}), i.e., 30 amino acids N-terminal to Aß region. This cleavage generates an amino terminal fragment and a 16 kD, membrane-associated C-terminal fragment.

The existence of two other proteases, ß and γ has been postulated based on the carboxyl terminal heterogeneity of soluble APP. A soluble APP fragment, truncated at the N-terminus of Aß (i.e., at the ß-secretase site) has been identified (Seubert, Oltersdorf et al. , 1993). Similarly, a potentially amyloidogenic, N-terminal fragment, truncated at the C-terminal of Aß (i.e., at the γ-secretase site), has also been found (Anderson, Chen et al. , 1992). Proteolytic cleavage of APP at the ß-secretase and γ-secretase sites, gives rise to the N-terminus and C-terminus, respectively, of Aß. Presumably, the 3 kD APP fragment termed 'p3' is generated from the C-terminal fragment of APP remaining in the membrane after α-secretase cleavage, by additional cleavage at the γ-secretase site (Haass, Hung et al. , 1993).

b. Characterization of Pathways Leading to Aß Production

Proteolytic processing of APP has been investigated with the goal of establishing the pathway(s) for Aß release. Until recently, Aß formation was thought to be the result of aberrant proteolytic processing (Sisodia, Koo et al. , 1990). Several groups have now shown that the Aß fragment (molecular weight 4 kD), and the p3 fragment (molecular weight 3 kD), are produced normally by cultured cells and are found in human cerebrospinal fluid (Seubert, Vigo-Pelfrey and Esch, 1992; Shoji, Golde et al. , 1992; Haass, Hung et al. , 1993).

As indicated above, the secretory pathway (1) precludes amyloid formation, while pathways (2) and (3) generate potentially amyloidogenic fragments. Also, "secretory" cleavage at the γ-secretase site can generate a potentially amyloidogenic N-terminal fragment. It is not known whether Aß is produced *in vivo* from any of the potentially amyloidogenic pathways cited above. The normal production of Aß may occur in other pathways not yet defined.

Conflict exists in the literature as to whether Aß production requires the C-terminal cytosolic domain of APP. One group of investigators (LeBlanc and Gambetti, 1994) has stated that the C-terminus of APP is required for Aß production while a second group (Haass, Hung et al. , 1993) has argued that the C-terminus is not essential for Aß production. The two groups employed similar methods. Using the eukaryotic expression vector Cep4ß, LeBlanc and Gambetti transfected the human K562 lymphoid cell line with 3 different constructs: 1.) APP_{695} 2.) APP_{695} truncated at the C-terminus, but containing

Aß and the entire transmembrane region and 3.) a C-terminal fragment of APP_{695} truncated at the N-terminus of Aß. Cells were metabolically labeled with ^{35}S methionine, proteins were immunoprecipitated with antibodies recognizing different APP epitopes, then separated on a 3 layer Tricine-SDS acrylamide gel. The gels were exposed to film for autoradiography or quantitated by phosphorimaging. These authors were able to observe a 4 kD band precipitated by 4G8 (an antibody to Aß $_{17-24}$) in cells transfected with construct (3), but were not able to observe such a band in cells transfected with construct (2). Cells transfected with construct (2) lack the NPTY (asparagine-proline-threonine-tyrosine) sequence located at amino acids 684-688 of APP_{695}. The latter sequence is a signal for receptor-mediated endocytosis. Therefore, LaBlanc and Gambetti argue that endocytosis is required for Aß production. However, a 3 kD fragment, the identity of which is presumably p3, was immunoprecipated from cells with construct (2).

In an effort to define the pathways by which Aß is released from APP, the effect of various compounds on Aß production in cultured cells has been quantitated (Busciglio, Gabuzda et al. , 1993; Haass, Hung et al. , 1993). Leupeptin, a lysosomal protease inhibitor, does not inhibit Aß production (Busciglio, Gabuzda et al. , 1993; Haass, Hung et al. , 1993). Ammonium chloride, a weak base, has been reported to dose-dependently reduce Aß production (Haass, Hung et al. , 1993) or to have no effect on Aß production (Busciglio, Gabuzda et al. , 1993). Monensin, an inhibitor of the distal Golgi, blocks Aß and p3 secretion. (Busciglio, Gabuzda et al. , 1993). Brefeldin A inhibits the secretion of Aß and p3 (Busciglio, Gabuzda et al. , 1993). The latter compound causes the Golgi to

collapse into the endoplasmic reticulum, and the trans-Golgi network to fuse with the endosomal system. Caffeine, which induces the release of calcium from intracellular stores, and the calcium ionophore A23187, increase the production of Aß in human kidney 293 cells transfected with APP_{751} (Querfurth and Selkoe, 1994). Thus, current studies indicate that Aß production is 1.) triggered by a rise in intracellular calcium 2.) requires maturation of APP in the Golgi, and 3.) may occur in an acidic compartment other than lysosomes.

4. Regulation of APP Expression

The mechanisms that regulate APP expression are only partially understood. The APP promoter is typical of those found in housekeeping genes in that it lacks a TATA box and has a high GC content (Salbaum, Weidemann et al. , 1988). The sequence between nucleotides -400 and -1 contains 72% GC and a high CpG to GpC ratio. [CpG sequences are a target for DNA methylation. Nucleotide positions are specified relative to the main transcriptional start site.] Transcription is initiated at multiple sites. The nucleotide sequence -200 to -100 contains a protein binding site. The 5' untranslated region of the APP gene contains two consensus sequences for the transcription factor AP-1 (at -350 and -45), a consensus sequence for a heat shock control element (at -317) and two consensus sequences for Alu I (positions -2436 to -2179 and -2020 to -1764). Thus, characterization of the APP promoter permits potential regulation of transcription by at least four mechanisms: 1.) methylation of cytosine residues 2.) protein binding to the GC rich region between -200 and -100 3.) binding of AP-1 to its recognition site and 4.)

stress-induced binding of heat shock factor to the heat shock control element (de Sauvage, Kruys et al. , 1992).

Two APP mRNA transcripts (3.2 kb and 3.4 kb) are observed on Northern blots of human brain. The 3.4 kb transcript contains a longer sequence representing the 3' untranslated region of the gene than does the 3.2 kb transcript. The two mRNAs are derived from alternative polyadenylation, rather than from alternative splicing. Although the 3' untranslated region contains three consensus sequences for polyadenylation, only two of them (at +2934 and +3185) are utilized to generate an mRNA transcript. *In Xenopus oocytes, the 3.4 kb mRNA transcript is translated into three times as much protein as the 3.2 kb species.* This is due to the increased translation of the 3.4 kb transcript, rather than to decreased stability of the 3.2 kb transcript. As indicated previously, neuritic plaques and dementia occur in Down's Syndrome (trisomy 21) as well as in Alzheimer's disease. In the former condition, plaque formation is thought to be due to a gene dosage effect, since the APP gene is located on chromosome 21. It is possible that APP overexpression facilitates plaque formation regardless of the means by which overexpression is induced. If so, conditions favoring APP overexpression arising from the preferential production of the 3.4kb mRNA transcript could cause plaque formation.

5. Normal Functions of APP

APP belongs to a family of highly conserved proteins (Sprecher, Grant et al. , 1993; Wasco, Bupp et al. , 1992; Wasco, Gurubhagavatula et al. , 1993; Rosen, Martin-Morris et al. , 1989). The evolutionary conservation of APP suggests that it has one or more

important functions. A full understanding of APP's normal functions has not been achieved. However, the data gathered to date suggest that APP may play an important role in many normal cellular activities including wound healing (Smith, Higuchi and Broze, 1990; Van Nostrand, Schmaier et al. , 1990), proliferation (Saitoh, Sundsmo et al. , 1989; Ninomiya, Roch et al. , 1993), adhesion (Chen and Yankner, 1991; Breen, Bruce and Anderton, 1991; Schubert, Jin et al. , 1989; Ghiso, Rostagno et al. , 1992), neurite extension (Small, 1994; Milward, Papadopoulos et al. , 1992; Araki, Kitaguchi et al. , 1991), survival under stress (Yamamoto, Miyoshi et al. , 1994; Mattson, Cheng et al. , 1993), and synaptic plasticity (Mattson, 1994). APP may also serve as a cell surface receptor (Nishimoto, Okamoto et al. , 1993; Kang, Lemaire and Unterbeck, 1987). A synopsis of the evidence for APP's role in several normal cell processes is presented below:

Wound Healing/Coagulation

Secreted forms of APP may play a role in coagulation and wound healing. Protein Nexin II is the name given to the N-terminal fragment of APP released into the extracellular fluid after cleavage of APP_{751} or APP_{770} by α-secretase. Protein Nexin II (containing the Kunitz protease inhibitor domain) is found in the α granules of platelets, and is released, along with other α granule markers, upon platelet activation by thrombin or collagen (Van Nostrand, Schmaier et al. , 1990). α granules are intracellular storage vesicles which fuse to the plasma membrane and release their contents at sites of injury.

Protein Nexin II is an effective inhibitor of coagulation factor XIa (Smith, Higuchi and Broze, 1990). It also inhibits the action of trypsin, chymotrypsin, epidermal growth factor binding protein, and the γ subunit of NGF (Van Nostrand, Schmaier et al. , 1990).

Cell Proliferation

Cell lines transfected with APP-antisense constructs exhibit poor cell growth (Saitoh, Sundsmo et al. , 1989; Ninomiya, Roch et al. , 1993). One such cell line, (A1), was created by tranfecting human lung fibroblasts with a full-length APP_{695} construct, in which the 100 amino acids at the carboxyl terminus were replaced with an antisense fragment (Saitoh, Sundsmo et al. , 1989). The growth of A1 is restored by the addition of conditioned media from parental fibroblasts. However, if conditioned media is treated to remove APP, it can not restore normal growth. The A1 cell line was used in conjunction with synthetic peptides corresponding to various APP fragments, to determine the APP sequence responsible for restoring fibroblast growth (Ninomiya, Roch et al. , 1993). A RERMS (arginine-glutamic acid-arginine-methionine-serine) sequence at APP 328-332 (APP_{695} numbering), is the shortest sequence sufficient to restore fibroblast growth in part. Growth can be restored fully by peptides encompassing 11 (APP 325-335) or 17 (APP 325-335) amino acids, both of which contain the RERMS sequence. Conditioned media from an APP C-100-transfected cell line in which the RERMS sequence was deleted is unable to restore growth, indicating that the RERMS sequence is the only APP sequence

responsible for promoting proliferation. The RERMS sequence is common to the 3 major APP isoforms.

Neuronal Survival

Soluble APP has been to shown to promote neuronal survival in serum-free media (Yamamoto, Miyoshi et al. , 1994; Araki, Kitaguchi et al. , 1991), and to protect neurons against injury induced by ischemia (Smith-Swintosky, Pettigrew et al. , 1994), hypoglycemia (Mattson, Cheng et al. , 1993) or glutamate (Mattson, Cheng et al. , 1993). In the latter study, the protection against hypoglycemia was abolished by antibodies directed toward APP 444-592 (APP_{695} numbering). It was also found that APP_{695} and APP_{751} dose-dependently lower resting calcium levels in rat hippocampal neurons, in the absence of any insult. Antibodies directed against APP 444-452 block the ability of APP_{695} and APP_{751} to lower intracellular calcium. Neuronal survival in serum-free media is supported dose-dependently by a synthetic peptide corresponding to APP 319-335 (17mer) (Yamamoto, Miyoshi et al. , 1994). N-terminal truncation of the 17mer to an 11mer (APP 325-335) greatly reduces its ability to support neuronal survival.

Finally, it has also been suggested that a heparin binding domain located at the amino terminus of APP contributes to neuronal survival (Small, 1994). Thus, three APP domains which contribute to neuronal survival have been identified, APP 319-335 (Yamamoto, Miyoshi et al. , 1994), APP 444-592 (Mattson, Cheng et al. , 1993) and the heparin binding domain (Small, 1994).

APP as a Cell-Surface Receptor

The protein sequence of APP contains features characteristic of cell-surface receptors (Kang, Lemaire and Unterbeck, 1987), indicating that APP may function in this manner. Further support for this notion is provided by the finding that a synthetic peptide corresponding to APP His 657-Lys 676 (APP_{695} numbering) dose-dependently stimulates the binding of ^{35}S-GTP-γ-S to the GTP binding protein, G_o (Nishimoto, Okamoto et al. , 1993). Nishimoto, Okamoto et al. have suggested that under some conditions, APP may activate G_o constitutively, and that such a situation may have negative consequences for cell viability. The presumption that APP functions as a receptor can not be verified until a ligand which binds membrane-bound APP is identified.

6. Actions of Aß

As noted earlier, it is now clear that soluble Aß is a normal constituent of biological fluids (Shoji, Golde et al. , 1992; Seubert, Vigo-Pelfrey and Esch, 1992; Haass, Schlossmacher et al. , 1992). The neurotrophic and neurotoxic actions of full length Aß are mimicked by a Aß fragment containing amino acids 25-35 ($Aß_{25-35}$) (Yankner, Duffy and Kirschner, 1990). At present, it is not known whether Aß has a physiological function. *In vitro*, $Aß_{1-40}$ and $Aß_{12-28}$ bind to ApoE, forming an extremely stable complex which resists dissociation by boiling in SDS (Strittmatter, Weisgraber et al. , 1993). The binding of Aß to ApoE is dependent on the presence of oxygen (Strittmatter, Weisgraber et al. , 1993). Complex formation requires Aß residues 12-28 and ApoE residues 244-272 (Strittmatter, Weisgraber et al. , 1993). Binding of Aß to ApoE3 occurs within hours, at

pH 4.6-7.6. In contrast, binding of ApoE4 occurs within minutes, at pH values greater than 6.6. Recently, ApoE binding has been shown to attenuate Aß toxicity dose-dependently in rat hippocampal cultures (Whitson, Mims et al. , 1994). Also, Aß $_{1-42}$ stimulates the release of bFGF and interleukin 1 (IL-1) from microglia and astrocytes (Araujo and Cotman, 1992). The release of bFGF and IL-1 from microglia can then cause astrocytes to proliferate and to produce microglial growth factors.

In 1989, Aß was reported to enhance the survival of hippocampal neurons in culture (Whitson, Selkoe and Cotman, 1989). A year later it was shown that Aß exposure can be neurotrophic or neurotoxic, depending on its concentration and neuronal age (Yankner, Duffy and Kirschner, 1990). Several groups confirmed the toxicity of Aß *in vitro* (Rush, Aschimies and Merriman, 1992; Emre, Geula et al. , 1992; Kowall, McKee et al. , 1992), but others could not (Mattson, Cheng et al. , 1992; Koh, Yang and Cotman, 1990; Podlisny, Stephenson et al. , 1992; Games, Khan et al. , 1992; Clemens and Stephenson, 1992). It is now apparent that purified Aß preparations may differ in their ability to aggregate, i.e., to assume the ß-pleated sheet conformation necessary for peptide assembly into fibrils (Pike, Burdick et al. , 1993; Yankner, 1992; Busciglio, Lorenzo and Yankner, 1992). Aggregation is required for toxicity (Pike, Burdick et al. , 1993). Free radical attack may promote Aß aggregation (Dyrks, Dyrks et al. , 1992).

The mechanism(s) by which Aß induces neurotoxicity are under active investigation. Aß $_{25-35}$, but not Aß $_{1-28}$, stimulates the release of nitric oxide from mouse neuroblastoma N1E-115 cells (Hu and El-Fakahany, 1993). It remains to be determined whether Aß-

induced release of NO is physiological, pathological or both. Several studies have found that Aß destabilizes calcium homeostasis (Joseph and Han, 1992; Mattson, Cheng et al. , 1992; Koh, Yang and Cotman, 1990). Aß and Aß $_{25-35}$ increase the susceptibility of cortical neurons to excitotoxin and calcium ionophore- induced damage by potentiating the rise in calcium provoked by these agents (Mattson, Cheng et al. , 1992). In NGF-treated PC12 cells, Aß $_{25-35}$ induces a dose dependent (10-400 µM) rise in intracellular calcium levels (Joseph and Han, 1992). This effect is observed in the presence of extracellular calcium but not in its absence. Aß effects on calcium homeostasis may be the result of its capacity to form calcium channels in planar bilayers (Arispe, Rojas and Pollard, 1993).

The effect of Aß $_{25-35}$ on calcium entry was investigated in cortical neurons (Weiss, Pike and Cotman, 1994). Nimodipine, an inhibitor of L-type voltage-dependent calcium channels, and Co^{+2}, a non-specific inhibitor of voltage-dependent calcium channels, protected cortical neurons from Aß $_{25-35}$ toxicity. The NMDA receptor antagonist, MK-801, and the kainate receptor antagonist, NBQX, were ineffective. The latter finding suggests that Aß toxicity is mediated, at least in part, by calcium entry through voltage-dependent channels.

Although Aß increases neuronal susceptibility to excitotoxic insults, its toxicity is not mediated by an excitotoxic mechanism (Pike, Burdick et al. , 1993; Busciglio, Yeh and Yankner, 1993; Weiss, Pike and Cotman, 1994). Pike et al found that hippocampal neurons from embryonic day 18 rats were sensitive to Aß toxicity during the first day

in vitro, a time at which these neurons are insensitive to excitatory amino acid toxicity. MK-801 did not attenuate Aß toxicity. This group also observed that, in contrast to EAA toxicity, Aß toxicity is not characterized by cell swelling. In another study, the glutamate antagonists, kynurenate, APV and CNQX, used alone or in combination, were unable to protect hippocampal neurons from Aß toxicity (Busciglio, Yeh and Yankner, 1993).

Aß toxicity is mediated at least in part by hydrogen peroxide (Behl, Davis et al. , 1994). This conclusion is based on experiments performed *in vitro* using exogenously supplied Aß, which yielded the following findings: 1.) Aß increases the intracellular accumulation of hydrogen peroxide and lipid peroxides 2.) catalase and antioxidants attenuate Aß toxicity 3.) Cell lines selected for resistance to Aß toxicity are also resistant to hydrogen peroxide 4.) Aß induces the expression of a transcription factor, NF-κB, that is activated by hydrogen peroxide. It is unknown whether Aß causes hydrogen peroxide accumulation by increasing its production or inhibiting its breakdown. The relevant mechanism may involve a flavin oxidase, because a flavin oxidase inhibitor, diphenylene iodonium, is also able to attenuate Aß toxicity.

Due to the existence of conflicting reports in the literature, it is not clear whether Aß toxicity is mediated primarily by apoptosis (Forloni, Chiesa et al. , 1993), necrosis (Behl, Davis et al. , 1994), or by a combination of mechanisms. Recently, Aß-induced neurotoxicity was shown to require tau protein kinase I (TPK I) (Takashima, Noguchi et al. , 1993). In primary cultures of rat hippocampal neurons, Aß-induced cell death was attenuated by a TPK I antisense oligonucleotide, and by inhibitors of RNA and protein

synthesis. The finding that RNA and protein synthesis are required for Aß-induced toxicity suggests that Aß provokes apoptosis, at least in this cell type.

C. The Role of Calcium in Neurodegenerative Disease

1. Calcium Homeostasis

A large variety of hormones and neurotransmitters exert their effects by eliciting a rapid, transient rise in intracellular Ca^{+2}. This can be done by facilitating calcium entry into the cell, or by inducing the release of calcium from intracellular stores (Majerus, Ross et al. , 1990; Hokin, 1985; Chuang, 1989; Berridge and Irvine, 1989; Berridge, 1987). Ca^{+2} then acts as a second messenger to elicit a cellular response. To maintain calcium's ability to act as a second messenger, cells must avoid sustained rises in intracellular Ca^{+2}.

The concentration of Ca^{+2} in extracellular fluid is approximately 1.3 mM (Orrenius, Burkitt et al. , 1992). The intracellular Ca^{+2} concentration is 0.1-0.2 µM (Orrenius, Burkitt et al. , 1992). Thus, a large concentration gradient for Ca^{+2} exists across the plasma membrane. An electrical gradient also spans the membrane; the cell interior is -60 mV relative to the exterior.

Calcium entry into cells occurs primarily through voltage-dependent or receptor-operated channels (Bertolino and Llinas, 1992). Low intracellular Ca^{+2} concentrations are maintained by the limited permeability of the cell membrane, buffering of intracellular Ca^{+2} by protein binding, compartmentation of Ca^{+2} within intracellular stores (endoplasmic reticulum, mitochondria, nucleus) and by the operation of active extrusion mechanisms.

The latter category includes rapid Ca^{+2} removal by the Na^{+}/Ca^{+2} exchanger, and slow removal by Ca^{+2} ATPase. The $Na^{+/}Ca^{+2}$ exchanger exchanges one Ca^{+2} for three Na^{+} (Orrenius, Burkitt et al. , 1992). The direction of transport depends on the membrane potential: Ca^{+2} flows inward when the cell is depolarized and outward when it is polarized. Ca^{+2}-ATPase exchanges a Ca^{+2} for a H^{+}, at the expense of one mole of ATP (Richter and Kass, 1991). It has a high affinity for Ca^{+2} and a low capacity for transport (Orrenius, Burkitt et al. , 1992).

A disturbance in any of the normal homeostatic mechanisms can lead to a sustained elevation of intracellular calcium. Sustained elevations of intracellular calcium can lead to perturbation of the cytoskeleton, impairment of mitochondrial function, and activation of phospholipases, proteases and endonucleases, and the generation of free radicals (Orrenius, McConkey et al. , 1989; Nicotera, Bellomo and Orrenius, 1992).

2. A Mechanism for Loss of Calcium Homeostasis: Glutamate Toxicity

Glutamate is the major excitatory neurotransmitter in the CNS in the brain and spinal cord. Its effects are mediated by multiple receptor types, including the NMDA receptor. The NMDA receptor is a ligand-gated ion channel capable of permitting a large calcium influx across the plasma membrane. Elevated concentrations of glutamate or aspartate can cause neuronal cell death by promoting excess calcium entry through NMDA receptor channels. In 1986, Olney coined the term "excitotoxicity", to refer to cell death mediated by high concentrations of excitatory amino acids acting at glutamate receptors. Glutamate toxicity has physiological relevance because it is believed to mediate ischemia-induced cell

death (Choi, 1988). Excitatory amino acids may also be involved in cell damage due to trauma or neurodegenerative disease (Olney, 1990).

During ischemia, large quantities of glutamate are released from damaged nerve terminals and glutamate uptake is reduced (Rothman, 1984). Surplus glutamate causes excessive receptor stimulation and an uncontrolled rise of intracellular calcium. Glutamate-induced neurotoxicity can be divided into two components; an acute component characterized by cell swelling due to Na^+,Cl^-, and H_2O influx, and a delayed component dependent on the presence of extracellular calcium (Choi, 1985). The delayed component can be ameliorated by NMDA receptor antagonists, but not by kainate or AMPA antagonists. The latter finding is an indication that the delayed component of glutamate toxicity is mediated primarily by calcium entry through NMDA receptor channels (Choi, 1992).

Calcium entry through NMDA receptor channels raises the intracellular calcium concentration, causing the activation of enzymes associated with calmodulin. One such enzyme is nitric oxide synthase (NOS) (Bredt and Snyder, 1990). NOS catalyzes the production of the free radical, nitric oxide, from arginine. Several lines of evidence indicate that NMDA toxicity is mediated by NO (Dawson, Dawson and London, 1991). First, NO production and NMDA toxicity are attenuated by NOS inhibitors and by arginine depletion of cell culture media. Secondly, sodium nitroprusside, which spontaneously releases NO, dose-dependently generates cGMP and induces cell death. Thirdly, NMDA- and sodium nitroprusside-induced toxicity are both reduced by

hemoglobin, an NO scavenger. Lastly, superoxide dismutase potentiates NMDA toxicity, by preventing the destruction of NO by superoxide.

The neurotoxicity of NO may be attributed in part, to its ability to activate poly(ADP-ribose) synthetase (PARS) (Zhang, Dawson et al. , 1994). PARS is a nuclear enzyme which adds multiple ADP-ribose units to protein when activated by DNA damage. The addition of each ADP-ribose unit requires one NAD^+, which must be regenerated at the expenditure of 4 ATPs. Therefore, PARS activation causes rapid energy depletion leading to cell death. PARS inhibitors partially inhibit NMDA- and NO-induced toxicity with potencies which parallel their potencies as inhibitors. The latter finding is evidence that PARS activation is a major mechanism mediating NO toxicity, but does not preclude the possibility that NO toxicity is also mediated by other mechanisms (Wink, Kasprzak et al. , 1991; Lepoivre, Chenais et al. , 1990; Drapier and Hibbs, Jr. 1986; McDonald and Moss, 1993; Nathan and Hibbs, Jr. 1991).

3. Loss of Calcium Homeostasis in Alzheimer's Disease

The evidence that loss of calcium homeostasis is involved in the etiology of Alzheimer's disease is extensive, and can only be summarized here. Earlier, the role of the amyloid precursor protein in Alzheimer's disease was described, and numerous studies were cited indicating that Aß destabilizes calcium homeostasis (Weiss, Pike and Cotman, 1994; Arispe, Rojas and Pollard, 1993; Joseph and Han, 1992; Mattson, Cheng et al. , 1992; Koh, Yang and Cotman, 1990). Conversely, a loss of calcium homeostasis may increase Aß production. This possibility is suggested by the finding that A23187 can

increase Aß production in cultured cells (Querfurth and Selkoe, 1994). The formation of the potentially toxic Aß fragment also compromises the production of soluble APP. The latter has been shown to protect neurons against hypoglycemia-induced injury and excitotoxicity, reduce resting calcium levels, and prevent the rise of intracellular calcium seen in response to hypoglycemia. (Mattson, Cheng et al. , 1993).

Technical problems have hindered the demonstration of altered calcium homeostasis in Alzheimer brain, but disrupted calcium homeostasis has been observed in fibroblasts (Kumar, Dunlop and Richardson, 1994; McCoy, Mullins et al. , 1993), platelets (Le Quan Sang, Mignot et al. , 1993) and lymphocytes (Adunsky, Baram et al. , 1991). In human fetal cerebral cortical neurons, elevated calcium levels have been shown to increase immunostaining by tau and ubiquitin antibodies, and to promote tau phosphorylation (Mattson, Engle and Rychlik, 1991). Tau is the primary protein component of neurofibrillary tangles and is hyperphosphorylated in AD brain (Grundke-Iqbal, Iqbal et al. , 1986).

4. Calcium Ionophore A23187

The term "ionophore" is used to describe structurally diverse compounds capable of transporting cations across biological membranes (Pressman, 1976). The calcium ionophore, A23187, possesses a lipophilic "backbone" which forms a cavity for cation insertion. Oxygen atoms extending into the interior of the cavity provide points of attachment to which cations can bind via electrostatic interactions. Upon complexation with oxygen, the solvation shell of the cation is removed and the positive charge

dispersed. A23187-bound cations are transported across biological membranes at high turnover rates, due to the shielding of positive charge within the molecule and the lipophilicity of the ionophore backbone.

A23187 (Figure 2) has two aromatic heterocyclic ring systems, and therefore exhibits changes in both flurorescence and absorbance upon complex formation (Pressman, 1976). It is soluble in ethanol and DMSO, but not in water. A23187 can transport calcium across the plasma membrane by means of a carrier mechanism in which Ca^{+2} is exchanged for $2H^{+}$ (Kolber and Haynes, 1981; Puskin, Visties and Wene, 1981) and can form channels in synthetic membranes (Balasubramanian, Sikdar and Easwaran, 1992) It must be present in the deprotonated, anionic state to bind cations (Pressman, 1976) Although A23187 induces arachidonic acid release and increased activity of PLA_2 (Clark, Littlejohn et al. , 1986; Thomas, Chap and Douse-Blazy, 1981; Hong, McLaughin et al. , 1985), lipid metabolism does not play a direct role in A23187-induced membrane permeabilization (Shier, DuBourdieu and Wang, 1991) Finally, A23187 also causes the release of Ca^{+2} from intracellular stores (Itoh, Kanmura and Kuriyama, 1985).

In NGF-treated PC12 cells, A23187 toxicity increases with time and concentration, and is primarily necrotic (Michel, Vyas et al. , 1994). A23187 toxicity has also been investigated in erthrocytes, a cell type in which ATP production is limited to glycolysis (Engstrom, Walsenstrom and Ronquist, 1993). In the presence of glucose, A23187 reduces energy charge, but stimulates glycolysis. Therefore, the A23187- induced effect on energy charge has been attributed to increased ATP expenditure, rather than decreased

ATP synthesis. In erythrocytes, ATP is used primarily to maintain Na^{+}/K^{+} ATPases and Ca^{+2} ATPases.

Figure 2. The Structure of the Calcium Ionophore A23187

A23187

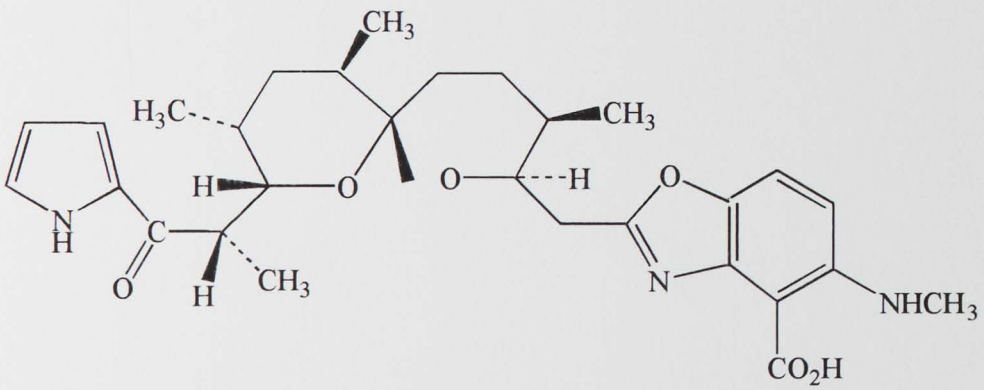

D. The Role of Free Radicals

1. Definition of Free Radical and Identification of Major Radical Species

Oxygen-derived free radicals may contribute to the pathological processes leading to several neurodegenerative diseases, including Alzheimer's disease. By definition, a free radical is an atomic or molecular species having one or more unpaired electrons. Most free radicals have only a fleeting existence, due to their great reactivity. Other highly reactive, oxygen-containing species, which do not meet the chemical definition of a free radical, are nevertheless, often referred to as such. These species are more appropriately called reactive oxygen species (ROS) and include singlet oxygen, hydrogen peroxide, peroxide, hydroperoxide, and epoxide metabolites of endogenous lipids and xenobiotics (Smith. 1992). The free radical theory of aging postulates that the accumulation of free-radical induced injuries over time is responsible for the aging process (Harman, 1992).

Molecular oxygen is a diradical, meaning that it has two unpaired electrons in separate orbitals which share the same spin. Since potential electron donors present two electrons with opposite spins in a single orbital, oxygen can not accept two electrons simultaneously. However, oxygen can be reduced by four consecutive transfers of 1e- as shown below (Cohen, 1994):

$$\begin{array}{lccccccccc} & & \overset{1e^-}{} & & \overset{1e^-}{} & & \overset{1e^-}{} & & \overset{1e^-}{} & \\ 1) & O_2 & \rightarrow & \bullet O_2^- & \rightarrow & H_2O_2 & \rightarrow & \bullet OH & \rightarrow & H_2O \\ & & & & \underset{2H^+}{} & & & & \underset{H^+}{} & \end{array}$$

The transfer of the first electron results in the formation of superoxide anion. The transfer of a second electron results in the production of hydrogen peroxide. The latter reaction can be catalyzed by superoxide dismutase or can occur spontaneously. The transfer of a third electron causes the conversion of hydrogen peroxide to the extremely reactive hydroxyl radical. Finally, transfer of a fourth electron produces water.

Superoxide is only moderately reactive, particularly in comparison to the hydroxyl radical. It is not a strong oxidant, but it can reduce iron (Reaction 2) or oxidize catecholamines (Reaction 3) (Cohen, 1994) as shown below:

2) $Fe^{+3} + \bullet O_2^- \rightarrow Fe^{+2} + O_2$

3) $\text{Quinone} + \bullet O_2^- + H^+ \rightarrow SQ\bullet + H_2O_2$

Hydrogen peroxide and the highly reactive hydroxyl radical can be produced by the Fenton reaction, in which transition metals, such as iron, copper or manganese, facilitate the reduction of molecular oxygen :

4) $O_2 + Fe^{+2} \rightarrow Fe^{+3} + \bullet O_2^-$

5) $2 \bullet O_2^- + 2H^+ \rightarrow H_2O_2 + O_2$

6) $H_2O_2 + Fe^{+2} \rightarrow \bullet OH + OH^- + Fe^{+3}$

The availability of iron for participation in the Fenton reaction is limited by iron binding proteins (Gutteridge, 1994). Two-thirds of body iron is contained within hemoglobin (Gutteridge, 1994). Lesser amounts of iron are carried by myoglobin, various enzymes, the iron binding proteins transferrin and lactoferrin, and the iron storage proteins ferritin and hemisiderin. In normal individuals, transferrin is only 1/3 bound by iron (Gutteridge, 1994). This means that the concentration of catalytic iron (i.e., available for the Fenton reaction) in plasma is essentially zero. Catalytic iron is usually bound to phosphate esters, organic acids, membrane lipids or DNA (Gutteridge, 1994). The hydroxyl radical produced by the Fenton reaction causes site-specific damage, most often to the non-protein species carrying the iron (Gutteridge, 1994).

The free radical NO functions physiologically in vascular relaxation, neuronal transmission and immune responses (Rengasamy and Johns, 1994). As indicated earlier, NO is formed from L-arginine in a reaction catalyzed by nitric oxide synthase. NO can react with superoxide to produce peroxynitrite anion, which, when protonated, decomposes to hydroxyl radical (Cohen, 1994):

7) $\bullet O_2^- + NO\bullet \rightarrow ONOO^-$

8) $ONOO^- + H^+ \rightarrow ONOOH$

9) $ONOOH \rightarrow \bullet OH + ONO\bullet$

Glutamate toxicity has been attributed to NO formation. However, despite its free radical character, in some instances NO formation may protect tissue from oxidative damage (Chiueh, 1994).

Free radicals are formed during numerous physiologic and pathologic processes, including electron leakage during oxidative phosphorylation, the metabolism of arachidonic acid, the autooxidation of catecholamines, the induction of cytochrome P450 reactions and ischemia/reperfusion injury. ROS are released by neutrophils during the respiratory burst (Coyle and Puttfarcken, 1993), and hydrogen peroxide is produced in peroxisomes (Wood and Youle, 1994).

2. Mechanisms of Free Radical-Induced Toxicity

The reactions typical of free radicals include radical addition, electron transfer, and atom abstraction (Smith. 1992). Through these mechanisms, free radicals can damage nucleic acids, proteins and lipids. Free radical attack can cause modification of amino acids (Floyd, 1990), protein crosslinking (aggregation) or protein fragmentation. The sulfhydryl groups of cysteine and the disulfide bonds of cystine residues are vulnerable to free radical attack (Jesberger and Richardson, 1991). The aromatic amino acids tryptophan, tyrosine and phenylalanine, are also vulnerable due to their unsaturated structures (Jesberger and Richardson, 1991). Free radical attack can cause changes in protein antigenicity and increased protein susceptibility to proteolysis and loss of function.

Free radical-induced DNA damage can be divided into base modifications and strand breaks. Hydroxyl radical will attack pyrimidines preferentially, then purines, and then the

deoxyribose moiety (Jesberger and Richardson, 1991). Modified bases that can be formed as a result of hydroxyl radical attack include 8-hydroxyguanine, 5-hydroxymethyluracil and thymine glycol (Floyd, 1990). Strand breaks are the result of hydroxyl radical attack on the 3' and 4' carbons of deoxyribose (Floyd, 1990). DNA is largely protected from free radical damage due to its helical arrangement, association with histones and relative isolation within the nucleus (Jesberger and Richardson, 1991). If free radical-induced damage does occur, efficient DNA repair mechanisms will be utilized. However, under some circumstances prooxidant forces may overwhelm repair mechanisms, leading to cell death or carcinogenesis.

Hydroxyl radicals can damage cell membranes by abstracting a hydrogen atom from the unsaturated bonds of membrane fatty acids and cholesterol (Moslen. 1992). The product of this reaction is a radical which reacts quickly with molecular oxygen to form a peroxyl radical. Peroxyl radicals can then abstract a hydrogen atom from a neighboring lipid to form a hydroperoxide and a new lipid radical capable of reacting with molecular oxygen. Thus, membrane damage is propagated in a chain reaction. Peroxidation of membrane lipids continues until the chain is broken by a chain terminator such as Vitamin E (α -tocopherol). Lipid peroxidation decreases membrane fluidity, and in doing so can alter membrane function. Loss of membrane fluidity has been shown to change the affinity of Na^+/K^+ ATPase for ATP (Mishra, Delivoria-Papadopoulos et al. , 1989). Calcium influx across the membrane may also change (Bast and Goris, 1989). Transition elements can play an important role in lipid peroxidation (Jesberger and Richardson, 1991).

Three types of evidence have been used to implicate free radicals in the etiology of pathological events. First, free radicals can be detected directly by electron paramagnetic resonance (EPR). However, the radicals that react with the greatest speed are found in very small concentrations, making them difficult to detect. Therefore, it is sometimes necessary to use a spin trap such as α-phenyl-t-butyl nitrone (PBN) to detect very highly reactive radicals. The radical will react with PBN to form a relatively stable nitroxide radical which can be then be analyzed by EPR. Secondly, one can obtain evidence of free radical generation by measuring the amount of product formed as a result of free radical attack on a substrate. Finally, evidence of free radical involvement has been obtained from studies employing free radical scavengers such as Vitamin E to protect against tissue injury, or scavenger depletion to potentiate injury.

3. Cellular Defense Mechanisms

In cells, numerous defense mechanisms have evolved to protect vital macromolecules from free radical damage. One of these mechanisms is the use of cytochrome oxidase to prevent the escape of intermediate free radicals during mitochondrial electron transport. However, a small percent of electron "leakage" still occurs. Therefore, the cell must also rely on other defense mechanisms to limit the effects of free radicals generated by this source, and other sources of free radicals. Free radical clearance and antioxidant regeneration are catalyzed by numerous enzymatic mechanisms. (Table 1.)

Non-enzymatic mechanisms for free radical protection include antioxidants (e.g., Vitamin E, ß-carotene, glutathione, Vitamin C), transition metal binders (transferrin,

ferritin, ceruloplasmin, albumin, metallothionein), and exporters (GSSG transporter, GS-conjugate transporter) (Moslen. 1992).

In comparison to other tissues, the brain is particularly vulnerable to oxidative stress. One reason for this vulnerability is the brain's almost exclusive reliance on aerobic respiration. In addition, iron accumulates in specific brain regions, especially the globus pallidus and substantia nigra, which may permit Fenton chemistry to occur under some circumstances (Olanow, 1993). The brain contains large concentrations of polyunsaturated fatty acids which provide a target for lipid peroxidation (Olanow, 1993), while it has only low concentrations of glutathione, glutathione peroxidase and Vitamin E (Olanow, 1993). Catalase is almost entirely absent from brain tissue. Since neurons are post-mitotic, large neuronal cell losses may compromise brain function.

Table 1. Enzymatic Mechanisms of Free Radical Clearance and Antioxidant Regeneration

Enzyme	Reaction Catalyzed	Location/ Comments
SOD	$2 \bullet O2^- + 2H^+ \rightarrow H_2O_2 + O_2$	CuZnSOD: cytoplasm/nucleus MnSOD: mitochondria Excellular SOD: plasma SOD levels are very low in extracellular fluids.
Catalase	$2 H_2O_2 \rightarrow 2H_2O + 1/2 O_2$ High Km for H_2O_2, first order kinetics	Peroxisomes, not extracellular fluids; catalase is specific for H_2O_2
Glutathione Peroxidase	$H_2O_2 + 2 GSH \rightarrow GSSG + 2 H_2O$ Low K_m for H_2O_2, Michaelis-Menton kinetics	Cytosol/mitochondria; Selenium dependent and independent forms of enzyme exist
Glutathione Reductase	$GSSG + 2 NADPH \rightarrow 2 GSH + 2 NADP^+$	Keeps GSH in reduced state
Glucose 6-phosphate Dehydrogenase	Glucose-6-phosphate + $NADP^+ \rightarrow$ 6-phosphoglucono-δ-lactone + NADPH + H^+	Rate limiting enzyme in pentose phosphate shunt

(Cotgreave, Moldeus and Orrenius, 1988)

4. Role of Free Radicals in Etiology of Alzheimer's Disease

A portion of the evidence implicating free radicals in the etiology of Alzheimer's disease has already appeared in previous sections of this document, but will be summarized here for the sake of clarity. First, the evidence implicating APP mutations in the development of familial Alzheimer's disease was reviewed (Wasco, Gurubhagavatula et al. , 1993). Later, it was noted that Aß toxicity is mediated, in part, by hydrogen peroxide *in vitro* (Behl, Davis et al. , 1994), and that $A\beta_{25-35}$ stimulates the release of nitric oxide from mouse neuroblastoma N1E-115 cells (Hu and El-Fakahany, 1993). It was also pointed out that Aß aggregation is promoted by free radical attack (Takashima, Noguchi et al. , 1993). Finally, Vitamin E has been reported to protect PC12 cells against Aß toxicity (Behl, Davis et al. , 1992).

5. Calcium Homeostasis and Free Radicals

In the present study, as in most, calcium- and free radical-induced toxicity are considered separately. But, one should bear in mind that disturbances in calcium homeostasis may promote free radical toxicity, and that the converse may also be true (Orrenius, Burkitt et al. , 1992). For example, the action of calcium-activated enzymes can lead to production of 1.) superoxide or 2.) hydroxyl radical:

1.) Under normal conditions, a step in the degradation of ATP is the xanthine dehydrogenase-catalysed production of uric acid and NADH from xanthine and NAD. During ischemia, xanthine dehydrogenase is converted to xanthine oxidase by the calcium-

activated protease calpain I. Xanthine oxidase catalyzes the same reaction as xanthine dehydrogenase, but uses molecular oxygen rather than NAD as the electron acceptor. Upon reperfusion, the 1 electron reduction of molecular oxygen results in the formation of superoxide radical.

2.) As mentioned earlier, NO production is catalyzed by the calcium/calmodulin dependent enzyme nitric oxide synthase. NO reacts with superoxide which results, ultimately, in the formation of hydroxyl radical (see Reactions 7-9 above).

E. Ganglioside Cytoprotection

1. The Importance of Membrane Lipids in Alzheimer's Disease

Gangliosides constitute a class of glycosphingolipids that are concentrated within the outer leaflet of neuronal cell membranes (Mahadik. 1992). Gangliosides of the gangliotetraose family have been shown to exert cytoprotection by diverse means (Mahadik. 1992). The structure of one such ganglioside, GM1, is shown in Figure 3. GM1 consists of 3 parts: a ceramide unit, an oligosaccaride chain and a N-acetylneuraminic acid (sialic acid) moiety. In this document, the term ganglioside will be used to denote members of the gangliotetraose family.

Gangliosides have provided protection against cell injury *in vivo* (Figliomeni, Bacci et al. , 1992; Emerich and Walsh, 1991; Emerich and Walsh, 1990; Shifman, 1991; Lipartiti, Lazzaro et al. , 1991; Seren, Rubini et al. , 1990) and *in vitro* (Favaron, Manev et al. ,

1988; Facci, Leon and Skaper, 1990; Skaper, Leon and Facci, 1991; Skaper, Facci and Leon, 1990; Skaper, Facci et al. , 1989). The cytoprotective efficacy of gangliosides has been demonstrated in animal models of cell damage caused by ischemia (Seren, Rubini et al. , 1990), anoxia (Skaper, Facci et al. , 1989), excitatory amino acids (Favaron, Manev et al. , 1988; Skaper, Leon and Facci, 1991; Skaper, Facci and Leon, 1990; Lipartiti, Lazzaro et al. , 1991) hypoglycemia (Facci, Leon and Skaper, 1990), diabetes (Figliomeni, Bacci et al. , 1992), and mechanical destruction of tissue (Shifman, 1991). In behavioral and biochemical studies, gangliosides have provided cytoprotection against neurotoxic damage induced by 6-hydroxydopamine (Kojima, Gorio et al. , 1984), MPTP (Date, Felten and Felten, 1989), AF64 (Emerich and Walsh, 1990), colchicine (Emerich and Walsh, 1991), ibotenic acid (Contestabile, Virgili et al. , 1990), and ethanol (Hungund, Reddy et al. , 1990). Studies demonstrating ganglioside efficacy have employed neurons from various brain regions including cortex (Favaron, Manev et al. , 1988; Skaper, Facci et al. , 1989), hippocampus (Skaper, Facci and Leon, 1990; Skaper, Facci et al. , 1989) and cerebellum (Skaper, Facci and Leon, 1990). Ganglioside efficacy has also been demonstrated in peripheral neurons (Figliomeni, Bacci et al. , 1992). Finally, beneficial effects of gangliosides have been observed in clinical studies of human stroke (Braune, 1991).

In addition to providing protection against numerous injuries, under some conditions GM1 is able to promote neuritogenesis and to potentiate the effects of NGF. GM1 is also able to promote PC12 cell survival in serum-free media in the absence of NGF.

2. Structural and Experimental Requirements for Ganglioside Cytoprotection

Preliminary information has emerged on the relationship between ganglioside structure and cytoprotective efficacy. Individual ganglioside preparations (GM1, GD1b, GT1b), as well as mixtures have shown the ability to provide cytoprotection (Figure 4). The usual order of potency for these compounds is GT1b > GD1b > GM1; enhanced potency is associated with additional sialic acid residues. AsialoGM1 (i.e., GM1 lacking the sialic acid moiety) is uniformly ineffective (Favaron, Manev et al. , 1988; Skaper, Leon and Facci, 1991; Skaper, Facci and Leon, 1990; Skaper, Facci et al. , 1989), illustrating the critical role of sialic acid in cytoprotection. Ganglioside potency is dependent on the number of sialic acid moieties, but roughly equivalent maximal efficacy can be achieved by GM1 and GT1b (Manev, Favaron et al. , 1990). The degree of GM1 cytoprotection depends on preincubation time (Skaper, Facci et al. , 1989). Longer preincubation periods provide a greater degree of cytoprotection, probably by allowing more time for ganglioside insertion into the plasma membrane. This interpretation is supported by the finding that increased GT1b content in plasma membranes is correlated with decreased neuronal cell death in response to a toxic dose of glutamate (Favaron, Manev et al. , 1988).

The synthetic gangliosides $LIGA_{20}$ and $LIGA_4$, were synthesized in an effort to overcome pharmacokinetic problems associated with GM1 (Figure 5). GM1 can not be administered orally, and is inserted slowly into plasma membranes (Manev, Favaron et al. , 1990). In contrast, $LIGA_{20}$ and $LIGA_4$ are inserted rapidly into plasma membranes, and

therefore have a faster onset of action than GM1 (Manev, Favaron et al. , 1990). $LIGA_4$ and $LIGA_{20}$ share the structure of GM1, except for the substitution of an acetyl ($LIGA_4$) or a dichloroacetyl ($LIGA_{20}$) group for the fatty acid at the 2-amino position of sphingosine. Future clinical use of the synthetic gangliosides will depend upon demonstration of adequate oral absorption and blood-brain barrier permeability.

Gangliosides provide potent cytoprotection of cerebellar granule cells against glutamate toxicity (Manev, Favaron et al. , 1990). The order of potency is $LIGA_{20}$ > $LIGA_4$ > PKS_3 > GM1, with EC_{50} values of 4.5, 5, 30, and 55 μM, respectively. PKS_3 (Figure 5) can be considered a derivative of sphingosine, with the addition of a dichloroacetyl group at the 2-amino position. Lyso GM1 (Figure 5), sphingosine, ceramide and sialic acid are not cytoprotective against glutamate toxicity in cerebellar granule cells (Manev, Favaron et al. , 1990).

In vitro, ganglioside cytoprotection is concentration-dependent and in the micromolar range. EC_{50} values for ganglioside cytoprotection do not vary widely, even among studies employing different methods of inducing cell injury and different neuronal populations. Ganglioside cytoprotection has been studied 1.) in cerebellar granule cells, against anoxia-induced damage (Skaper, Facci et al. , 1989) 2.) in cerebellar granule cells against aspartic acid-induced toxicity (Skaper, Facci and Leon, 1990) and 3.) in hippocampal pyramidal neurons against glutamate toxicity (Skaper, Leon and Facci, 1991). The EC_{50} values for GM1 in the latter three studies were 25, 35 and 30 μM, respectively.

Figure 3. The Structure of GM1

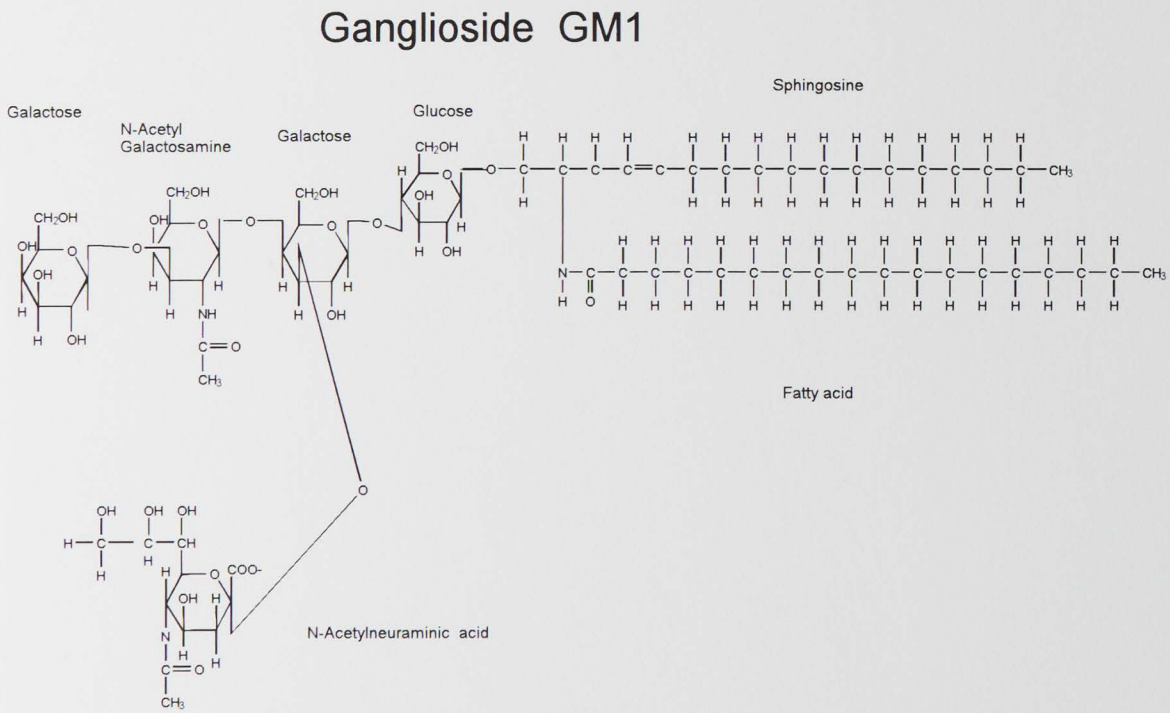

N-acetylneuraminic acid is also known as sialic acid. AsialoGM1 has the structure of GM1, except that it does not contain sialic acid.

Figure 4. Schematic Diagrams of Selected Gangliosides

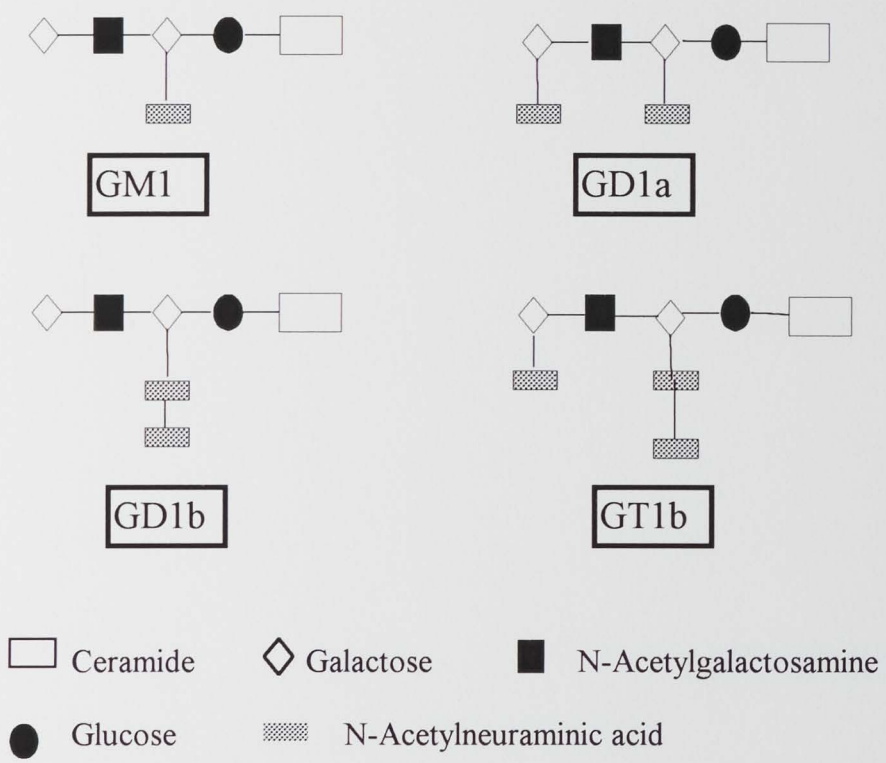

Figure 5. Schematic Diagrams: $LIGA_4$, $LIGA_{20}$, PKS_3 and LysoGM1

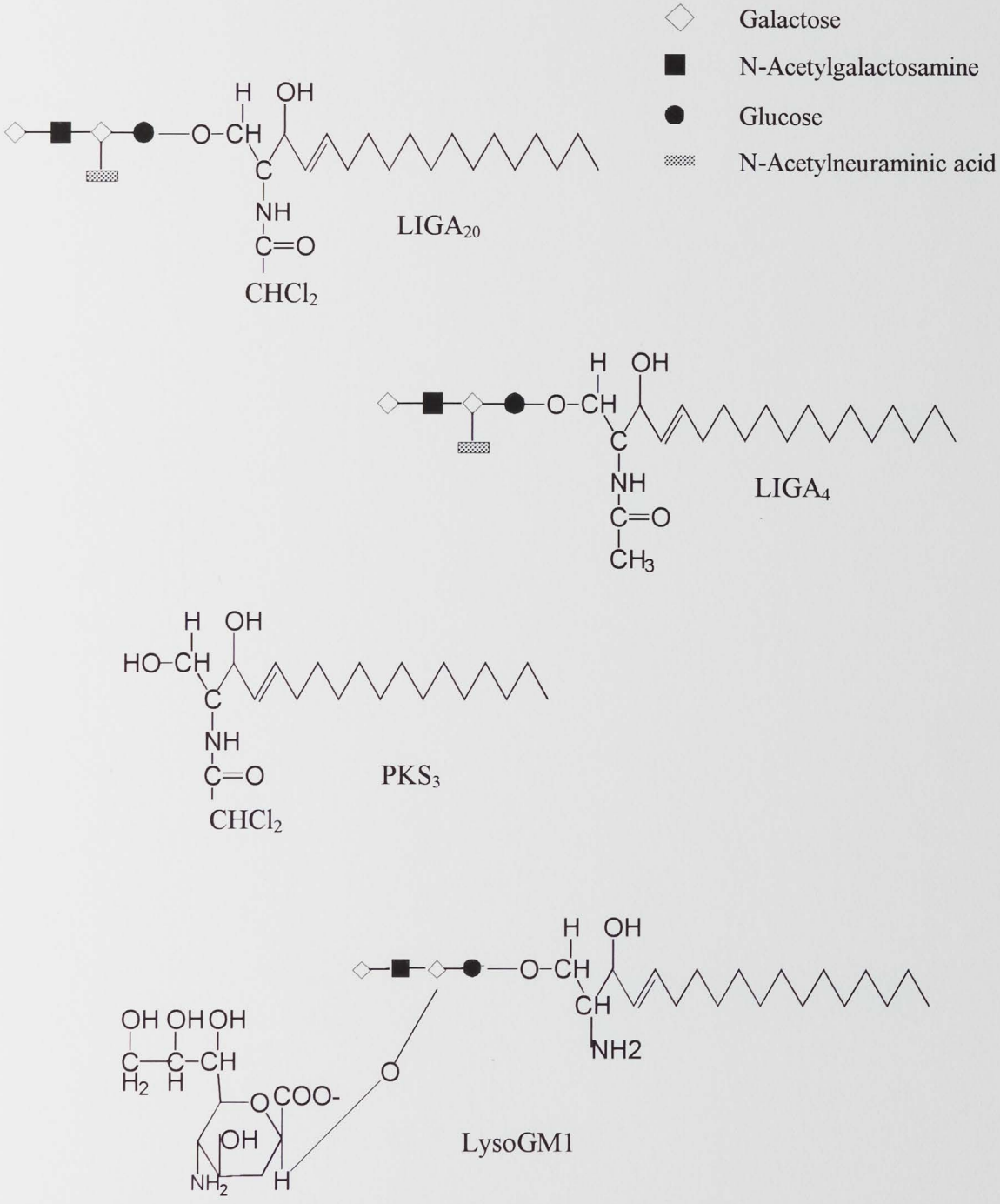

The ability of gangliosides to confer cytoprotection depends to a large extent on time of administration. In the three *in vitro* studies cited above, GM1 did not provide cytoprotection when administered after cell injury. However, in three *in vivo* studies (Figliomeni, Bacci et al. , 1992; Shifman, 1991; Seren, Rubini et al. , 1990) cytoprotection was observed even though the only neuronal exposure to exogenous ganglioside occurred post-injury. A report on ganglioside efficacy in diabetes (Figliomeni, Bacci et al. , 1992) is especially interesting. Animals were made diabetic by a single injection of streptozocin. Ganglioside or saline was administered i.p. daily for 1 month, with treatment beginning two or 17 weeks after injection. Both short-term and long-term diabetic rats showed improved axonal transport of cytoskeletal proteins (tubulin and actin) in sciatic nerve compared to controls. Improvement was more pronounced in animals exposed to ganglioside 2 weeks after injury than in animals treated 17 weeks after injury. This study illustrates several points: 1.) Gangliosides may be useful in conditions characterized by chronic neuronal damage of unknown origin. 2.) Gangliosides can be efficacious *in vivo*, even when administered a long time after neuronal injury. However, maximal benefit is achieved by early treatment. 3.) Multiple mechanisms of ganglioside cytoprotection may account for discrepancies between *in vivo* and *in vitro* results, with regard to time of drug administration.

3. Potential Mechanisms of Ganglioside Cytoprotection

The mechanism(s) of ganglioside cytoprotection is (are) unknown. For several reasons, there are likely to be multiple mechanisms involved. First, adult mammalian brain

contains over 90 different ganglioside species (Yu & Saito. 1989): this diversity undoubtedly reflects the functional requirements of cells. Secondly, the relevant "mechanism of action" is likely to depend on the type of injury involved (i.e., ischemic, mechanical, toxin-induced, etc.) and on whether the injury is acute or chronic (such as in diabetes or CNS neurodegenerative diseases). Furthermore, mechanisms of cytoprotection defined *in vitro* may not reflect the actual mechanism contributing to cell survival *in vivo*. For these reasons, identification of a single mechanism of action is unlikely.

Current thought on the mechanism of ganglioside cytoprotection is dominated by four hypotheses. These are that gangliosides 1.) are "receptor abuse dependent antagonists" (RADAs), as defined below 2.) exert cytoprotection by maintaining the structure and function of the plasma membrane 3.) provide cytoprotection by inhibiting nitric oxide formation (Dawson, Hung et al. , 1995) and 4.) confer cytoprotection by stimulating receptor kinases for trophic factors.

a. Receptor Abuse-Dependent Antagonism

Manev (Manev, Favaron et al. , 1990) coined the term "receptor abuse-dependent antagonists" to describe a new category of potential therapeutic agents. RADAs exert cytoprotection by antagonizing events occurring subsequent to ligand-receptor binding. By definition, only agents which do not bind the receptor of interest, can be classified as RADAs. RADAs inhibit the sequelae of abusive receptor stimulation, but do not alter physiologic signal transduction. Gangliosides are the only compounds currently assigned

to this class. Evidence in suppport of this hypothesis is contained within 5 reports (De Erausquin, Manev et al. , 1990; Manev, Favaron et al. , 1990; Manev, Favaron et al. , 1989; Favaron, Manev et al. , 1988; Vaccarino, Guidotti and Costa, 1987).

There is evidence that gangliosides confer cytoprotection against glutamate toxicity by attenuating a sustained glutamate-evoked translocation of protein kinase C (PKC) from the cytoplasm to the plasma membrane. The steps between PKC translocation and neuronal death have not been defined. Sustained PKC translocation is mediated by a delayed and prolonged elevation of intracellular calcium, evoked by toxic concentrations of glutamate. This action is believed to occur 1.) in the absence of ganglioside binding to glutamate receptors at transmitter binding sites 2.) without ganglioside interference in the operation of glutamate-operated cationic channels.

b. Ganglioside Protection of Plasma Membranes

Glutamate release during ischemia induces the opening of ionotropic NMDA receptors which are highly permeable to calcium. The resulting rise in intracellular calcium can lead to cell death via activation of phospholipases, causing the breakdown of membrane lipids and the release of free fatty acids. Calcium-dependent activation of phospholipase A_2 occurs during ischemia and anoxia (Nicotera, Bellomo and Orrenius, 1992). Phospholipase A_2 catalyzes the release of arachidonic acid from membrane phospholipids. Phospholipase C catalyzes the conversion of phosphatidylinositol 4,5-bisphosphate (PIP_2) into IP_3 and diacylglyerol. The loss of free fatty acids causes decreased membrane fluidity, which in turn, alters the function of ion channels, receptors and enzymes (Mahadik. 1992).

In a gerbil model of global ischemia, GM1 treatment increased membrane fatty acids (palmitic, stearic, oleic, linoleic, and arachidonic) in ischemic tissue, but not in non-ischemic tissue (Mahadik. 1992). This effect may be responsible for ganglioside protection against loss of membrane enzyme activity and maintenance of ionic homeostasis (Mahadik. 1992). Loss of Na^+/K^+ ATPase activity during ischemia is thought to result from a conformational change in the enzyme, due to the loss of membrane lipids (Karpiak, Mahadik and Wakade, 1990). GM1 treatment of gerbils after unilateral common carotid artery occlusion ameliorated the loss of Na^+/K^+ ATPase activity in cortical membranes (Karpiak, Li and Mahadik, 1986).

Gangliosides have been shown to reduce the availability of substrate for free radical generating reactions during ischemia (Mahadik, Hawver et al. , 1989), and to preserve levels of radical-metabolizing enzymes (Mahadik. 1992). Ganglioside treatment after focal ischemia attenuates the loss of membrane fatty acids, including arachidonic acid (Hungund, Gokhale et al. , 1990; Mahadik, Hawver et al. , 1989). Free radicals are generated from arachidonic acid during eicosanoid synthesis. Ganglioside preservation of arachidonic acid within plasma membranes limits eicosanoid synthesis, and the free radical generation which accompanies it. Ganglioside treatment prevents the increase in cyclooxygenase and lipoxgenase metabolites which occurs during ischemia/reperfusion injury (Petroni, Bertazzo et al. , 1989).

c. Inhibition of Nitric Oxide Formation

Gangliosides bind calmodulin (Higashi, Omori and Yamagata, 1992), and are able to modulate enzyme activity by binding to both calmodulin and a calmodulin-dependent enzyme (cyclic nucleotide phosphodiesterase (Higashi and Yamagata, 1992). As noted previously, glutamate toxicity is mediated by nitric oxide (Dawson, Dawson and London, 1991). Recently, evidence has been presented that gangliosides mitigate glutamate-induced toxicity by inhibiting nitric oxide synthase (NOS), a calmodulin-dependent enzyme (Dawson, Hung et al. , 1995). In cell homogenates, a series of gangliosides inhibited NOS with the same order of potency as for inhibition of cyclic nucleotide phosphodiesterase. The most potent ganglioside was GT1b. AsialoGM1 and GM3, did not bind calmodulin and did not inhibit NOS. The ability of GT1b to inhibit NOS activity was reversed by increasing concentrations of calmodulin. Three non-ganglioside, calmodulin-binding drugs were found to inhibit NOS to the extent of their ability to bind calmodulin. In human kidney 293 cells, (previously transfected with cDNA for NOS and stimulated by A23187), the order of potency established for ganglioside binding to calmodulin was the same as that established for inhibition of NOS. The order of potency generated for NOS inhibition in 293 cells agreed with that generated in cell homogenates. Finally, in primary cultures of rat cortical cells, the ability of a given ganglioside to attenuate NMDA toxicity corresponded to its ability to inhibit NOS.

d. Stimulation of receptor kinases for trophic factors

Gangliosides may exert cytoprotective effects by binding to receptor kinases for neurotropic factors such as NGF. This hypothesis is based on evidence that GM1 can potentiate the protective actions of NGF (Cuello, Garofalo et al. , 1989), attenuate injury arising from NGF depletion (Ferrari, Batistatou and Greene, 1993), and stimulate NGF-induced neurite outgrowth (Ferrari, Fabris and Gorio, 1983).

NGF binds to two receptor sites, trk A and p75, with high and low affinity, respectively (Ross, 1991). NGF stimulates the autophosphorylation of Trk A, and GM1 increases NGF-induced autophosphorylation (Whittemore, Loo and Cotman, 1995; Mutoh, Tokuda et al. , 1995). In the absence of NGF, GM1 stimulates autophosphorylation of Trk A, and phosphorylation of Trk A's protein targets (Mutoh, Tokuda et al. , 1995). GM1 binds to Trk A, but does not bind to similar receptors (Mutoh, Tokuda et al. , 1995).

F. A23187 and Aß

In view of the similarities between the ionophore A23187 and Aß, it may be useful to regard Aß as an ionophore. Both A23187 and Aß are able to elevate intracellular calcium and to form membrane pores (Arispe, Rojas and Pollard, 1993; Balasubramanian, Sikdar and Easwaran, 1992). Dihydropyridines, which block L-type calcium channels, attenuate Aß and A23187 toxicity (Matsuda, 1995; Weiss, Pike and Cotman, 1994). (The ability of dihydropyridines to attenuate Aß toxicity has been cited as evidence that Aß has an effect

on L-type calcium channels. In the case of A23187, dihydropyridines were shown to be protective effect in a model lacking voltage-gated calcium channels.) Finally, Vitamin E protects PC12 cells against Aß toxicity (Behl, Davis et al. , 1992), and inhibits the A23187-induced efflux of creatine kinase from skeletal muscle (Phoenix, Edwards and Jackson, 1991). Clearly, oxidative stress may be a component of A23187-induced injury, but such injury does not occur in the absence of extracellular calcium.

G. Goals of this Study

The literature contains reports of 1.) Aß-induced destabilization of calcium homeostasis and 2.) the involvement of free radicals in Aß-induced cell death. The present study was designed to determine whether overexpression of APP C-100 in a neuronal-like cell line had similar consequences for cell viability. Specifically, a major goal of this study was to evaluate the effect of APP C-100 overexpression on cell susceptibility to calcium and hydrogen peroxide toxicity. To test the hypothesis that APP C-100 expression destabilized calcium homeostasis, concentration response curves for the calcium ionophore, A23187 (calcimycin), were established in APP C-105-transfected PC12 cells and vector-transfected controls. Similarly, to determine whether APP C-100 overexpression influenced cell vulnerability to free radicals, concentration response curves for hydrogen peroxide were established in APP C-105-transfected PC12 cells and vector-transfected controls.

A second goal of this study was to determine whether the ganglioside GM1 offered protection against A23187-induced and hydrogen peroxide-induced injury. The literature contains many reports that GM1 protects cells from diverse toxic insults, both *in vitro* and *in vivo*. GM1 was shown to protect Neuro 2A cells from A23187 toxicity (Nakamura, Wu and Ledeen, 1992). We sought to confirm that GM1 also protected the PC12 cell line from A23187 toxicity, and to examine whether GM1 protected PC12 cells from hydrogen peroxide toxicity.

H. Characteristics of the Cell Line, PC12

APP C-105 was overexpressed in the neuronal-like cell line, PC12. The PC12 cell line is derived from a catecholamine-secreting tumor (pheochromocytoma) of rat adrenal medulla (Greene and Tischler, 1976). In the absence of nerve growth factor (NGF), PC12 cells retain a high degree of similarity to adrenal chromaffin cells and replicate continuously. The presence of NGF induces PC12 cells to enter a post-mitotic state, in which they assume many of the characteristics of sympathetic neurons. NGF-treated PC12 cells exhibit neurite outgrowth, prominent cytoskeletal development, the ability to generate action potentials, and increases in the number of sodium channels, cholinergic muscarinic receptors, and opiate receptors (Fujita, Lazarovici and Guroff, 1989; Greene and Tischler, 1982). A key difference between sympathetic neurons and PC12 cells is that, unlike sympathetic neurons, PC12 cells do not require the continuos presence of

NGF for survival. PC12 cells will survive in the absence of NGF, if maintained in serum-containing media, or in a serum-free media that has been supplemented appropriately (Rukenstein, Rydel and Greene, 1993).

I. APP C-100-transfected PC12 Cells

Yankner was the first to describe the NGF-induced death of APP C-100-transfected PC12 cells (Yankner, Dawes et al. , 1989). PC12 cells, and NIH-3T3 cells (a fibroblast-like cell line) were transfected with one of the following APP constructs: 1.) full length APP_{695} 2) the Aß fragment or 3.) a fragment extending from Aß to the carboxyl terminus (APP C-100). PC12 cells transfected with construct (3) died when induced to differentiate by NGF, but remained viable in the absence of NGF. In contrast, NIH-3T3 cells transfected with construct (3) did not differentiate, and did not die in the presence of NGF. Conditioned media from PC12 or NIH-3T3 clones transfected with construct (3) caused the death of non-transfected, NGF-treated PC12 cells. PC12 or NIH-3T3 cells transfected with constructs (1) or (2) survived in the presence of NGF.

In the present study, PC12 cells were stably transfected with a vector containing a DNA sequence encoding APP C-105, corresponding to construct (3) above (J. Wells, E. N. Rodgers Veterans Memorial Hospital, Bedford, MA). (A stably transfected clone is one that has incorporated one or more copies of a vector into its genome. Daughter cells inherit copies of the vector.) This fragment does not contain a signal peptide for protein

secretion. The promotor used in the present study (Moolten and Wells, 1993) differs from that used by Yankner. Stably-transfected clones were selected by their ability to grow in neomycin sulfate (G418). Since the modified NTK vector encoding APP C-105 contains a gene for neomycin resistance which is normally lacking in PC12 cells, the ability of a clone to grow in neomycin sulfate indicates that at least one copy of the vector has been incorporated into its genome. Neomycin-resistant clones were characterized by Southern, Northern and Western blotting. The latter studies provided evidence for the incorporation of vector-derived DNA in the PC12 genome (Southern blot), the production of mRNA corresponding to vector-derived DNA (Northern blot), and the actual production of aggregated APP C-105 (Western blots). Although APP C-105 overexpression was confirmed, it is not known whether vector-derived APP C-105 is inserted into the membrane.

II. METHODS

A. Materials

RPMI 1640 media, A23187, heat-inactivated horse serum, newborn calf serum, penicillin-streptomycin, bovine serum albumin, poly-d-lysine (molecular weight 70,000-150,000), MTT, insulin, and N,N,-dimethylformamide were purchased from Sigma Chemical Company, St. Louis, MO. Hydrogen peroxide was purchased from Fisher Scientific, Fair Lawn, NJ. Tissue culture plastics were obtained from Costar, Cambridge, MA. Lipofectant Reagent, G418 (neomycin sulfate), nerve growth factor and Proteinase K were purchased from Gibco BRL. Nitrocellulose (Hybond ECL) and the ECL Western Blotting Detection System (catalog # RPN 2109) were purchased from Amersham. Coomassie Brillant Blue G-250 and Mini-PROTEAN II Ready gels (catalog # 161-0903) were obtained from Biorad. Tri-Reagent™, a total RNA isolation reagent, was purchased from Molecular Research Center, Cincinnati, OH. Immobilon P was purchased from Millipore, Bedford, MA. ^{32}P-dCTP was purchased from Du Pont/New England Nuclear, Boston, MA. XAR film was acquired from Kodak. An oligolabelling kit was purchased from Pharmacia. Centriprep-3 concentrators were purchased from Amicon, Beverly, MA. Taq polymerase was purchased from Perkin Elmer, Norwalk, CT.

PC12 cells were the gift of G. Siek (PerSeptive Biosystems, Framingham, MA). J. Wells (E.N. Rodgers Veterans Memorial Hospital, Bedford, MA) produced the APP C-105-transfected PC12 cell lines. A polyclonal rabbit antibody to the carboxyl terminus

of APP, known as "C8", was the kind gift of D. Selkoe, Harvard Medical School. This antibody was raised against a synthetic peptide corresponding to amino acids 676-695 of APP_{695} (Proceedings of the National Academy of Sciences 85:7341 - 7345, 1988). Horseradish peroxidase (HRP)-conjugated goat anti-rabbit IgG (catalog # 611-1322) came from Rockland, Gilbertsville, PA. All other reagents were obtained from commercial sources and were of the highest possible quality.

B. Cell Maintenance

PC12 cells were grown in RPMI 1640 media, supplemented with 10% heat-inactivated horse serum, 5% newborn calf serum, 25 units/ml penicillin G and 25 μg/ml streptomycin. Flasks were pre-treated with 4 μg/ml poly-d-lysine to promote cell adhesion. The cells were maintained at 37°C, in an environment containing 5% CO_2.

C. Transfection of PC12 Cells with a Vector Containing DNA Sequence Corresponding to APP C-105

1. Construction of Vector

To provide a means of introducing APP C-105 into PC12 cells, a vector containing the DNA sequence corresponding to APP C-105 was constructed. The latter vector was made by modifying the retroviral vector, NTK (Moolten and Wells, 1993), originally

derived from the Moloney leukemia virus (Moolten and Wells, 1993). NTK includes a neomycin-resistance gene, driven by the long terminal repeat (LTR) promoter. It also includes the thymidine kinase (TK) gene and the TK promoter. The new vector was constructed by replacing NTK's thymidine kinase gene with a DNA fragment coding for the C-terminal 105 amino acids of APP. To remove the TK gene, the NTK vector was treated with Bgl II-Cla I. Then, a C-terminal fragment of human APP_{751} cDNA, (generated by digestion of APP_{751} cDNA with Bgl II-Cla I), was ligated to the vector. Constitutive expression of the C-terminal fragment is driven by the TK promoter. NTK's neomycin resistance gene permitted the selection of transfected clones in neomycin sulfate. Control cell lines were transfected with an unaltered NTK.

2. Establishment of Stable Cell Lines

Recipient PC12 cells were grown in flasks to 60-80% confluence. Ten to twenty micrograms of DNA were dissolved in 50 μl of water. To the DNA, 30-50 micrograms of Lipofectant Reagent in 50 μl of distilled water were added. The mixture was incubated for 15 minutes at room temperature. Meanwhile, the media was removed from flasks containing recipient PC12 cells, and the cells were rinsed in serum-free N2 media. To each flask, 3 ml of serum-free N2 media and 100 μl of the lipofectant mixture were added. The flasks were incubated at 37°C for 4-6 hours. RPMI media containing 15% serum was then added to the flasks, after which incubation continued for an additional 12-14 hours. Clones were selected by adding 400 μg/ml of G418 (neomycin sulfate) to the flasks for 2-

3 weeks, with media changes every 2-3 days. Resistant clones were subcloned and expanded.

D. Procedures for Characterization of APP C-105-transfected Cell Lines

1. Southern Blots

Genomic DNA was isolated from APP C-105-transfected and vector-transfected PC12 cell lines. A polymerase chain reaction (PCR) was performed using a 5'-3' primer for the TK promoter, a 3'-5' primer for the APP fragment, dNTPs, and Taq polymerase. The double-stranded PCR product was run on a 1% agarose gel. The gel was washed, then transferred to an Immobilon membrane. After washing, the Immobilon membrane was baked at 80°C for 1 hour in a vacuum oven. The membrane was probed with a ^{32}P-APP_{751} C-100 fragment (generated by digestion of APP_{751} with Bgl II-Cla I). The details of this procedure are given below.

a. DNA Isolation

Cell pellets were resuspended in a solution of 10 mM EDTA, 1% SDS, and 100 mM Tris, pH 8. Proteinase K was added to resuspended cells at a ratio of 100 μg Proteinase K per ml of suspension. Digestion was allowed to proceed overnight at 50°C. The solution was extracted with phenol, then spun at 1000 x g for 5 minutes. After separation of organic and aqueous phases, the aqueous phase was extracted with chloroform, and spun

at 1000 x g for 5 minutes. Again, organic and aqueous phases were separated, and the organic phase discarded. To precipitate DNA, 0.1 volume of 3 M sodium acetate and 2.5 volumes of cold ethanol were added to the aqueous phase. Precipitation was allowed to proceed overnight. Next, the precipated DNA was collected by centrifugation at 5000 x g for 15 minutes. The pellet was rinsed in cold, 70% ethanol and spun down again at 5000 x g for 5 minutes. Finally, the ethanol was discarded and the DNA pellet was resuspended in water. To determine the quantity and purity of each DNA preparation, absorbance was measured at 260 and 280 nm, as described in *Current Protocols in Molecular Biology* (1995).

b. PCR Amplification

PCR amplification was carried out using an instrument from Ericorp, Inc. Genomic DNA was subjected to boiling for 10 minutes at 100°C, then maintained at 50°C for up to 10 minutes. A reaction buffer was prepared consisting of 2 µl of 10X Taq buffer, 0.2 µg of a TK 5'-3' fragment (forward sequencing primer), 0.2 µg of APP_{751} C-105 3'-5' fragment (reverse sequencing primer), and 3.2 µl of each dNTP stock. (Each dNTP stock was 1.25 mM.) The final volume of the reaction buffer was adjusted to 10 µl. Ten µl of Reaction Buffer was added to each sample. The samples were subjected 25 - 30 cycles of amplification, each of which was designed as follows: 94°C for 15 seconds, 45°C for 20 seconds, 72°C for 40 seconds.

c. Gel Electrophoresis and Transfer of PCR Product to Membrane

A 1% agarose gel prepared as follows: 1% agarose was dissolved into 100 ml of 1X TAE by boiling. The warm agarose solution was poured into a horizontal mold (11 x 14 cm) and allowed to solidify for 1 hour. PCR products were added to sample wells, then electrophoresed in 1X TAE, at 100 volts, for 2 hours. The gel was washed in 0.05 N NaOH for 20 minutes, then in 0.5 M Tris/1.5 M NaCl for 20 minutes. Both washes were performed on a rotary shaker. A sponge was placed in a container of 20X SSC. Two pieces of Whatman 3MM paper and a piece of Immobilon membrane were cut to the size of the gel. The Whatman paper was soaked in distilled water. The Immobilon membrane was hydrated in 95% ethanol, then washed in distilled water to remove all traces of ethanol. The following items were placed, in order, on top of sponge: A piece of Whatman 3MM, the gel, the Immobilon P membrane, the second piece of Whatman 3MM paper. A stack of paper towels and a weight were placed on top of the transfer apparatus. Transfer was allowed to proceed overnight. After disassembly of the transfer apparatus, the Immobilon membrane was washed 2 - 3x in 2X SSC and allowed to dry for 5 minutes on a paper towel. The membrane was baked at 80°C for 1 hour in a vacuum oven, then stored at -20°C until further use.

d. Prehybridization

A prehybridization step was performed in order to block non-specific binding sites on the Immobilon membrane. Salmon sperm DNA was boiled for 10 minutes, then added to

10 ml of Hybridization Buffer, to a final concentration of 100 μg/ml. This buffer and the Immobilon membrane were placed in a plastic bag and prehybrization was allowed to proceed at 42°C for 2-6 hours.

Figure 6. Schematic Diagram of Modified NTK, the Plasmid Vector Used to Transfect PC12 Cells with the APP C-105 DNA Sequence

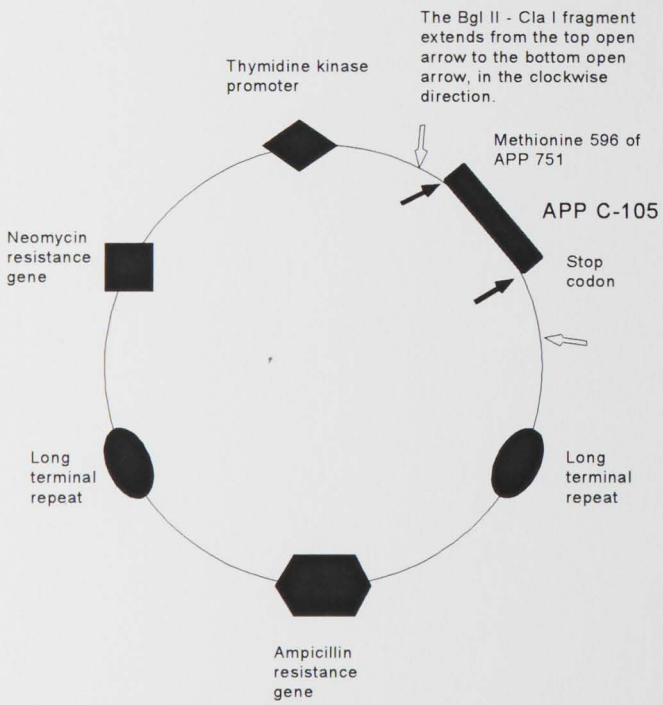

e. Labeling of DNA Probe Encoding APP C-105 with ^{32}P-dCTP

A DNA sequence encoding APP C-105 was labeled with radioactive phosphorous using ^{32}P-dCTP (Du Pont/NEN) and a commercial oligolabeling kit (Pharmacia). After labeling, the probe was run over a Sephadex G-50 column (2 cm x 1 cm bed), to remove unincorporated ^{32}P-dCTP. Both procedures were performed as described in the directions for the oligolabeling kit.

f. Hybridization of ^{32}P- DNA Probe to Membrane and Autoradiography

The ^{32}P- DNA probe was boiled for 10 minutes and then added to 25 ml of Hybridization Buffer. The pre-hybridization buffer (in which the Immobilon membrane had been incubated as described above) was discarded, and replaced by the ^{32}P- DNA probe contained in Hybridization Buffer. Hybridization was allowed to proceed overnight at 42°C. The labeled membrane was washed in a large beaker as follows:

Temperature	Wash Solution	Washing Protocol
Room temp.	2X SSC, 0.1% SDS	3X, 15 min./wash
60°C	2X SSC, 0.1% SDS	3X, 15 min./wash
60°C	0.2% SSC, 0.1% SDS	3X, 15 min./wash

Autoradiography was performed by exposing the blot to XAR film for 24 hours at -80° C.

g. Reagent Preparation

N2 media: DMEM/F12 medium containing 5 μg/ml insulin, 100 μg/ml human transferrin, 20 nM putrescine dihydrochloride, 30 nM sodium selenite, and antibiotic.

10X Taq Buffer: 50X Denhardt's, 5 g Ficoll, 5 g polyvinylpyrolidone, 5 g BSA (Fraction 5), H_2O to 500 ml

1X TAE: 0.04 M Tris Acetate, 0.001 M EDTA. Solution was adjusted to pH 8.

20X SSC: 3M NaCl, 0.3M sodium citrate

Hybrization Buffer: 6X SSC, 0.5% SDS, 5X Denhardt's, 50% formamide

2. Northern Blot

Total RNA was isolated from APP C-105-transfected and control PC12 cells, using Tri-Reagent™ according to the manufacturer's directions. RNA was applied to a 1% agarose gel as described above in Methods, Section D.1.c. The rest of the procedure was performed in the same manner as described above for Southern Blots.

3. Western Blots

a. Preparation of Cell Lysates

Cells were removed from flasks by pipeting and harvested by centrifugation at 500 x g. The media was discarded, then 5 ml of ice-cold phosphate buffered saline (PBS) was added to the pellet. After a second centrifugation, the PBS was discarded and the pellet was reconstituted in 200 μl of Wu Lysis Buffer. After addition of Wu Lysis Buffer, cell lysates were kept on ice until they could be transferred to Eppendorf tubes. Cell lysates

were spun at 4°C and 16,000 x g for 10 minutes. The supernatants were transferred to a second set of Eppendorf tubes, flash-frozen, then stored at -80°C. Prior to freezing, a 50 µl aliquot of each cell lysate was reserved (on ice) for determination of protein concentration.

b. Preparation of Conditioned Media

Cells were grown in RPMI media containing 15% serum. The serum-containing media was discarded. Cells were washed with RPMI media containing 3µM insulin, then allowed to grow in the latter media for 2 days. At this point, conditioned media was removed from the flasks and filtered through a 0.2 micron filter to remove cells and debris. Conditioned media was centrifuged 3x in an Amicon Centriprep 3 concentrator, with removal of filtrate after each spin. All spins were performed at 4° C and 3000 x g. Typically, the first spin was 3 hours, and the second and third spins were 1 hour.

c. Bradford Protein Assay

The Bradford protein assay was performed as described in *Current Protocols in Molecular Biology* (1995). A standard curve was constructed, then sample protein values were determined by interpolation. Comassie Blue Solution was prepared as follows: 100 mg of Coomassie Brilliant Blue G-250 was dissolved in 50 ml of ethanol (200 proof). One hundred milliliters of 85% phosphoric acid were added to the dissolved dye. The volume was brought to 1 liter with distilled water, then the solution was filtered through Whatman #1 paper. Next, a 5 mg/ml solution of BSA was prepared in water. A known

volume of sample, standard (12.5, 25, 50, 75, 100ug BSA) or 0.15 M NaCl (100 µl) was added to 13 x 11 mm glass tubes in duplicate. The volume in each tube was adjusted to 100 µl with 0.15 M NaCl. Five ml of Coomassie Blue Solution was added to each tube containing sample or standard. Tubes were incubated for 2 minutes at room temperature. Absorbance was read at 595 nm.

d. Conditions for Western Blotting

Samples were thawed quickly at 37°C, then immediately placed on ice. All samples were diluted to 3.4 µg protein/µl in Wu Lysis Buffer. Next, 29.2 µl of each sample was added to 5.8 µl of 6X Sample Buffer and boiled for 3 minutes. The entire volume of boiled sample (35 µl, i.e., 99.3 µg total protein) was added to the gel. Samples were electrophoresed on a 4- 20% polyacrylamide gradient minigel prepared in 0.375 M Tris-HCl pH 8.8 using 1X Running Buffer. Electrophoresis was performed at 200 volts for 1 hour. After electrophoresis, the gels were equilibrated for 20 minutes in Transfer Buffer. The gel was transferred to nitrocellulose. The blot was stored in cellophane at 4°C prior to immunoblotting. The blot was incubated in Blocking Buffer for 1 hour at room temperature, exposed to primary antibody for 1 hour at room temperature, then washed three times. ("C8" antibody was diluted 1:1200 in Blocking Buffer.) The washes were performed for 1.) 15 minutes in Wash Buffer 1 2.) 15 minutes in Wash Buffer 2, and 3.) 30 minutes in Wash Buffer 1. After washing, the blot was exposed to secondary antibody (HRP-conjugated antibody directed against rabbit IgG, diluted 1:5000 in Blocking Buffer)

for 1 hour. Finally, the blot was developed using the ECL Western Blotting Detection Kit according to the kit directions.

e. Reagent Preparation

PBS, pH 7.3: 137 mM NaCl, 2.7 mM KCl, 4.3 mM $Na_2HPO_4.7H_2O$, 1.4 mM KH_2PO_4

Wu Lysis Buffer: 300 μg/ml leupeptin, 1% Triton-X 100, 0.01% EDTA,1 mM PMSF in 50 mM Tris, pH 7.6.

6X Sample Buffer: 7 ml 4x Tris-HCl/SDS, pH 6.8, 3 ml glycerol, 1 g SDS, 0.93 g DTT, 1.2 mg bromophenol blue. Add water to 10 ml, store at -80°C.

5X Running Buffer: 124 mM Tris base, 0.5 M glycine, 5% SDS. pH should be 8.3. Do not adjust.

Transfer Buffer: 25 mM Tris base, 192 mM glycine, 20% (v/v) methanol, pH 8.3

Blocking Buffer: 5% Carnation powdered milk, 1.5% BSA, 0.01 M Tris, pH 8.0, 0.15 M NaCl, 0.05% Tween

Wash Buffer 1: 1% BSA, 0.01 M Tris, pH 8.0, 0.15 M NaCl, 0.05% Tween

Wash Buffer 2: 1% BSA, 0.01 M Tris, pH 8.0, 0.15 M NaCl, 0.05 % Tween, 0.1% Triton X-100

f. Densitometry

Scanning of films, from immunoblotting experiments, was performed by using a densitometer (Molecular Dynamics). Individual protein bands in the gels were scanned by volume integration. Background values were determined for each gel/film and were

subtracted from protein band readings to obtain corrected OD values of protein bands. The densitometry was performed under the guidance of Dr. Anil Amaratunga.

E. Experimental Protocol for Generation of Concentration Response Curves

Tissue culture plates were treated overnight, or for at least 3 hours, with 4 μg/ml of poly-d-lysine. Subsequently, plates were washed twice in sterile, distilled water. A23187 was reconstituted in DMSO to a concentration of 5 mM, aliquoted, and then stored at –80°C until needed. A cell suspension containing 30,000-40,000 cells/ml was prepared in RPMI media containing 15% serum. Aliquots (1 ml) of this suspension were dispensed into wells on a poly-d-lysine-coated tissue culture plate. After plating, cells were incubated overnight to permit cell adhesion to tissue culture plastic. The serum-containing media was removed from wells containing adherent cells, then the cells were washed with Hank's Buffer or serum-free RPMI media (i.e., RPMI media containing 3μM insulin). Cells were exposed to various concentrations of toxin (A23187 or hydrogen peroxide) prepared in serum-free RPMI media. All diluted A23187 solutions, and the negative control solution were adjusted to contain the same concentration of DMSO. A solution of 0.1% Triton X-100 in serum-free RPMI media was added to several wells (causing total cell death) in order to determine the background absorbance (i.e., blank). Cells were exposed to toxin for 22 hours at 37°C and 5% CO_2. After 22 hours, the MTT assay was performed as described below. In total, the cells were exposed to toxin for 24 hours. In

some experiments, cells were preincubated with GM1, or exposed to GM1 and a toxin concurrently.

F. MTT Cell Viability Assay

The MTT assay is based on the ability of living cells to cleave the ring structure of a colorless tetrazolium salt, [3-(4,5-dimethylthiazole-2-yl)-2-5, -diphenyl tetrazolium bromide; MTT] resulting in the formation of an insoluble, colored formazan. Formazan must be solubilized in order to obtain a homogeneous solution whose optical density can be measured. In the original assay described by Mosmann (Mosmann, 1983), formazan was solubilized in acidified isopropanol. After the addition of isopropanol, each sample required vigorous trituration, followed by spectrophometric analysis. Sample precision was unacceptable when the assay was performed in this manner, due to variability introduced during the mixing step. Trituration of samples was both time-consuming and labor-intensive. In addition, the precipitation of serum proteins by isopropanol precluded use of this assay when cells were bathed in serum-containing media.

A modified MTT assay has been described (Hansen, 1989). The assay calls for the addition of Extraction Buffer (described below) rather than isopropanol to samples, followed by an overnight incubation at 37°C. A mixing step is not required and acceptable precision is obtained. Precipitation of serum proteins does not occur in media containing less than 25% serum. Therefore, the modified MTT assay was adopted.

The modified assay is performed by adding 200 µl of MTT (500 mg/ml in phosphate buffer solution) to each well, followed by a 2 hour incubation at 37°C to allow dye incorporation. To solubilize the formazan, 1 ml of Extraction Buffer (20% W/V SDS in a 1:1 solution of N,N,dimethyl formamide/water, pH 4.7) is added to each well and the plate is incubated overnight. Finally, the amount of product is measured spectrophotometrically at 570 nm. The percentage of cells surviving at a given concentration of toxin was calculated as given below:

$$\% \text{ of control} = \frac{\text{MTT absorbance in the presence of toxin}}{\text{MTT absorbance in the absence of toxin (control)}} \times 100$$

The differential vulnerability of clones to hydrogen peroxide or A23187 was determined by plotting percent survival against toxin concentration.

G. Generation of Graphs and Statistical Analysis

Composite concentration response curves were established for each clone by plotting the mean of the average value (i.e., the percentage of cells surviving at a given concentration of toxin) obtained from each experiment vs toxin concentration. The data were plotted and subjected to regression analysis using SigmaPlot version 5.01 for DOS (Jandel Scientific, San Rafael, CA.). The 95% confidence limits of each regression line were

calculated. ANOVA was performed using the SigmaStat Statistical Analysis System version 1.02 for DOS (Jandel Scientific, San Rafael, CA.). P values ≤ 0.05 were regarded as significant.

III. RESULTS

A. Relationship Between Cell Number and the MTT Assay

When the modified MTT assay was performed as described under Methods, a linear relationship between MTT reduction (absorbance) and cell number was obtained (Figure 7). In one experiment, a PC12 cell suspension was prepared, and the number of cells/ml determined by trypan blue exclusion. Nine dilutions of this suspension were made, each containing 100-100,000 cells/ml. One milliliter of each dilution was plated into three wells on a tissue culture plate. The MTT assay was performed immediately. The data were subjected to linear regression, and the 95% confidence limits of the regression line (broken lines) were calculated. Error bars represent the standard deviation.

A linear relationship was also obtained in a second assay, using the APP C-105-transfected clone, BT108, and PC12 cells (Figure 8). Regression lines generated for the PC12 and BT108 clones have correlation coefficients of .999 and .991, respectively. The relationship between absorbance and cell number remained linear over a range of 5000-300,000 cells. In the latter assay, BT108 cells reduced more MTT per cell than PC12 cells. Comparison of the two assays shows that absorbance values can vary from day-to-day for a given number of PC12 cells (Figure 7 and Figure 8).

Figure 7. Linearity of the Modified MTT Assay

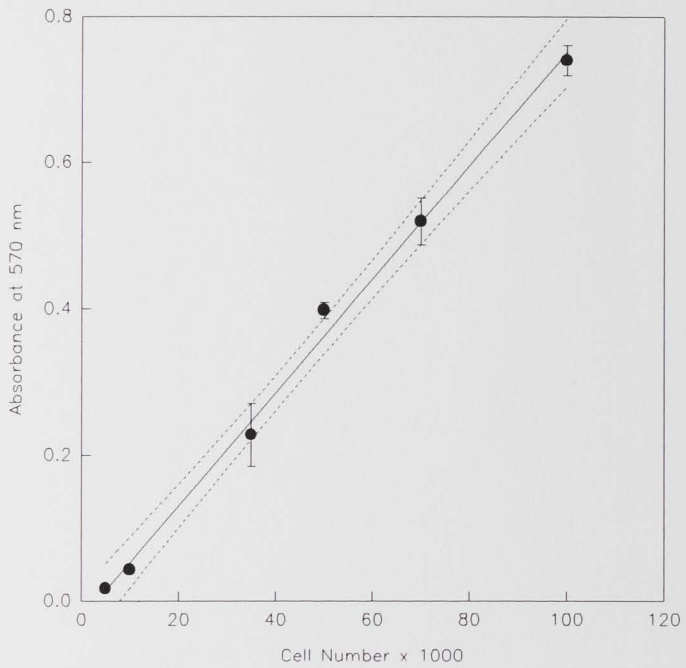

In one experiment, the number of cells per milliliter in a suspension of non-transfected PC12 cells was determined by trypan blue exclusion. Nine dilutions of this suspension were made. One milliliter of each dilution was plated into triplicate wells on a 24-well plate. The MTT assay was performed immediately. The data were subjected to linear regression. Dotted lines represent the 95% confidence limits of the regression line. Error bars represent the standard deviation.

Figure 8. Cell Number vs. Absorbance in the MTT Assay

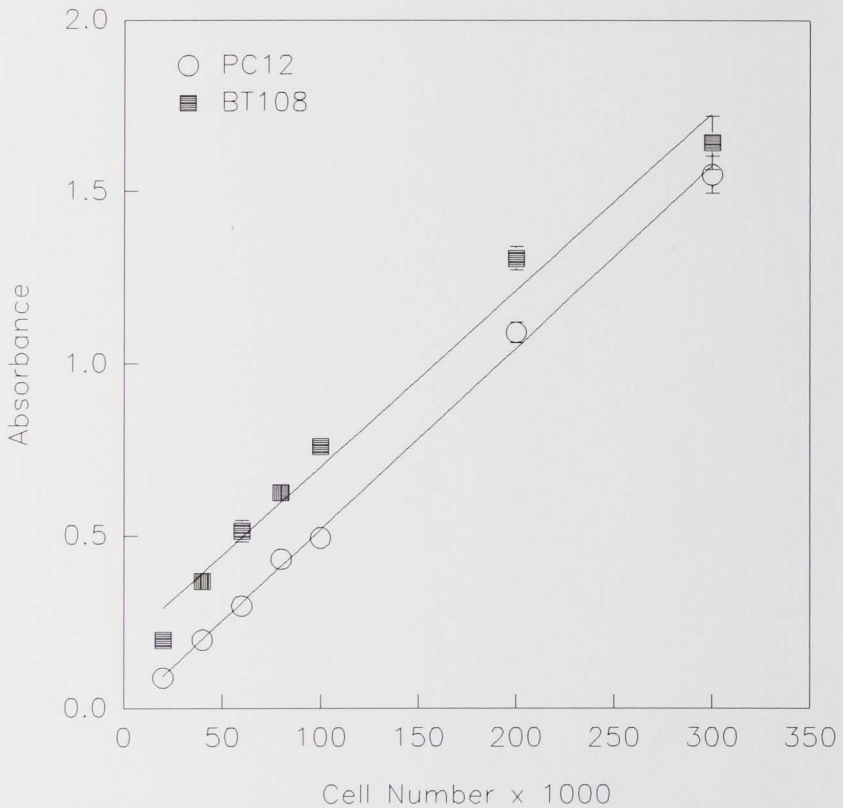

BT108 is an APP C-105-transfected clone.

B. Characterization of APP C-105-transfected Cell Lines

1. Southern Blot

APP C-105-transfected PC12 clones (BT108, BT111, ATF11) and wild type (non-transfected) PC12 cells were subjected to Southern analysis as described under Methods. As expected, the presence of DNA corresponding to APP C-105 was detected in APP C-105-transfected clones, but not in wild type (non-transfected) PC12 cells (Figure 9). This analysis was performed prior to the creation of the vector-transfected clones, PLNTK6 and PLNTK3; therefore, wild type PC12 cells were used as a control.

2. Northern Blot

APP C-105-transfected PC12 clones (BT111, BT110, ATF11) and wild type (non-transfected) PC12 cells were subjected to Northern analysis as described under Methods. Messenger RNA corresponding to APP C-105 was detected in APP C-105-transfected clones, but not in wild type PC12 cells (Figure 10).

3. Western Blots

Two Western blots were performed to verify the translation of the APP C-105 fragment into protein. For the first blot, *cell lysates* were prepared from APP C-105-transfected (BT111, BT108, BT110, ATF11), vector-transfected (PLNTK6), and wild type (non-transfected) PC12 cells (Figure 11). The lysates were probed with C8, an antibody which recognizes the carboxyl terminus of APP (APP $_{676\text{-}695}$). (C8 was obtained

from D. Selkoe.) Inspection of the blot does not reveal the existance of any remarkable differences between APP C-105-transfected clones and controls. However, densitometry shows that in comparison to controls, bands 3 and 4, with apparent molecular weights of 45,000 and 60,000 kD, are increased in all four APP C-105-transfected clones (Table 2).

A second Western blot was performed using *conditioned media,* rather than cell lysates (Figure 12). Using C8 antibody, three protein fragments containing the C-terminus of APP were detected in conditioned media from an APP C-105-transfected clone (BT111; Figure 12). The fragments have molecular weights ranging from 27,500- 42,400 kD and are **not** present in vector-transfected controls (PLNTK6) or non-transfected PC12 cells. APP C-105 has a molecular weight of approximately 11 kD. Therefore, the bands observed in conditioned media from the BT111 clone likely represent aggregates of APP C-105.

In conclusion, using an antibody directed against the C-terminus of APP, altered protein expression was observed in cell lysates and conditioned media from APP C-105-transfected clones.

4. Growth of APP C-105-transfected Clones and Controls

The growth of an APP C-105-transfected cell line (BT111) was compared to that of a vector-transfected control (PLNTK6) in one experiment. Cells were grown in serum-containing or serum-free media containing 3 μM insulin. Relative cell number (i.e., amount of MTT reduction) was determined at the time of plating (day 0) and on days 1, 3 and 4. The same number of BT111 and PLNTK6 cells were plated on day 0. Both

BT111 and PLNTK6 cells multiplied in the presence of serum-containing media, but BT111 cells grew at a faster rate than did controls. Control cells grown in RPMI media containing 3 μM insulin survived, but did not multiply. In contrast, BT111 cells multiplied in this medium.

5. Enhanced Survival of APP C-105-transfected Clones in the Absence of Insulin

PC12 cells survive in serum-containing media, or in several serum-free formulations to which one or more growth factors have been added (Rukenstein, Rydel and Greene, 1993). Specifically, PC12 cells are able to survive in serum-free RPMI media containing 3 μM insulin. PC12 cells incubated in serum-free, insulin-free RPMI media undergo apoptotic cell death due to growth factor deprivation (Greene, 1978). In one experiment, evidence was obtained indicating that APP C-105 expression increases the ability of PC12 cells to survive in the absence of growth factors, i.e., in the absence of serum and insulin (Figure 14). This experiment was performed due to a laboratory observation that vector-transfected clones seemed to die more readily when cells were washed briefly in Hank's buffer prior to incubation in RPMI containing 3 μM insulin. Since Hank's buffer does not contain serum or insulin, this observation suggested that APP C-105 expression decreased cell death due to growth factor deprivation.

Each test or control clone was dispensed into wells on a 24-well plate. The plating media (RPMI media containing 15% serum) was removed from all wells. Twelve wells on each plate were washed with RPMI media containing 3 μM insulin, then incubated in the

latter medium. The remaining wells were washed with Hanks Buffer, then incubated in serum-free, insulin-free RPMI media. After a 12-hour incubation, the MTT assay was performed. Cell survival in serum-free, insulin-free RPMI media was calculated as a percentage of cell survival in RPMI media containing 3 μM insulin. Two-way ANOVA indicated a significant difference in the mean values obtained for the three clones, after allowing for the presence or absence of insulin ($p < .001$). There was also a significant interaction between clonal type and insulin ($p \leq .001$). Pairwise comparisons were performed using the Student-Newman-Keuls Test. In serum-free, insulin-free media, the survival of BT108 and BT111 cells was significantly increased in comparison to control ($p \leq .05$). The latter finding must be confirmed by replication of this experiment.

Figure 9. Southern Blot of APP C-105-transfected Clones and Non-transfected PC12 Cells

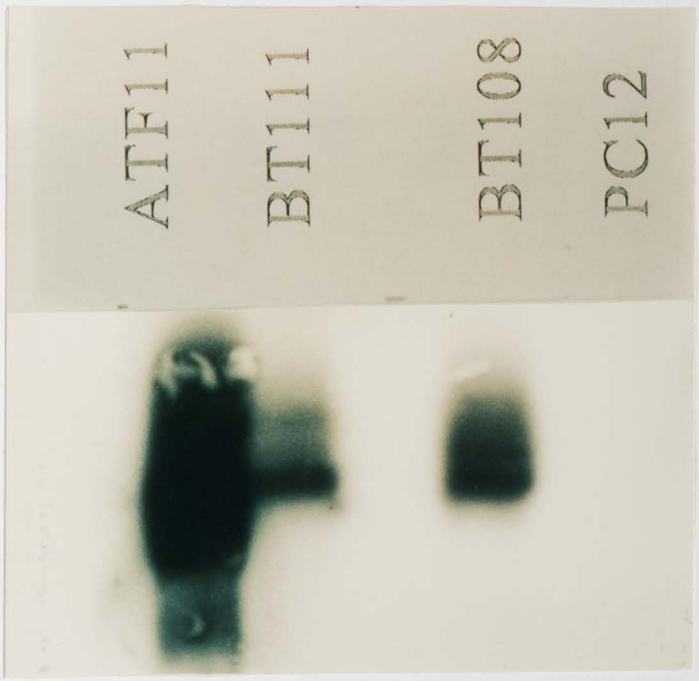

Genomic DNA was isolated from APP C-105-transfected clones (ATF11, BT111, and BT108) and vector-transfected PC12 cell lines. A polymerase chain reaction (PCR) was performed using a 5'-3' primer for the TK promoter, a 3'-5' primer for the APP C-105 fragment, dNTPs, and Taq polymerase. The double-stranded PCR product was run on a 1% agarose gel. The gel was washed, then transferred to an Immobilon membrane. After washing, the Immobilon membrane was baked at 80°C for 1 hour in a vacuum oven. The membrane was probed with a ^{32}P-APP_{751} C-100 fragment (generated by digestion of APP_{751} with Bgl II-Cla I). Autoradiography was performed by exposing the membrane to XAR film for 24 hours at -80° C. Details of this procedure are as described under Methods.

Figure 10. Northern Blot of APP C-105-transfected Clones and Non-transfected PC12 Cells

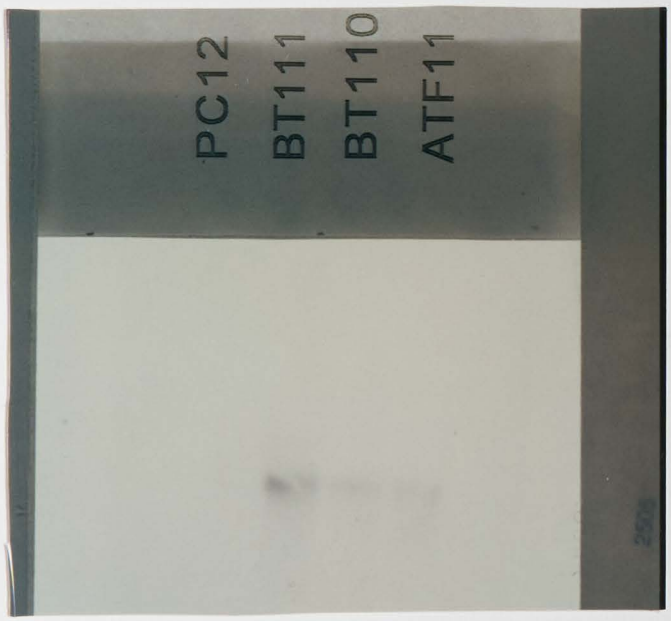

Total RNA, isolated from APP C-105-transfected clones (BT111, BT110, ATF11) and non-transfected PC12 cells, was applied to a 1% agarose gel. The gel was washed, then transferred to an Immobilon membrane. After washing, the Immobilon membrane was baked at 80°C for 1 hour in a vacuum oven. The membrane was probed with a ^{32}P-APP_{751} C-100 fragment (generated by digestion of APP_{751} with Bgl II-Cla I). Autoradiography was performed by exposing the membrane to XAR film for 24 hours at -80°C.

Figure 11. Western Blot of Cell Lysates, Using an Antibody Directed Against the C-terminus of APP

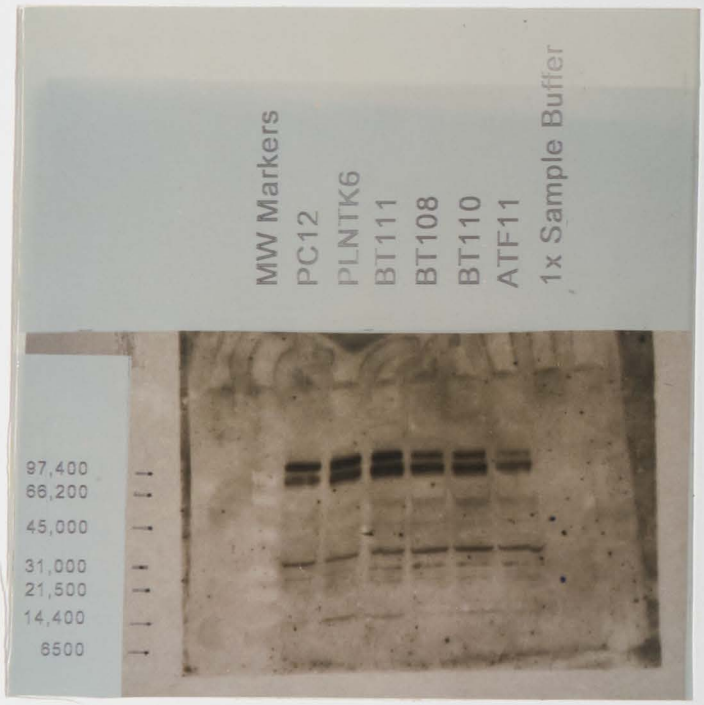

ATF11, BT110, BT111, BT108 are APP C-105-transfected clones. PLNTK6 is a vector-transfected control. Non-transfected PC12 cells were used as an additional control. Cell lysates were electrophoresed on a 4- 20% polyacrylamide gradient minigel, transferred to nitrocellulose, washed, then probed with C8, an antibody to APP $_{676\text{-}695}$. After further washing, the nitrocellulose membrane was exposed to an HRP-conjugated antibody directed against rabbit IgG. The blot was developed using the ECL Western Blotting Detection Kit.

Table 2. Densitometric Analysis of a Western Blot: Examination of Cell Lysates Using An Antibody Directed Against the C-terminus of APP

Percent of Controls				
Band	BT111	BT108	BT110	ATF11
1	106.6	111.9	103.6	133.5
2	110.8	99.7	103.5	82.0
3	**134.9**	**129.8**	**176.6**	**135.5**
4	**142.9**	**128.7**	**128.9**	**115.5**
5	105.0	107.1	115.5	107.6
6	99.3	92.9	90.8	94.2
7	112.8	97.3	93.2	113.8
8	102.8	55.5	75.8	94.1

A Western blot was subjected to densitometric analysis. Eight bands were quantified for each clone. Bands are listed in order of molecular weight, with band 1 having the highest molecular weight band seen on the blot, and band 8 the lowest. Data were obtained in four APP C-105 transfected clones (BT111, BT108, BT110 and ATF11) and in two control clones, wild type (non-transfected) PC12 cells and the vector-transfected clone, PLNTK6. The raw number for each band in an APP C-100-transfected clone was divided by the average of the band data for the two control clones, then multiplied by 100.

Figure 12. Western Blot of a Conditioned Medium, Using an Antibody Directed Against the C-terminus of APP

BT111is an APP C-105-transfected clone. The vector-transfected clone, PLNTK6, and wild type (non-transfected) PC12 cells were used as controls. Conditioned media were electrophoresed on a 4 - 20% polyacrylamide gradient minigel, transferred to nitrocellulose, washed, then probed with C8, an antibody to APP $_{676\text{-}695}$. After further washing, the nitrocellulose membrane was exposed to an HRP-conjugated antibody directed against rabbit IgG. The blot was developed using the ECL Western Blotting Detection Kit. Three faint bands (with molecular weights ranging from 27,500- 42,400 kD) appear in the APP C-105-transfected clone, BT111, but are absent from controls.

Table 3. Densitometric Analysis of a Western Blot: Examination of Cell Lysates Using an Antibody Directed Against the C-terminus of APP

Percent of Controls	
Band	BT111
1	131.1
2	120.6
3	126.1

A Western blot was subjected to densitometric analysis. Data were obtained in the APP C-105 transfected clone, BT111, and in two control clones, wild type (non-transfected) PC12 cells and the vector-transfected clone, PLNTK6. Three bands were quantified for the BT111 clone, and three areas corresponding to these bands were quantified in the two control clones. (Bands are visible in the lane for the BT111 clone only.) Bands are listed in the order of molecular weight, with band 1 having the highest molecular weight seen on the blot, and band 3 the lowest. The raw number obtained for each BT111 band was divided by the average of the data obtained for the two controls, then multiplied by 100. However, due to high non-specific binding in the PLNTK6 lane for the area corresponding to BT111 band 1, the BT111 band 1 value was divided by the value obtained for the corresponding area in the PC12 lane.

Figure 13. Clonal Growth in RPMI Media Containing 15% Serum or 3 μM Insulin

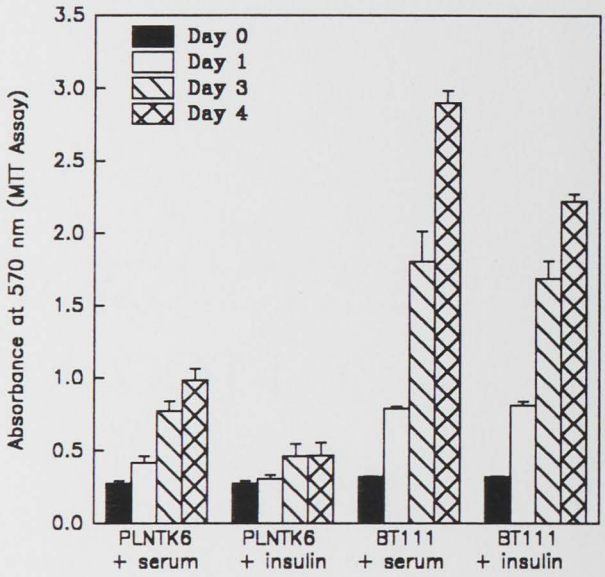

BT111 is an APP C-105-transfected clone and PLNTK6 is a vector-transfected control. In one experiment, clonal growth in RPMI media containing 15% serum was compared to that in serum-free RPMI media containing 3 μM insulin. The MTT assay was performed on days 0, 1, 3 and 4. Error bars represent the standard deviation of triplicate determinations. Both APP C-105-transfected cells and controls multiplied in serum-containing RPMI media, but the former grew at a faster rate. Controls survived but did not multiply when grown in serum-free RPMI media containing 3 μM insulin. In contrast, APP C-105-transfected cells divided in the absence of serum.

Figure 14. The Effect of APP C-105 Expression on Cell Survival in the Absence of a Growth Factor

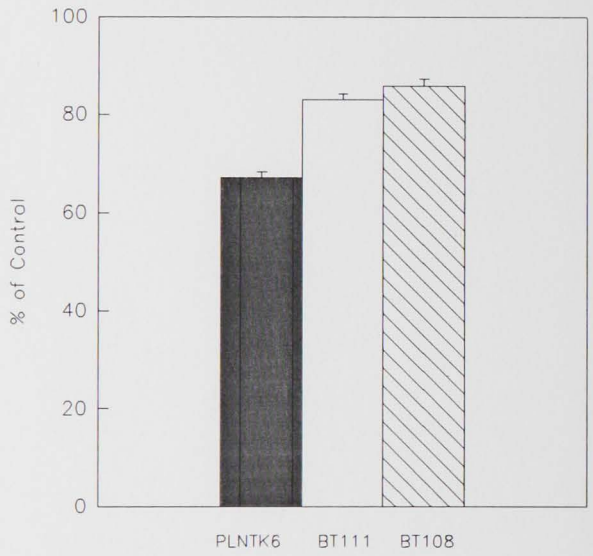

BT111 and BT108 are APP C-105-transfected clones. PLNTK6 is a vector-transfected control. In one experiment, cells were plated in RPMI media containing 15% serum, washed, then grown in RPMI media containing 3 μM insulin or in serum-free, insulin-free RPMI media for 12 hours. PC12 cells grown in serum-free, insulin-free RPMI media undergo apoptotic cell death due to growth factor deprivation (Rukenstein, Rydel and Greene, 1993). Clonal survival in serum-free, insulin-free RPMI media was calculated as a percentage of clonal survival in RPMI media containing 3 μM insulin (control). In comparison to controls, APP C-105 transfected clones are resistant to growth factor deprivation.

C. NGF-Induced Death of APP C-105-transfected Clones

When treated with NGF, wild type PC12 cells assume many of the characteristics of sympathetic neurons. In contrast, NGF treatment causes the death of APP C-100-transfected PC12 cells when the latter are grown in a serum-containing medium. The latter response is critically dependent on the presence of the C-terminus of APP (Yankner, Dawes et al. , 1989). In five experiments, the APP C-105-transfected clones produced in this laboratory were treated with NGF to gather evidence supporting or refuting the proposition that successful transfection had occurred (Figure 15 - Figure 19). Two of these experiments were performed in serum-free media (Figure 15, Figure 16) and three were performed in serum-containing media (Figure 17, Figure 18, Figure 19).

The following protocol was used for experiments performed in *serum-free media*: Cells were plated in RPMI media containing 15% serum and were allowed to incubate overnight. The following day (day 0), the plating media was removed, and the cells were washed with Hanks Buffer to remove any traces of serum. The plating media was replaced by RPMI media containing 1 μM insulin, or RPMI media containing 1 μM insulin and 50 ng/ml of NGF. The cells were maintained until day 6, when the MTT assay was performed. Cell number did *not* decrease in any of the four APP C-105-transfected cell lines tested. (Data for BT111 and BT110 clones appear in Figure 15. Data for BT108 and ATF11 clones are shown in Figure 16.) In fact, NGF-treatment increased cell number in both controls and APP C-105-transfected cell lines.

Different results were obtained when APP C-105-transfected cells were treated with NGF in the presence of *serum-containing media* (Figure 17, Figure 18, Figure 19). In the first experiment, an APP C-105-transfected clone (ATF11) and control (non-transfected PC12 cells) were grown in serum-containing media for six days, in the presence or absence of NGF (Figure 17). On day 6, the MTT assay was performed. ANOVA revealed a significant difference between APP C-105-transfected cells and controls ($p < .001$), and an interaction between clonal type and the presence of NGF ($p < .001$). Pairwise comparisons were performed using the Student-Newman-Keuls Test. The latter analysis indicated the existence of a statistically significant decrease in the number of ATF11 cells in the presence of NGF. No change occurred in the number of non-transfected PC12 cells.

In the second experiment, an APP C-105-transfected clone (BT111) and a vector-transfected control (PLNTK6) were exposed to NGF in serum-containing media for 5, 6 or 7 days before the MTT assay was performed (Figure 18). ANOVA revealed a significant difference between BT111 cells and controls ($p=.005$), and an interaction between clonal type and length of NGF treatment ($p<.001$). Pairwise comparisons were performed using the Student-Newman-Keuls Test. This analysis indicated that the number of control cells increased significantly on day 7, in comparison to day 5 ($p<.05$). In contrast, the number of BT111 cells was significantly reduced on day 6 in comparison to day 5 ($p<.05$), and on day 7 in comparison to day 6 ($p<.05$).

In the third experiment, three APP C-105-transfected clones (ATF11, BT111, and BT108) and controls (non-transfected PC12 cells) were exposed to NGF in serum-containing media (Figure 19). The MTT assay was performed on days 0, 1, 3 and 4. Two-way ANOVA was performed using data generated in the four clones on days 3 and 4. An interaction occurred between clonal type and days of NGF treatment ($p=.001$). A significant difference among clones was identified, after allowing for differences in the length of NGF treatment ($p=.042$). Similarly, a significant difference between days 3 and 4 was found, after allowing for the effect of clonal type ($p<.001$). Pairwise comparisons were performed using the Student-Newman-Keuls Test. The latter analysis revealed that PC12 cell number was significantly increased on day 4, in comparison to day 3 ($p<.05$). The number of BT111 cells and ATF11 cells did not change significantly on day 4 in comparison to day 3. There was a significant increase in BT108 cell number on day 4 in comparison to day 3 ($p<.05$). However, this increase was smaller than the increase which occurred in control cells. Clearly, in APP C-105-transfected clones, the rate of increase in cell number is slowed by treatment of cells with NGF in a serum-containing medium. Theoretically, the latter decline in rate could be due to a slowdown in cell replication. However, microscopic observations indicate that NGF treatment induces cell death. The MTT result indicate that more than four days of NGF treatment are required for the rate of cell death to exceed the rate of cell replication. Comparison of Figures 17 and 18 to Figure 19 shows that NGF-induced toxicity requires 6 days to become manifest in APP C-105-transfected clones.

In conclusion, the results of three experiments indicate that APP C-105-transfected cells die when treated with NGF in the presence of serum-containing media for six days.

Figure 15. NGF Does Not Induce the Death of APP C-105-transfected clones in Serum-free Medium

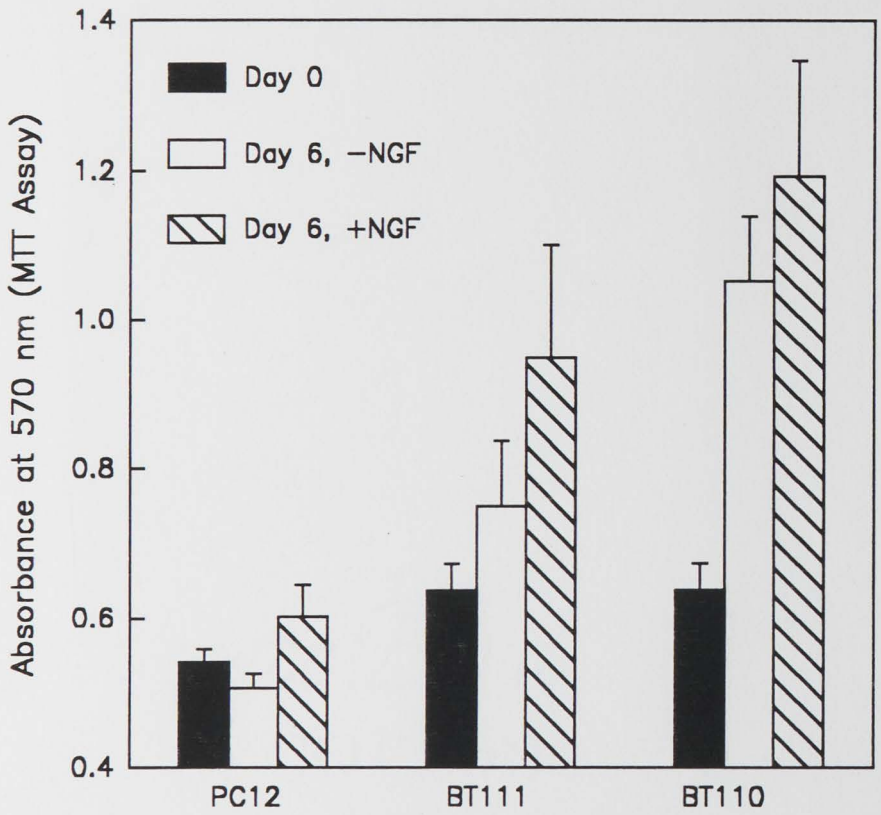

The APP C-105-transfected clones, BT111 and BT110, and non-transfected PC12 cells (controls) were plated at the same cell density. Cells were exposed to NGF in serum-free RPMI media containing 1 μM insulin, or to the same media without NGF, for 6 days. MTT absorbance was measured on the day of plating (Day 0) and on Day 6. APP C-105-transfected clones and controls exhibited an increase in cell number when exposed to NGF in serum-free RPMI media containing 1 μM insulin.

Figure 16. NGF Does Not Induce the Death of APP C-105-transfected Clones in Serum-free Medium

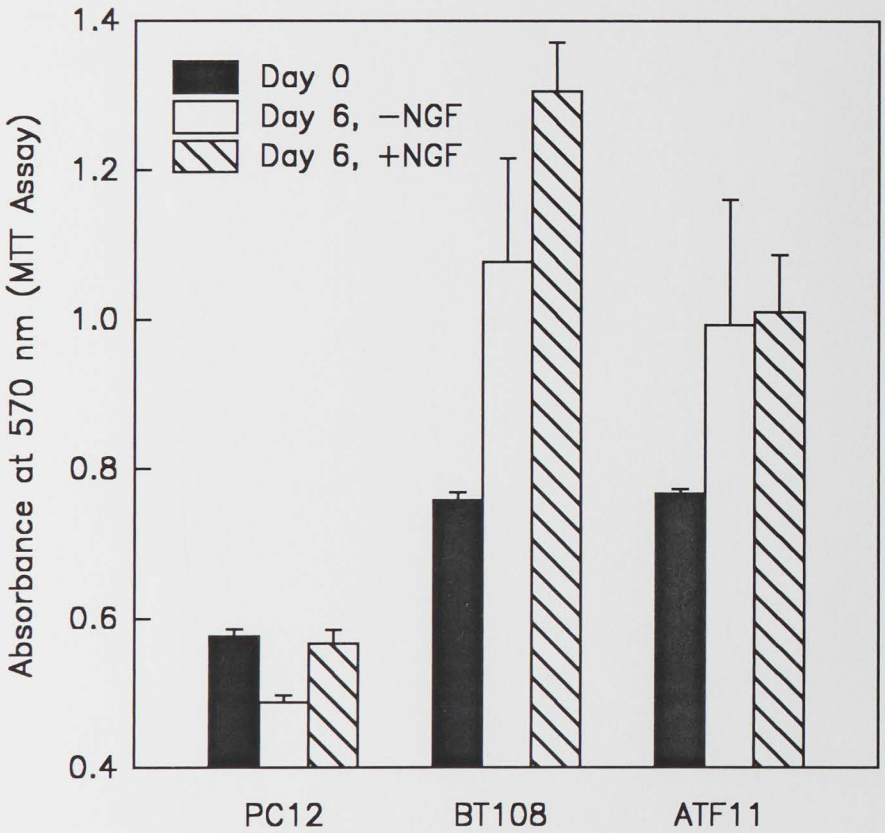

The APP C-105-transfected clones, BT108 and ATF11, and wild type PC12 cells (non-transfected controls) were plated at the same cell density. Cells were exposed to NGF in serum-free RPMI medium containing 1 μM insulin, or to the same medium without NGF, for 6 days. MTT reduction (absorbance) was measured on the day of plating (Day 0) and on Day 6. Cell number did not decrease when APP C-105-transfected clones were exposed to NGF in serum-free RPMI medium containing 1 μM insulin.

Figure 17. In the Presence of a Serum-containing Medium, NGF Induces a Reduction in Cell Number in an APP C-105-transfected Clone: Experiment 1

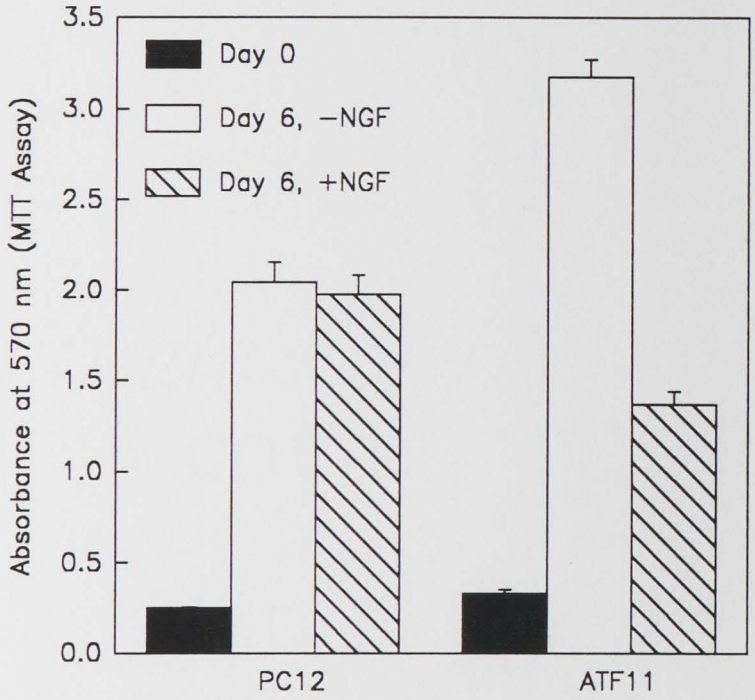

The APP C-105-transfected clone, ATF11, and wild type PC12 cells (non-transfected controls) were plated at the same cell density. Cells were exposed to NGF in RPMI media containing 15% serum, or to the same medium without NGF, for 6 days. MTTreduction was quantitated on the day of plating (Day 0) and on Day 6. Wild type PC12 cells replicated to roughly the same extent in the presence or absence of NGF. ATF11 cells replicated faster than wild type PC12 cells in the absence of nerve growth factor, suggesting that APP C-105 expression promotes cell replication. After 6 days of NGF treatment, fewer ATF11 cells were present than wild type PC12 cells.

Figure 18. NGF Induces Death of APP C-105-transfected Cells in Serum-containing Medium: Experiment 2

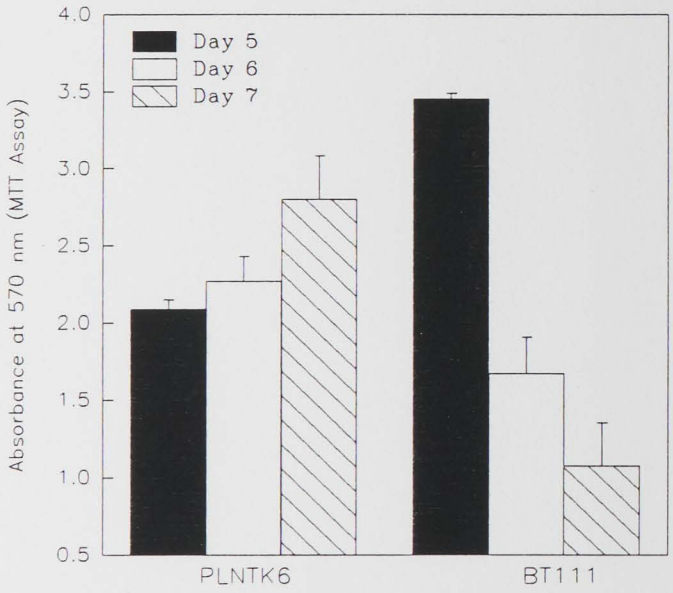

The APP C-105-transfected clone, BT111, and wild type PC12 cells (non-transfected controls) were plated at the same cell density. Cells were exposed to NGF in RPMI medium containing 15% serum. The MTT assay was performed on days 5, 6 and 7. APP C-105-transfected clones died when exposed to NGF in serum-containing RPMI medium.

Figure 19. In APP C-105-transfected Clones, the Rate of Increase in MTT Reduction Between Days 3 and 4 is Slowed by Treatment with NGF in a Serum-containing Medium: Experiment 3

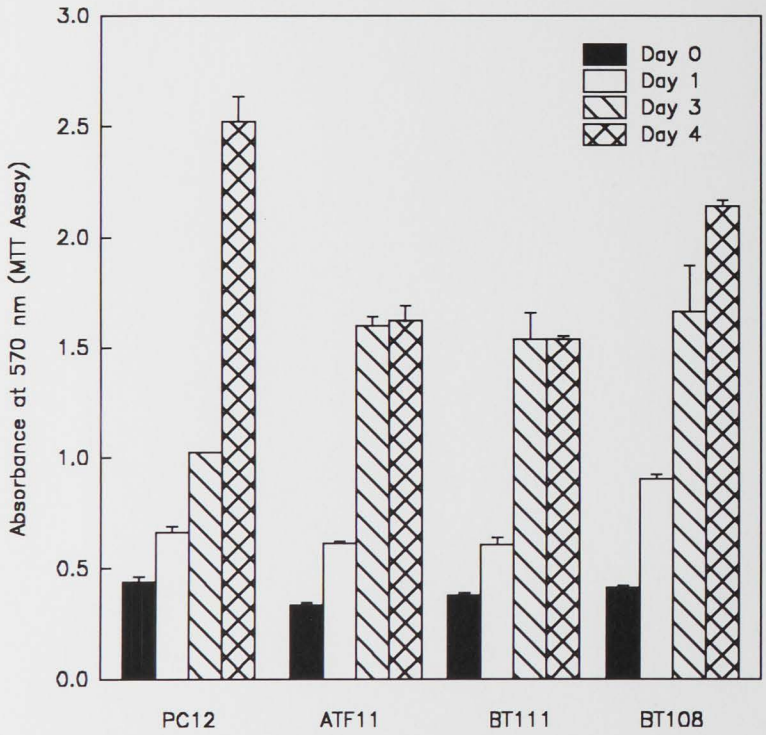

The APP C-105-transfected clones, ATF11, BT111, and BT108 and wild type PC12 cells (non-transfected controls) were exposed to NGF for four days in RPMI media containing 15% serum. MTT reduction (absorbance) was measured on day 0 (the day of plating) and on days 1, 3 and 4. Significant differences in MTTreduction were observed for APP C-105-tranfected clones and controls on days 3 and 4. See text.

D. Toxicity of A23187 in APP C-105-transfected Clones and Controls

To determine whether APP C-105 expression enhances PC12 cell susceptibility to calcium-induced injury, experiments designed to produce concentration response curves for the calcium ionophore A23187 were performed. Concentration response curves for A23187 were obtained in two APP C-105-transfected clones (BT108, BT111) and a vector-transfected control (PLNTK6). (These data appear in Figure 20 and Figure 21. For the sake of clarity, the same data for the PLNTK6 clone are presented in both figures.) Data were obtained for five A23187 concentrations ranging from 0.25- 5 μM. Different regression lines were generated for BT108 and PLNTK6 clones, indicating an enhanced susceptibility of the BT108 clone to A23187 toxicity. The 95% confidence limits of the two regression lines did not overlap, suggesting that a real difference exists. By the same analysis, the sensitivity of the BT111 clone was not significantly different from that of control (Figure 21). The regression coefficients and the correlation coefficient of each composite concentration curve, and the EC_{50} for A23187 obtained in each clone are shown in Table 4. Data for the PLNTK6, BT111 and BT108 clones were produced in 5, 6 and 4 experiments, respectively. In one experiment, a concentration response curve was obtained for the vector-transfected clone, PLNTK3, rather than for the PLNTK6 clone. This was done to permit data collection for an APP C-100-transfected clone, since the PLNTK6 clone was temporarily unavailable. (Data for the PLNTK3 clone are not shown.)

In summary, the data indicate that the BT108 clone is significantly more susceptible to A23187-induced injury than control. The sensitivity of the BT111 clone to A23187-induced toxicity is not statistically different from that of control.

Table 4. Values Derived from Composite Concentration Response Curves for A23187

	PLNTK6	BT108	BT111
$ß_0$ (intercept)	45.8	21.8	29.9
$ß_1$ (slope)	-49.0	-31.7	-46.8
Correlation coefficient	.981	.990	.964
EC_{50} for A23187 (μM)	0.9	0.15	0.4

Table 4 shows regression equations, correlation coefficients and EC_{50} values derived from composite concentration response curves for A23187. BT111 and BT108 are APP C-105-transfected clones; PLNTK6 is a vector-transfected control.

Figure 20. Concentration Response Curves for A23187 in an APP C-105-transfected Clone and a Vector-transfected Control

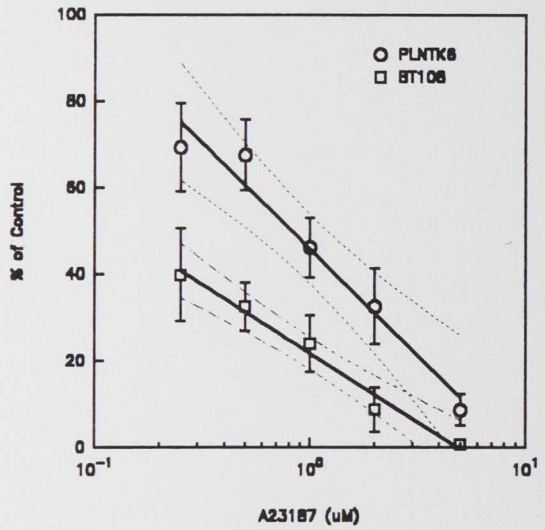

The cytotoxicity of A23187 was quantitated using the MTT assay. PLNTK6 is a vector-transfected control and BT108 is an APP C-105-transfected clone. Data obtained in five (PLNTK6) or four (BT108) experiments were averaged to produce a composite concentration response curve for each clone, which was subjected to linear regression. Broken lines indicate the 95% confidence limits of each regression line. Error bars represent the standard error. The regression coefficients and the correlation coefficient of each composite concentration response curve, and the EC_{50} for A23187 in each clone appear in Table 4. Since the 95% confidence limits of the regression lines for the BT108 and PLNTK6 clones do not overlap, it can be concluded that the BT108 clone is more vulnerable to A23187 toxicity than control.

Figure 21. Concentration Response Curves for A23187 in an APP C-105-transfected Clone and a Vector-transfected Control

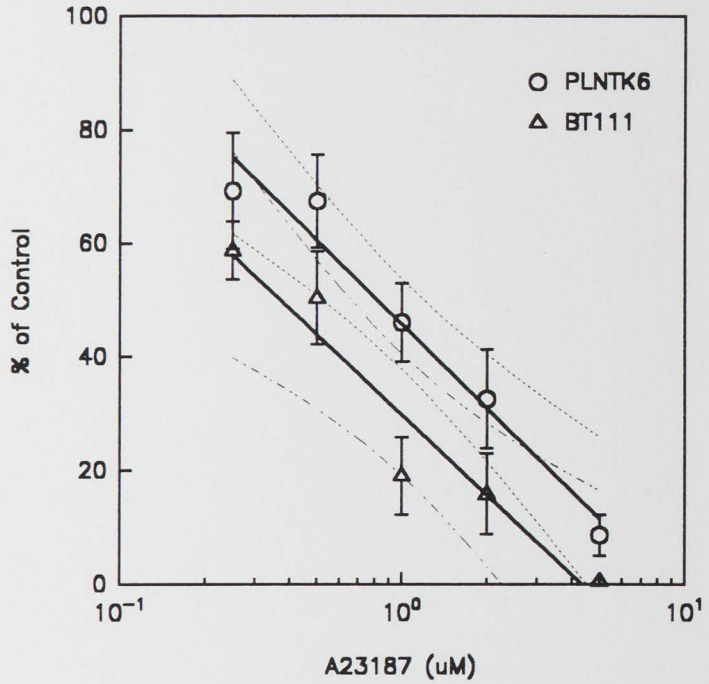

The cytotoxicity of A23187 was quantitated using the MTT assay. PLNTK6 is a vector-transfected control and BT111 is an APP C-105-transfected clone. Data obtained in five (PLNTK6) or six (BT111) experiments were averaged to produce a composite concentration response curve for each clone, which was subjected to linear regression. Broken lines indicate the 95% confidence limits of each regression line. Error bars represent the standard error. The regression coefficients and the correlation coefficient of each composite concentration response curve, and the EC_{50} for A23187 in each clone appear in Table 4. Since the 95% confidence limits of the regression lines for the BT111 and PLNTK6 clones overlap, it can not be concluded that the BT111 clone is more vulnerable to A23187 toxicity than control.

E. Toxicity of Hydrogen Peroxide in APP C-105-transfected Clones and Controls

The percentage of cells killed by a given dose of hydrogen peroxide is dependent on the number of cells exposed, i.e., hydrogen peroxide toxicity decreases with increasing cell number (Watson, Askew and Sandle, 1994). The latter finding was verified in one experiment in which PC12 cells were plated at densities ranging from 40,000 - 160,000 cells/ml, then exposed to 10 μM hydrogen peroxide (Figure 22). Therefore, an effort was made to ensure that APP C-105-transfected clones and controls were present at the same cell density in experiments designed to assess relative vulnerability to hydrogen peroxide.

Concentration response curves (Figure 23) for hydrogen peroxide were generated in three APP C-105-transfected clones (BT111, BT108 and BT110) and two vector-transfected control clones (PLNTK6 and PLNTK3). Cells were exposed to hydrogen peroxide in RPMI containing 3 μM insulin or to the same medium without hydrogen peroxide (control) for 24 hours. Cell survival at each concentration of hydrogen peroxide was calculated as a percentage of cell survival in the absence of hydrogen peroxide (i.e., RPMI containing 3 μM insulin only). Data were obtained for hydrogen peroxide concentrations ranging from 5-50 μM. Composite curves for each clone were constructed using data produced in three (PLNTK6, PLNTK3, BT110) or six (BT111, BT108) experiments. Identical data for the PLNTK6 clone are presented in three figures: Figure 23, Figure 24,

and Figure 25. APP C-105 overexpression increased resistance to hydrogen peroxide to a large extent in two clones (BT108, BT110; Figure 24) and to a smaller extent in a third (BT111) (Figure 25).

The data for the BT111 clone are marked by large standard errors occurring at multiple concentrations of hydrogen peroxide. In some assays, BT111 sensitivity to hydrogen peroxide toxicity was comparable to that of the BT108 clone, while in other assays, BT111 sensitivity was similar to controls. The data for the BT111 clone indicate that other factors in addition to APP C-105 expression influence cellular resistance to hydrogen peroxide.

A control experiment was performed to confirm that the increased resistance of APP C-105-transfected clones to hydrogen peroxide could not be attributed to variations in doubling times among clones (Figure 26). This was done in view of the findings that APP C-105-transfected clones may replicate faster than controls (Figure 13) and that hydrogen peroxide toxicity decreases with increasing cell number (Figure 22). APP C-105-transfected clones and controls were exposed to hydrogen peroxide within three hours of plating, to eliminate any possibility of cell replication. The doubling time of wild type PC12 cells is 48-96 hours (Greene and Tischler, 1982). Under these conditions, the APP C-105-transfected clone, BT108, was less sensitive to hydrogen peroxide than wild type PC12 cells. However, the BT111 clone could not be shown to be resistant to hydrogen peroxide because the 95% confidence limits of the regression lines for BT111 and PC12 overlapped. As indicated previously, BT111 exhibited a large amount of inter-assay

variation that was not observed with other APP C-100-transfected clones. (This variation was also observed in concentration response curves for A23187 performed in the BT111 clone.) Since the BT108 clone was shown to be resistant to hydrogen peroxide in this experiment, the increased resistance to hydrogen peroxide previously observed can be attributed to APP C-105 expression, rather than to the influence of cell number on hydrogen peroxide toxicity.

Figure 22. The Effect of Initial Cell Number on Survival in the Presence of Hydrogen Peroxide

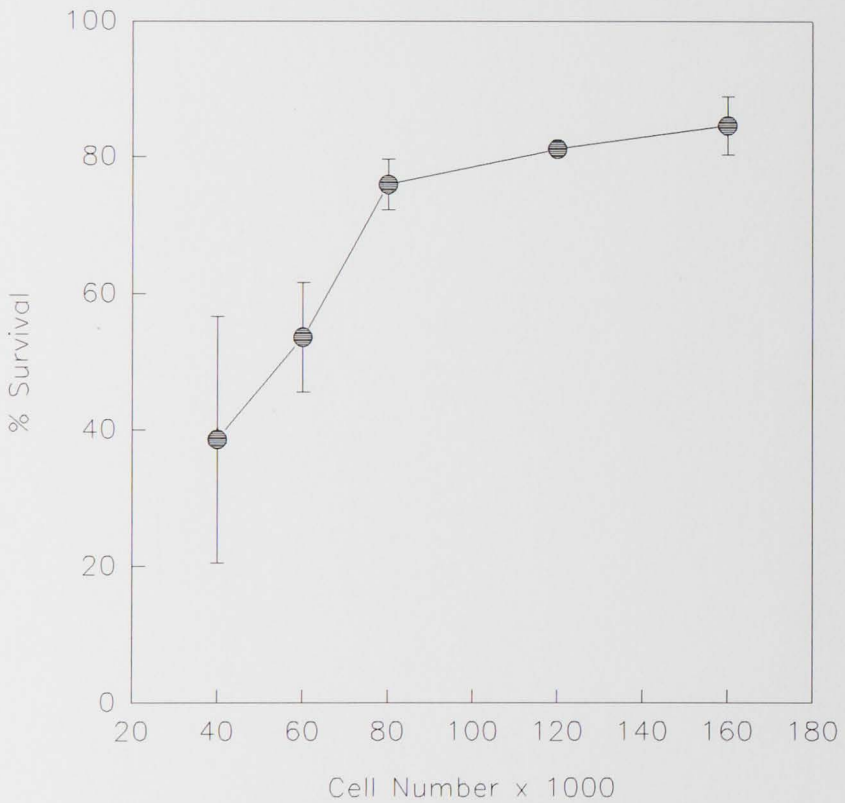

Wild type (i.e., non-transfected) PC12 cells were plated in RPMI media containing 15% serum at densities between 40,000-160,000 cells/ml. After 2 hours, the plating media was removed and the cells were washed with RPMI media containing 3 μM insulin. At each cell density, cells were exposed to 10 μM hydrogen peroxide or to a negative control solution for 24 hours. The data show that the extent of hydrogen peroxide toxicity decreases with increasing cell number.

Table 5. Values Derived from Composite Concentration Response Curves for Hydrogen Peroxide

	PLNTK6	PLNTK3	BT111	BT110	BT108
$ß_0$ (intercept)	86.9	110.8	107.7	100.6	107.1
$ß_1$ (slope)	-4.0	-4.7	-3.3	-1.7	-1.2
$ß_2$	.047	.052	.030	none	none
Correlation coefficient	.999	.999	.997	.999	.996
H_2O_2 EC_{50} (μM)	10	10.5	21	31	47

Table 5 shows regression coefficients, correlation coefficients and EC_{50} values derived from composite concentration response curves for hydrogen peroxide. BT111, BT110 and BT108 are APP C-105-transfected clones; PLNTK6 and PLNTK3 are vector-transfected controls.

Figure 23. Survival of PC12 Cell Clones in the Presence of Hydrogen Peroxide

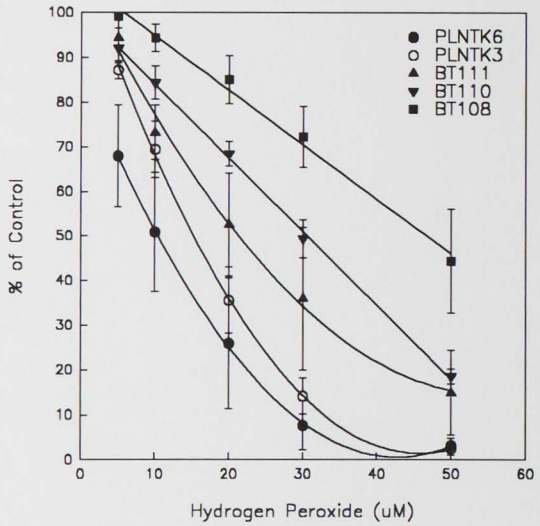

Cells were exposed to hydrogen peroxide in RPMI containing 3 μM insulin, or to RPMI containing 3μM insulin only (control) for 24 hours. Cell survival at each concentration of hydrogen peroxide was calculated as a percentage of cell survival in the absence of hydrogen peroxide (control). PLNTK6 and PLNTK3 are vector-transfected clones (controls); BT111, BT110 and BT108 are APP C-105-transfected clones. Data obtained from 3 (PLNTK6, PLNTK3, BT110) or 6 (BT111, BT108) experiments were averaged to produce composite concentration response curves for each clone. Composite curves were then subjected to first-order or second-order regression.

Figure 24. Concentration Response Curves for Hydrogen Peroxide in PC12 Clones, Including 95% Confidence Limits

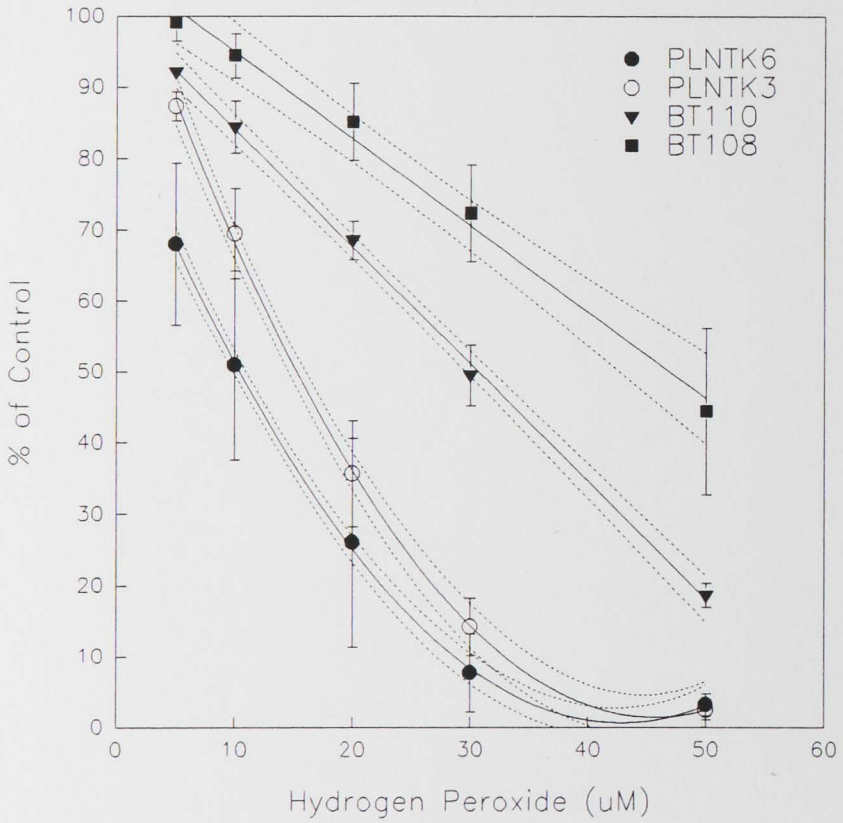

The cytotoxicity of hydrogen peroxide was quantitated using the MTT assay. Broken lines indicate the 95% confidence limits of the composite concentration response curve. Error bars represent the standard error. BT110 and BT108 are APP C-105-transfected clones, PLNTK6 and PLNTK3 are vector-transfected controls.

Figure 25. Concentration Response Curves for Hydrogen Peroxide in an APP C-105-transfected Clone and Vector-transfected Controls, Including 95% Confidence Limits

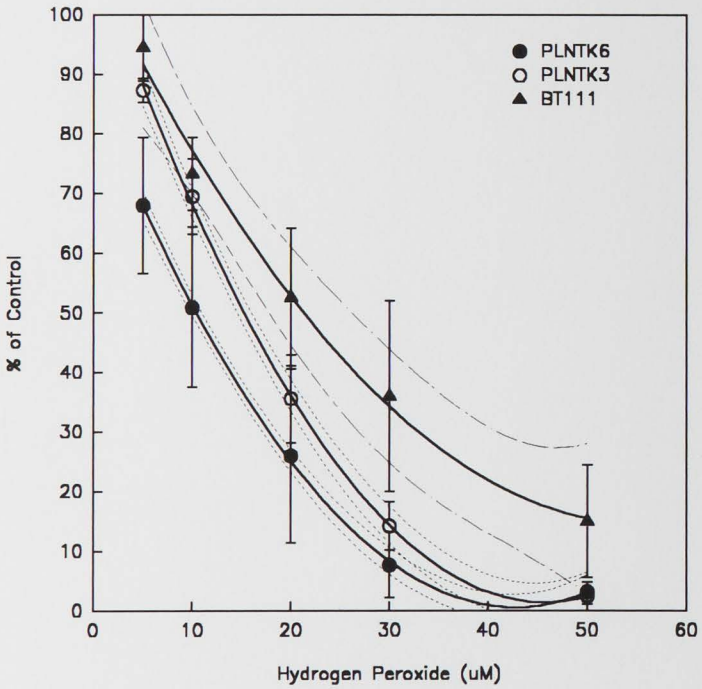

The cytotoxicity of hydrogen peroxide was quantitated using the MTT assay. For clarity, the 95% confidence limits for the PLNTK3 and PLNTK6 cell lines are shown with short broken lines; those for BT111 are shown with long, broken lines. Error bars represent the standard error. BT111 is an APP C-105-transfected clone; PLNTK3 and PLNTK6 are vector-transfected controls.

Figure 26. Concentration Response Curve for Hydrogen Peroxide: Cells Plated Only 3 Hours Before Hydrogen Peroxide Exposure

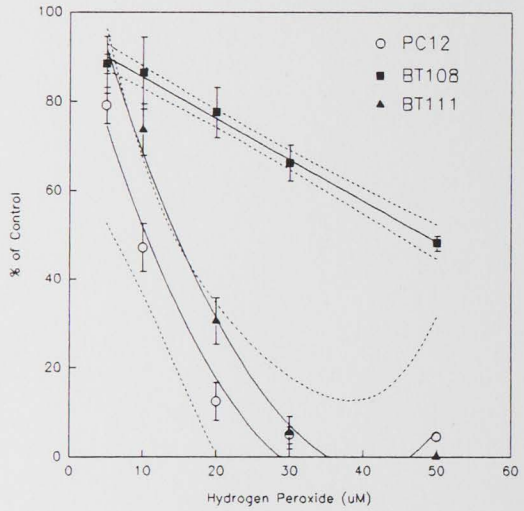

To confirm that the apparent resistance of APP C-105 transfected clones is not due to an effect of cell number on hydrogen peroxide toxicity, cells were plated only three hours prior to hydrogen peroxide exposure in a single control experiment. BT111 and BT108 are APPC-105-transfected clones; PC12 indicates wild type controls. Error bars represent the standard deviation of triplicate determinations. Dotted lines represent the 95% confidence levels of the regression lines for BT108 and PC12. (For clarity, the 95% confidence limits of the regression line for BT111 are not shown.) Under these conditions, BT108 is resistant to hydrogen peroxide; the 95% confidence limits of the BT108 regression line do *not* overlap with those for PC12. However, the 95% confidence limits for the BT111 and PC12 regression lines do overlap. Therefore, in this experiment it can not be shown that the BT111 clone is resistant to hydrogen peroxide. In respect to the BT108 clone, resistance to hydrogen peroxide can be attributed to APP C-105 expression, rather than to the influence of cell number on hydrogen peroxide toxicity.

F. Lack of GM1 Protection Against Hydrogen Peroxide

To determine whether GM1 protected PC12 cells against hydrogen peroxide, concentration response curves for GM1 were obtained in three experiments. Cells were exposed concurrently to hydrogen peroxide and increasing concentrations of GM1, for 24 hours. In each experiment, data were obtained for a vector-transfected clone (PLNTK3, PLNTK6) and one or more APP C-105-transfected clones (BT108, BT111). The number of concentration response curves generated for each clone is as follows: BT108, 3; BT111, 2; PLNTK6, 2; PLNTK3, 1. The BT108 and BT111 clones were exposed to 40 μM hydrogen peroxide, whereas the PLNTK6 and PLNTK3 clones were exposed to 20 μM hydrogen peroxide. This was done because in preliminary experiments it was found that treatment of controls with 40 μM hydrogen peroxide caused total cell death, but treatment of APP C-105-transfected clones with 20 μM hydrogen peroxide did not cause sufficient cell death to permit recognition of any protective effect GM1 might have against hydrogen peroxide-induced toxicity. Composite data for each clone are shown in Figure 27. Data obtained in the BT108, BT111 and PLNTK6 clones were subjected to two-way ANOVA. (PLNTK3 data were not included in the latter analysis.) GM1 did not significantly alter the survival of cells exposed to hydrogen peroxide in any of the clones tested.

The effect of GM1 on cell survival *in the absence of hydrogen peroxide* was examined in one experiment (Figure 28). Concentration response curves were generated for the APP C-105-transfected clone, BT108, and the vector-transfected clone, PLNTK3. Cells

were exposed to RPMI media containing 3 μM insulin, or to RPMI media containing 3 μM insulin and increasing concentrations of GM1 for 24 hours. Cell survival at a given concentration of GM1 was calculated as a percentage of cell survival in the absence of GM1. Triplicate determinations were performed at GM1 concentrations of 10, 25, 50, 75 and 100 μM. Two-way ANOVA indicated a significant difference in cell survival between the two clones ($p=.003$), and a significant effect of GM1 on cell survival ($p<.001$). 100 uM GM1 decreased cell survival by approximately 10% in both clones. The deleterious effect of GM1 on cell survival in the absence of hydrogen peroxide must be confirmed by replication of this experiment.

G. GM1 Protection Against A23187

It had been reported previously that GM1 protects Neuro-2A cells from A23187 toxicity (Nakamura, Wu and Ledeen, 1992). A similar finding was made in one experiment performed using non-transfected PC12 cells. Cells were exposed to 0.5 μM A23187 only, or to A23187 and increasing concentrations of GM1 for 24 hours. GM1 increased cell survival in a dose-dependent manner (Figure 29).

Figure 27. Concentration Response Curves for GM1, in the Presence of Hydrogen Peroxide

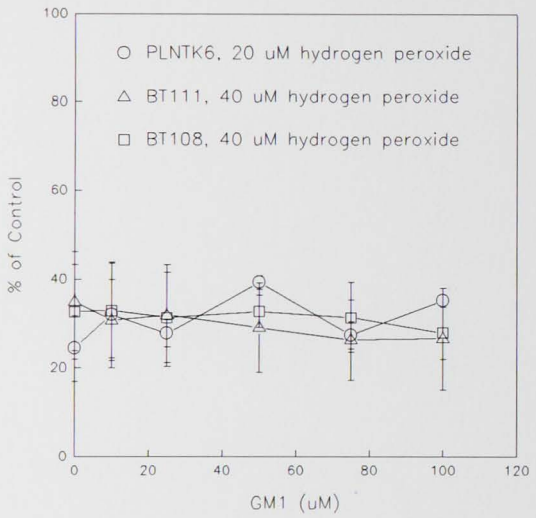

BT111 and BT-108 are APP C-105-transfected clones and PLNTK6 is a vector-transfected clone. Cells were exposed to RPMI containing 3 μM insulin only, RPMI containing 3 μM insulin and 20/40 μM hydrogen peroxide, or to RPMI containing 3 μM insulin, 20μM/40μM hydrogen peroxide and increasing concentrations of GM1 for 24 hours. Cell survival in the presence of hydrogen peroxide, or cell survival in the presence of hydrogen peroxide and a given concentration of GM1 was calculated as a percentage of cell survival in absence of any toxin (i.e., cell survival in RPMI containing 3 μM insulin). Three experiments were performed. In each experiment, concentration response curves for at least one APP C-105-transfected clone and one vector-transfected control were obtained. The number of concentration response curves for each clone is as follows: BT108, 3; BT111, 2; PLNTK6, 2. In one assay, the vector-transfected control PLNTK3 was used instead of PLNTK6. (Data not shown.) Error bars represent the standard error. GM1 did not alter the survival of cells exposed to hydrogen peroxide in any of the clones tested.

Figure 28. Concentration Response Curve for GM1 in the Absence of Hydrogen Peroxide

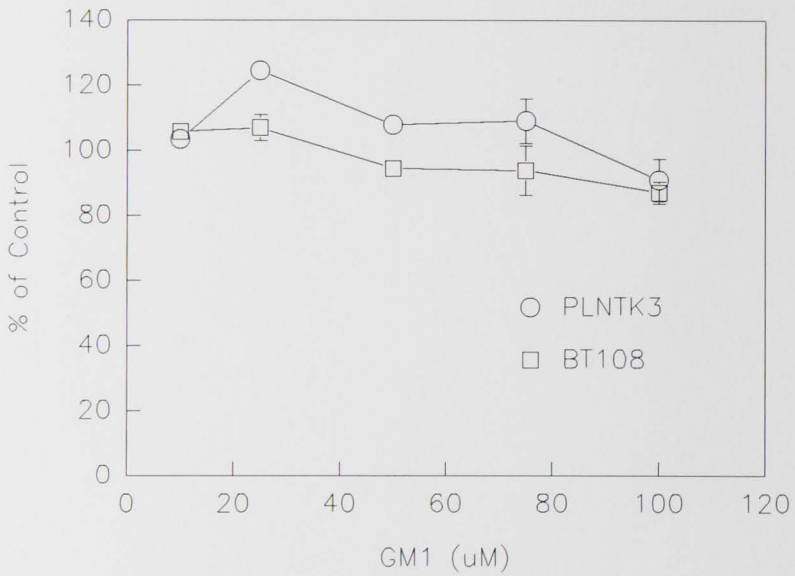

In one experiment, cells were exposed to RPMI media containing 3 μM insulin, or to RPMI media containing 3 μM insulin and increasing concentrations of GM1. Cell survival at a given concentration of GM1 was calculated as a percentage of cell survival in the absence of GM1. PLNTK3 is a vector-transfected clone and BT108 is an APP C-105-transfected clone. GM1 (100 uM) decreased cell survival by approximately 10% in both clones.

Figure 29. GM1 Protects Against A23187 Toxicity in Wild Type (Non-transfected) PC12 Cells

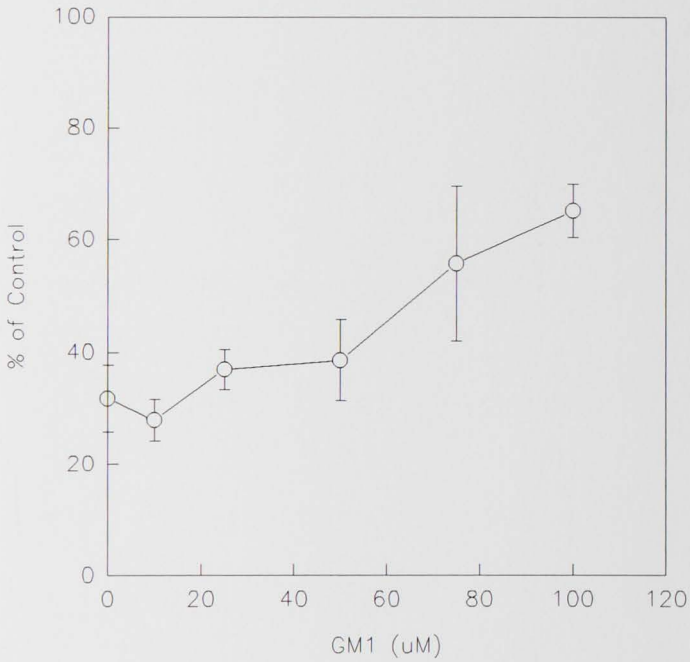

Wild type (i.e., non-transfected) PC12 cells were exposed to RPMI media containing 3 μM insulin and 0.01% DMSO, 0.5 μM A23187 only, or to 0.5 μM A23187 and increasing concentrations of GM1 for 24 hours. GM1 increased cell survival in a dose-dependent fashion. In the absence of GM1, 31.8% survival was obtained after cell exposure to 0.5 μM A23187. Survival after A23187 treatment was calculated as a percentage of cell survival in RPMI media containing 3 μM insulin and 0.01% DMSO. Error bars represent the standard deviation of triplicate determinations.

IV. Discussion

A. APP C-105-transfected Clones

The results of this study indicate that APP C-105 expression can alter PC12 cell vulnerability to toxic insults. Specifically, APP C-105 overexpression induces PC12 cell resistance to hydrogen peroxide and increased sensitivity to A23187. In addition, our results show that GM1 does not protect against hydrogen peroxide in APP C-105-transfected clones or vector-transfected controls. Finally, the results of a single experiment indicate that GM1 attenuates A23187-induced toxicity. (Obviously, the latter experiment must be replicated before any conclusion about GM1's effect on A23187 toxicity in PC12 cells can be drawn.) These results are based on the indirect measurement of cell number using the MTT assay. Typically, other cytotoxicity assays measure plasma membrane permeability to vital stains (e.g., trypan blue) or the activity of intracellular enzymes released by cell lysis (e.g. lactate dehydrogenase). The MTT assay is unique among cytotoxicity assays in that it is 1.) reversible and 2.) an early indicator of Aß-induced toxicity (Shearman, Ragan and Iversen, 1994). To produce meaningful data, an understanding of the variables influencing MTT reduction and solubilization is required. The precautions taken to assure reliable data collection will be described below.

An hypothesis that could account for the altered sensitivity of APP C-105-transfected cells to both hydrogen peroxide and calcium will be advanced. Also, several explanations for the lack of GM1 effectiveness against hydrogen peroxide toxicity will be proposed.

1. APP C-105-transfected PC12 Cells Overexpress APP C-105

To create APP C-105-transfected or vector-transfected clones, PC12 cells were exposed to a modified NTK vector containing the DNA sequence corresponding to APP C-105, or to unaltered NTK, respectively, in the presence of Lipofectant reagent. Transfected cells were selected in the presence of neomycin sulfate. Clonal survival in neomycin sulfate is indicative of vector incorporation into the genome, since the latter is required to permit expression of a neomycin-resistance gene. Therefore, we know that each of the APP C-105-transfected clones employed in this study received at least one, and perhaps several, copies of the vector containing the DNA sequence encoding APP C-105. We have demonstrated by Southern and Northern blotting that APP C-105-transfected clones are producing DNA and mRNA respectively, corresponding to APP C-105. Furthermore, we have shown that protein expression is altered in APP C-105-transfected clones by Western analysis. Using an antibody to $APP_{675-695}$, we found that two peptides, with apparent molecular weights of approximately 45,000 and 60,000 kD, are overexpressed in *cell lysates* derived from APP C-105-transfected clones. Also, three peptides containing the C-terminus of APP were found in *conditioned medium* from an APP C-105-transfected cell line (BT111), but were absent in controls. The latter had apparent molecular weights ranging from 27,500-42,400 kD. Since APP C-100 has a molecular weight of 11 kD, the peptides found in cell lysates and conditioned

medium likely represent aggregates of APP C-100. Finally, we have shown that our APP C-105-transfected clones die when treated for with NGF for at least six days in serum-containing medium, a behavior which has previously been reported for APP C-100-transfected clones (Fukuchi, Kamino et al. , 1992; Yankner, Dawes et al. , 1989). The death of APP C-105-transfected cells in response to NGF is additional evidence that the clones employed in this investigation overexpress APP C-105.

The mechanism by which NGF induces the death of APP C-100 transfected clones is not understood. It is important to note that one laboratory has obtained APP C-100-transfected clones which do not die in response to NGF (Sandhu, Kim et al. , 1996). The NGF-induced death of APP C-100-transfected cells may depend on the cell line chosen for transfection and the vector employed. These factors will be discussed at greater length below.

In model systems in which APP C-100 overexpression confers sensitivity to NGF, there is reason to believe that the latter effect is *not* mediated by Aß. In Sagara's laboratory, APP C-100-transfected clones were selected for resistance to Aß (Sagara, Dargusch et al. , 1996). Resistance is mediated, in part, by increases in catalase and GSH peroxidase activity. Therefore, one would expect NGF, which increases catalase and GSH peroxidase activity (Jackson, Sampath et al. , 1994), to protect against Aß toxicity. However, the opposite is true. This may

indicate that NGF-induced cell death does not involve Aß, or that some APP C-100-transfected clones do not produce Aß.

2. NGF-induced Cell Death Does Not Occur in Serum-free Media

In the present study, NGF provoked the death of APP C-105-transfected cells in the presence of serum, but not in its absence. This indicates that in addition to NGF, one or more serum-borne factors are required to induce the death of APP C-105-transfected cells. The failure to observe NGF-induced cell death in serum-free media is in agreement with a previous report, in which NGF-induced cell death was shown to occur at a slower rate in serum-free media than in serum-containing media in APP C-104-transfected PC12 cells (Kozlowski, Spanoyannis et al. , 1992).

In the present study NGF actually *increased* cell survival in the absence of serum. This is due to the fact that cells were exposed to NGF in serum-free media containing 1 μM insulin. Since 3 μM insulin is required for maximal PC12 survival in serum-free media (Rukenstein, Rydel and Greene, 1993), NGF enhanced the survival of PC12 cells exposed to an inadequate concentration of insulin. During NGF treatment in serum-free medium, APP C-105-transfected clones replicated to a greater extent than did controls. This indicates that APP C-105 may replace serum-borne mitogenic factors.

3. Model Systems for APP C-100 Overexpression

The effect of APP C-100 expression on a given parameter is dependent on the model system used for investigation (Wolozin, Bacic et al. , 1992). Clones which overexpress APP C-100 have been created from several parental cell lines, using different vectors. Commonly used vectors differ with respect to 1.) the number of APP C-terminal amino acids encoded 2.) the viral origin of the promotor sequence used to express APP C-100 3.) the location of the translation start site and 4.) the amount of non-coding sequence incorporated.

In the present study, we did not determine whether our APP C-105-transfected PC12 cells overexpress Aß. Although the overexpression of Aß in APP C-100-transfected cells has been reported (Macq, Philippe and Octave, 1994; Dyrks, Dyrks et al. , 1993), Aß overexpression in the current model can not be assumed.

B. MTT Cell Viability Assay

1. General Principles

The tetrazolium salt MTT is reduced (cleaved) within living cells to produce a colored formazan, which absorbs light maximally at 570m. In 1983, Mossman demonstrated that a linear relationship between formazan production (absorbance) and cell number could be obtained (Mosmann, 1983). In this report, Mossman

stated that since MTT was reduced within the mitochondria of living cells, dead cells were unable to induce formazan production. In essence, a 'living' cell was defined as one in which cellular respiration occurred (Mosmann, 1983). This assumption was based on Slater's work, who showed that inhibitors of mitochondrial electron transport could decrease MTT reduction (Slater, Sawyer and Strauli, 1963). However, Slater did not provide evidence that MTT reduction was confined to the inner mitochondrial membrane. Recently, it has been shown that most MTT reduction occurs in the cytosol and that mitochondrial MTT reduction accounts for only a small percentage of total cellular MTT reduction (Berridge and Tan, 1993). In addition, MTT reduction has been reported to occur in the absence of viable mitochondria (Loveland, Johns et al. , 1992). In light of recent reports, the MTT assay defines a 'living' cell as one that has sufficient reducing power in the form of NADH and NADPH to convert MTT to formazan. NADPH is produced primarily by the pentose phosphate pathway; NADH is produced by glycolysis and the tricarboxylic acid cycle.

The original MTT assay could measure 200-50,000 cells (Mosmann, 1983). The sensitivity of the modified assay is decreased in comparison to the original assay, but reproducibility is much improved (Hansen, 1989). The linear relationship between absorbance and cell number in the MTT assay is dependent on 1) the pH of the Extraction Buffer and 2) a lack of bacterial contamination in cell cultures. If the Extraction Buffer pH is less than 4, formazan will be converted

back to MTT; if greater than 5, absorbance values will be falsely elevated (Hansen, 1989). Contamination of cell cultures causes erroneous absorbance values, because bacteria as well as mammalian cells are able to convert MTT to formazan.

2. Possible Sources of Error

APP C-105 overexpression was found to confer resistance to hydrogen peroxide and increased vulnerability to A23187. It is necessary to consider whether one or more systematic errors could have occurred which would lead to these results. Potentially, clonal differences in the amount of formazan produced per cell could influence comparisons between APP C-105-transfected cells and vector-transfected clones. To eliminate the latter possibility, clonal viabilities were not compared on the basis of raw formazan production. Instead, the percentage of living cells at a given concentration of toxin was calculated. The differential vulnerability of clones to hydrogen peroxide or A23187 was determined by plotting percent survival against toxin concentration.

Experiments designed to evaluate the vulnerability of APP C-105-transfected cells to A23187 were performed in serum-free RPMI media containing 3 μM insulin. If APP C-105-transfected clones were more likely than controls to die in serum-free media, one might erroneously draw the conclusion that APP C-105 expression increases sensitivity to A23187. Death of PC12 cells in serum-free

media occurs due to a lack of growth factors. However, the ability of APP C-105-transfected clones to survive in serum-free, insulin-free media is *enhanced*, when compared to that of control cells (Figure 14). For this reason, the increased vulnerability of APP C-105-transfected clones to A23187 is unlikely to be artefactual.

Diligent efforts were made to avoid contamination of all clones, and culture media were tested for the presence of contamination periodically. This was done by spreading a thin film of culture media onto agar plates and examining the plates 48 hours later for bacterial growth.

D. APP C-105 Expression Enhances Vulnerability to A23187

The ability to maintain calcium homeostasis, here defined as the ability of a cell to maintain a low concentration of intracellular calcium while in the presence of a much larger extracellular calcium concentration, is compromised by overexpression of APP C-105. This conclusion is based on the finding that A23187, a calcium ionophore, is more toxic to APP C-105-transfected clones than to controls. Aß may be responsible for the observed effect of APP C-105 overexpression on calcium homeostasis, since the disruption of calcium homeostasis by Aß has been reported (Weiss, Pike and Cotman, 1994; Mattson, Cheng et al. , 1992; Koh, Yang and Cotman, 1990; Arispe, Rojas and Pollard, 1993; Joseph and Han, 1992). Studies describing the deleterious effect of Aß on

the ability of cells to maintain low concentrations of intracellular calcium formed the basis for the current work and have already been discussed.

1. A23187 and Aß

In several ways, Aß is similar in its behavior to A23187. For this reason, it may be useful to regard Aß as an ionophore. Both A23187 and Aß are able to form membrane pores (Arispe, Rojas and Pollard, 1993; Balasubramanian, Sikdar and Easwaran, 1992). Dihydropyridines, which block L-type calcium channels, attenuate both Aß and A23187 toxicity (Matsuda, 1995; Weiss, Pike and Cotman, 1994). The ability of dihydropyridines to attenuate Aß toxicity has been cited as evidence that Aß has an effect on L-type calcium channels. However, dihydropyridines were shown to protect against A23187 toxicity in a model lacking voltage-gated calcium channels. This indicates that such protection is mediated by a mechanism which is independent of the dihydropyridines' ability to block L-type calcium channels. Finally, the antioxidant Vitamin E protects PC12 cells against Aß toxicity (Behl, Davis et al. , 1992), and inhibits the A23187-induced efflux of creatine kinase from skeletal muscle (Phoenix, Edwards and Jackson, 1991). The latter finding suggests that oxidative stress may be a component of A23187-induced injury. However, it is clear that A23187-induced injury is initiated by calcium, since the latter does not occur in the absence of extracellular calcium.

2. Potential Mechanisms

Calcium homeostasis is maintained by the limited permeability of the plasma membrane, the operation of extrusion mechanisms, the binding of calcium to intracellular proteins, and sequestration of calcium within organelles (endoplasmic reticulum, mitochondria and nuclei). Specific mechanisms by which APP C-105 expression could increase cellular vulnerability to calcium include, but are not limited to, the following:

1. *Imposition of an energy deficit.* APP C-105 overexpression could increase ATP hydrolysis or decrease ATP synthesis. A lack of available ATP would cause the failure of Na^{+}/K^{+} ATPase and Ca^{+2} ATPase, and thereby elevate resting calcium levels. Aß and hydrogen peroxide have been shown to activate poly(ADP-ribose) synthetase (PARS), an enzyme involved in DNA repair (Zhang, Pieper and Snyder, 1995). Activation of PARS causes depletion of its substrate, NAD^{+}. Since NAD^{+} is also required for the glycolytic conversion of glyceraldehyde 3-phosphate to 1,3-biphosphoglycerate, Aß-induced activation of PARS can inhibit glycolytic generation of ATP. Hydrogen peroxide toxicity is attenuated by inhibition of PARS (Marini, Frabetti et al. , 1993)

2. *Disruption of gap junctions.* Production of a gap junctional protein, connexin 43, is induced in PC12 cells overexpressing a C-terminal fragment of APP (C-97) (Lynn, Marotta and Nagy, 1995). Unlike normal PC12 cells or vector-transfected controls, APP C-97- transfected clones are able to transmit intercellular calcium waves. Transmission occurs in the absence of extracellular calcium and is blocked by inhibitors of gap junctional communication (Lynn, Marotta and Nagy, 1995). Therefore, the possibility exists that APP

C-97 may be able to disrupt calcium homeostasis by permitting the inappropriate propagation of calcium waves.

3. *Alteration of protein expression.* APP C-105 overexpression could decrease the expression of a calcium binding protein, such as calretinin. Neurons in which calretinin is expressed are resistant to A23187 (Lukas and Jones, 1994) and Aß (Pike and Cotman, 1995) toxicity *in vitro*.

If APP C-105 overexpression increases Aß secretion, the latter could disturb calcium homeostasis by 1.) directly increasing intracellular calcium or 2.) limiting the ability of cells to lower intracellular calcium after a calcium challenge.

E. APP C-105 Expression Decreases Vulnerability to Hydrogen Peroxide

1. Hydrogen Peroxide Toxicity

Hydrogen peroxide has numerous effects on cell function. These effects include, but are not limited to, the capacity 1.) to inflict DNA damage and activate polyADP ribose polymerase (Nath, Enright et al. , 1994; Schraufstatter, Hinshaw et al. , 1986) 2.) cause depletion of ATP (Hyslop, Hinshaw et al. , 1988) and NAD^+ (Schraufstatter, Hinshaw et al. , 1985) 3.) activate the pentose phosphate shunt (Schraufstatter, Hinshaw et al. , 1985) 4.) raise intracellular calcium (Golconda, Ueda and Shah, 1993; Kimura, Maeda and

Hayashi, 1992) 5.) disrupt the plasma membrane and cytoskeleton (Hinshaw, Sklar et al. , 1986) and 6.) inhibit protein synthesis (Jornot, Petersen and Junod, 1991).

The present data indicate that APP C-105-transfected cells are more resistant to hydrogen peroxide toxicity. This unexpected result must be placed in the context of a recent report that PC12 cells can be selected for resistance to Aß and hydrogen peroxide by 4 month exposure of cells to 20 μM Aß $_{25-35}$ (Sagara, Dargusch et al. , 1996). 20 μM Aß $_{25-35}$ is a concentration sufficient to kill the majority of PC12 cells exposed to it. The latter finding suggests that our APP C-105-transfected cells may be exposed chronically to high concentrations of Aß, produced from APP C-105. Further, in this laboratory it has been shown that APP C-105-transfected cells are resistant to Aß, as well as to hydrogen peroxide (John Wells, unpublished observations).

The increased resistance of cells grown in the presence of high concentrations of Aß has been attributed to observed increases in GSH peroxidase and catalase activity (Sagara, Dargusch et al. , 1996). In our system, we did not determine these parameters.

2. Aß Resistance is a Complex Phenomenon

Several observations suggest that increased enzyme activity might account only partially for the enhanced resistance to hydrogen peroxide and Aß, observed in Aß-resistant PC12 clones (Sagara, Dargusch et al. , 1996), and in APP C-105 transfected clones. First, both the Aß-resistant clones isolated by Sagara, and the APP C-105-transfected clones created in this laboratory exhibit a changed morphology in comparison to parental (non-transfected) PC12 cells. Sagara's Aß-resistant clones have a flattened

appearance, and possess more cytoplasmic vesicles and vacuoles than non-resistant PC12 cells. Our APP C-105-transfected clones also had a flattened appearance that is distinctly different from non-transfected PC12 cells and vector-transfected controls. Sagara's group studied Aß-resistance in the rat CNS cell line, B12. Aß-resistant B12 clones adopt a morphology similar to Aß-resistant PC12 clones. However, B12 cells do not assume a changed morphology when transfected with cDNA for catalase and glutathione peroxidase (Sagara, Dargusch et al. , 1996). Therefore, it is clear that increased enzyme activity alone is not sufficient to confer the morphology typical of cells selected for Aß resistance. Secondly, an Aß-resistant B12 clone has been isolated that is devoid of catalase mRNA or enzyme activity. The latter clone does exhibit increased glutathione peroxidase activity. Thirdly, in another study, catalase and glutathione peroxidase activity were not increased in hydrogen peroxide-resistant PC12 cells (Jackson, Sampath et al. , 1994).

3. A Hypothesis to Explain the Current Findings

As detailed above, there is evidence to suggest that APP C-105-induced resistance to hydrogen peroxide may involve extensive changes in cellular function. The present data contain a second clue to the nature of the mechanism mediating APP C-105-induced resistance to hydrogen peroxide: hydrogen peroxide-resistant clones are also more vulnerable to calcium (A23187) toxicity. This is an odd finding since sustained elevation of intracellular calcium is required for manifestation of hydrogen peroxide-induced cell death (Halleck, Richburg and Kauffman, 1992). BAPTA and quin2 (intracellular calcium chelators) protect against hydrogen peroxide-induced cell death and double stranded DNA

breaks. One would expect hydrogen peroxide-resistant clones to be calcium (A23187)-resistant, rather than calcium-sensitive. Concentration response curves for A23187 in APP C-105-transfected clones and controls indicate that the ability to maintain calcium homeostasis is compromised in APP C-105 transfected clones. Hydrogen peroxide toxicity may be mediated by a multi-step process culminating in the elevation of intracellular calcium. If so, resistance to hydrogen peroxide might be achieved by increasing the clearance of hydrogen peroxide before the latter could initiate a cascade of events leading to the elevation of intracellular calcium.

Ideally, one mechanism would account for the effects of APP C-105 overexpression on cellular vulnerability to hydrogen peroxide and calcium. We speculate that APP C-105 overexpression induces mobilization of free radical defenses at the expense of cellular resources needed to maintain calcium homeostasis. The latter occurs as a result of enhanced NADPH production by the pentose phosphate shunt. To illustrate the plausibility of this hypothesis, the pentose phosphate shunt and the possible fates of glucose 6-phosphate will be reviewed (Stryer. 1988).

The brain requires a continuos supply of glucose, since it relies totally on glucose for its fuel supply (except during starvation). Glucose is phosphorylated to glucose 6-phosphate rapidly upon cell entry. It can then be converted to pyruvate via glycolysis, or enter the pentose phosphate shunt. The reactions of the pentose phosphate shunt provide ribose 5-phosphate for nucleic acid synthesis and NADPH for reductive biosyntheses. The shunt has oxidative and non-oxidative branches (Figure 30). All

reactions occur in the cytosol. In the oxidative branch of the shunt, three reactions occur sequentially. The sum of these reactions is as follows:

$$\text{glucose 6-phosphate} + \text{NADP}^+ + \text{H}_2\text{O} \rightarrow \text{ribulose 5-phosphate} + 2\ \text{NADPH} + 2\ \text{H}^+ + \text{CO}_2$$

It can be seen that 1 molecule of ribulose 5-phosphate and 2 NADPH are produced for each molecule of glucose 6-phosphate. The first reaction in the oxidative branch is the rate-limiting step for the production of ribose 5-phosphate. Glucose 6-phosphate is converted to 6-phophoglucono-δ-lactone, by the action of glucose 6-phosphate dehydrogenase (G6P dehydrogenase). This reaction is essentially irreversible, and its rate is controlled by the availability of $NADP^+$. NADPH inhibits the activity of G6P dehydrogenase.

In the first two reactions of the non-oxidative branch, ribose 5-phosphate or xylulose 5-phosphate are produced from ribulose 5-phosphate (Figure 30). In the last three reactions, ribose 5-phosphate and xylulose 5-phosphate are converted to the glycolytic intermediates, fructose 6-phosphate and glyceraldehyde 3-phosphate (Figure 30). The non-oxidative reactions of the pentose phosphate pump are reversible, and therefore permit adjustment of NADPH and ribose 5-phosphate concentrations to meet cellular requirements. Three possible situations are listed below:

Situation 1 Equal cellular requirements for ribose 5-phosphate and NADPH

Situation 2 More ribose 5-phosphate than NADPH is needed

Situation 3 More NADPH than ribose 5-phosphate is needed

In Situation 1, most glucose 6-phosphate is consumed by the oxidative branch of pentose phosphate pump as described in the equation above. Ribulose 5-phosphate is then converted to ribose 5-phosphate in the first reaction of the non-oxidative branch. In Situation 2, most glucose 6-phosphate is converted to fructose 6-phosphate and glyceraldehyde 3-phosphate via the glycolytic pathway. The latter two products are converted by by reversal of reactions 3-5 in the non-oxidative branch of the pentose phosphate shunt to ribose 5-phosphate. In Situation 3, ribose 5-phosphate is produced in the same manner as in Situation 1, then converted by reactions 3-5 of the non-oxidative branch into fructose 6-phosphate and glyceraldehyde 3-phosphate. The latter enter 1.) a gluconeogenic pathway to produce glucose 6-phosphate or 2.) the glycolytic pathway to produce pyruvate. If the intermediates fructose 6-phosphate and glyceraldehyde 3-phosphate enter the glycolytic pathway, both ATP and NADH are produced. However, if these intermediates enter the gluconeogenic pathway, a large amount of NADPH is produced but no ATP is produced. It is important to note that the final reaction in gluconeogenesis, i.e., the conversion of glucose 6-phosphate to glucose, does not occur in brain. Brain does not contain glucose 6-phosphatase, the enzyme necessary to catalyze this reaction.

We hypothesize that Aß induces hydrogen peroxide production, and in so doing, concurrently stimulates the oxidative branch of the pentose phosphate shunt and blocks glycolytic ATP synthesis (Schraufstatter, Hinshaw et al. , 1985). Aß causes the accumulation of intracellular hydrogen peroxide (Behl, Davis et al. , 1994), which in turn, depletes intracellular glutathione (Schraufstatter, Hinshaw et al. , 1985). Glutathione (γ-glutamylcysteinylglycine, GSH) is a thiol-containing tripeptide which plays a crucial role in the defending cells against hydrogen peroxide toxicity. Glutathione protects against hydrogen peroxide toxicity by 1.) reducing intracellular peroxides via glutathione peroxidase 2.) maintaining reduced disulfide bonds in proteins and 3.) facilitating the non-enzymatic reduction of free radicals (Meister and Anderson, 1996).

The reduced form of glutathione (GSH) constitutes about 90% of the total intracellular pool. It is regenerated from oxidized glutathione (GSSG) in a reaction catalyzed by glutathione reductase:

$$GSSG + 2\ NADPH \rightarrow 2\ GSH + 2\ NADP^{+}$$

Aß may increase cellular requirements for reduced glutathione. The need to regenerate GSH stimulates NADPH production by the pentose phosphate shunt (Figure 31). NADPH is produced via the G6P-catalyzed conversion of glucose 6-phosphate to 6-phosphoglucono-lactone and the 6-phosphogluconate

dehydrogenase-catalyzed conversion of 6-phosphogluconate to ribulose 5-phosphate.

In addition, Aß-induced hydrogen peroxide release may inhibit glycolysis, causing ATP depletion (Hyslop, Hinshaw et al. , 1988). Hydrogen peroxide inhibits the glycolytic enzyme glyceraldehyde 3-phosphate dehydrogenase by three independent mechanisms: 1.) direct inactivation of the enzyme 2.) reduction of the intracellular concentration and redox potential of nicotinamide cofactors and 3.) a shift in the pH away from the enzyme optima (Hyslop, Hinshaw et al. , 1988). Glyceraldehyde 3-phosphate dehydrogenase inhibition leads to the accumulation of glyceraldehyde 3-phosphate, dihydroxyacetone phosphate and fructose 1,6 bisphosphate. Therefore, Aß may cause increased entry of fructose 6-phosphate and glyceraldehyde 3-phosphate into the gluconeogenic pathway, *resulting in heightened NADPH production at the expense of ATP synthesis*. The decreased vulnerability of APP C-105-transfected PC12 cells to hydrogen peroxide may be due to the fact that NADPH production permits the regeneration of GSH. Moreover, the increased vulnerability of APP C-105-transfected cells to A23187 may occur due to the failure of ATP-dependent calcium defense mechanisms.

If APP C-105-tranfected clones are exposed to elevated concentrations of Aß, intracellular hydrogen peroxide concentrations may also be elevated, and chronic stimulation of the pentose phosphate shunt could occur. This hypothesis could be tested

by examining NADH/NADPH or GSH/GSSG ratios in APP C-105-transfected cells and controls.

Figure 30. Pentose Phosphate Shunt

Oxidative Branch

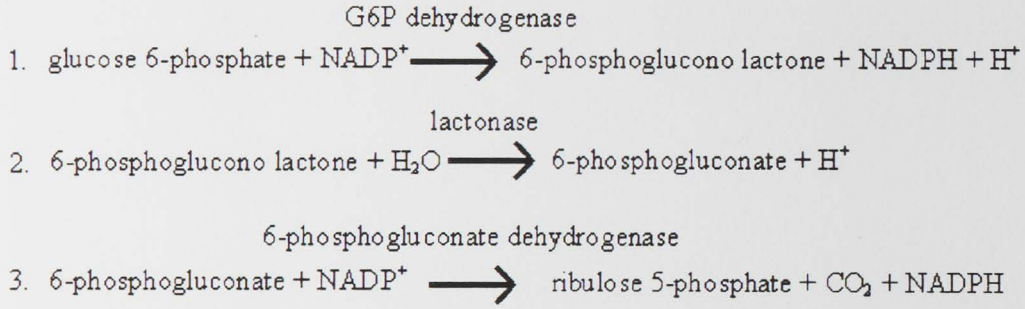

Non-oxidative Branch

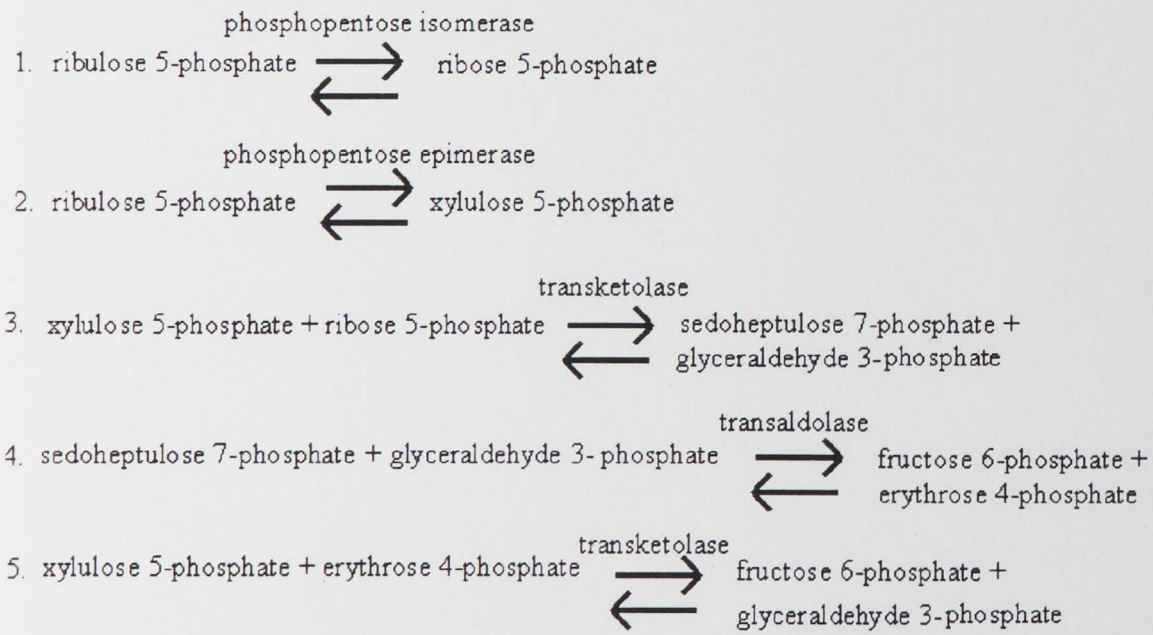

Figure 31. The Effect of Aß on the Pentose Phosphate Shunt and Glycolysis

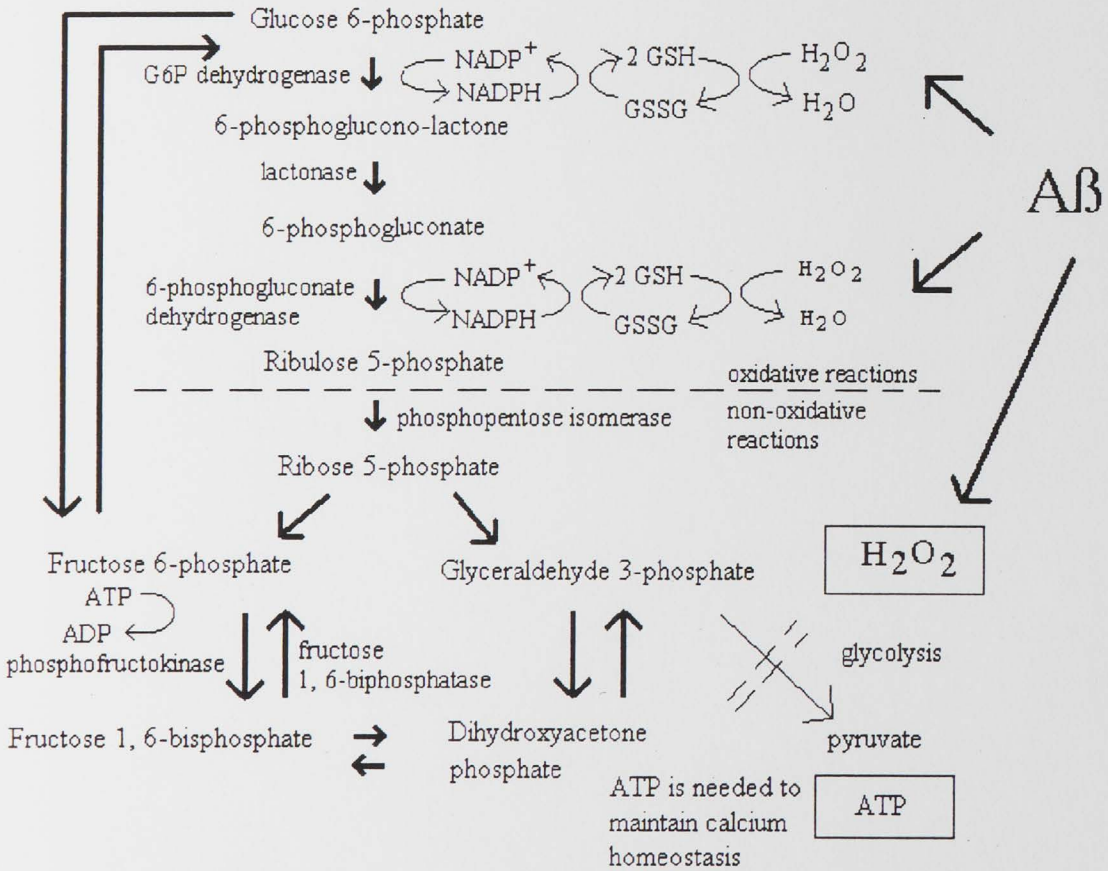

F. Gangliosides

1. Protection Against A23187-induced Toxicity

The results of one experiment agree with a previous observation that GM1 protects against A23187-induced cell death (Nakamura, Wu and Ledeen, 1992). Although the mechanism of this action is not known, a control experiment minimized the possibility that a trivial mechanism is involved; GM1 does not act by precipitating A23187, thus preventing it from crossing cell membranes. (Data not shown.)

Several compounds in addition to GM1 have been found to protect against A23187-induced cell death and/or to inhibit A23187-induced biochemical changes. The lipid-soluble antioxidant, Vitamin E (Figure 32), inhibits the A23187-induced efflux of creatine kinase (a cytosolic enzyme) from skeletal muscle (Phoenix, Edwards and Jackson, 1991). In the latter study, the relative importance of various structural groups for inhibition of A23187-induced creatine kinase efflux by Vitamin E was determined (Phoenix, Edwards and Jackson, 1991). Using structural analogs, it was found that 1.) Vitamin E's ability to function as an antioxidant (conferred by its chromanol hydroxyl group) is unrelated to its ability to inhibit A23187-induced creatine kinase efflux 2.) inhibition of efflux depends on the length of the isoprenoid side chain, but not on its degree of unsaturation and 3.) inhibition of efflux does not require the presence of chromanol methyl groups.

Vitamin E's side chain and chromanol methyl groups are thought to provide it with sites of attachment to membrane phospholipid fatty acids. However, in the latter study all Vitamin E analogs containing an isoprenoid chain were found to inhibit creatine kinase efflux, *independent* of the nature of the head group. In view of these findings, attachment of Vitamin E might not be required for inhibition of A23187-induced creatine kinase efflux.

The effects of dihydropyridine-type and non-dihydropyridine-type calcium antagonists on A23187-induced damage were studied in perfused rat liver and isolated hepatocytes (Matsuda, 1995). *In vivo* and *in vitro*, the dihydropyridine-type calcium antagonists, nitrendipine and nifedipine, prevented A23187-induced LDH release. The non-dihydropyridine antagonists, verapamil and diltiazem, were ineffective. (The protection observed *in vivo* was not due to an effect on the vasculature.) Since the plasma membrane of rat hepatocytes does not contain voltage-gated or receptor-operated calcium channels, nitrendipine and nifedipine do not protect against A23187-induced damage by acting as calcium channel antagonists. A23187-induced cytotoxicity may be mediated by intracellular signalling pathways, since inhibitors of calmodulin and protein kinase C attenuated A23187-induced LDH release *in vitro* (Matsuda, 1995).

In another study, sphingosine (a PKC inhibitor) inhibited the A23187-induced release of arachidonic acid and increase in PLA_2 activity (Chakraborti, Michael and Patra, 1991). Sphingosine's effect occurred at high concentrations of A23187, at

which protein kinase C is translocated from the cytosol to the membrane. GM1 contains a molecule of sphingosine.

Figure 32. The Structure of Vitamin E

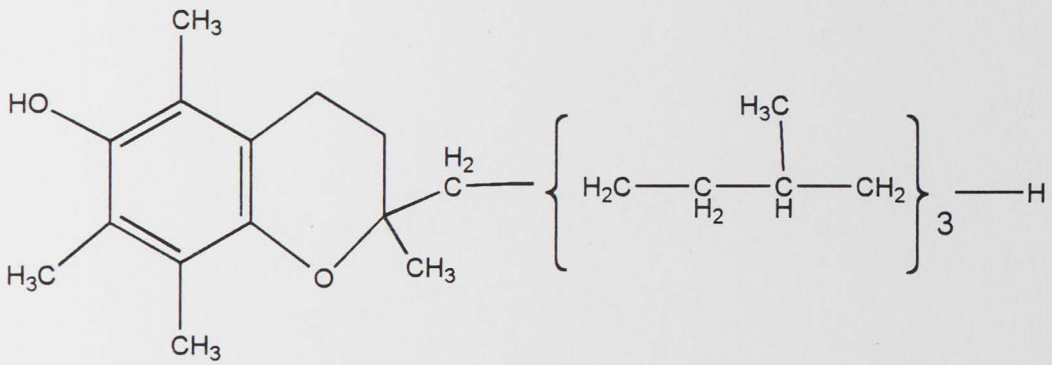

2. Possible Explanations for the Failure of GM1 to Protect Against Hydrogen Peroxide

In the present work, a protective effect of GM1 against hydrogen peroxide toxicity was not observed. This is surprising, since ganglioside efficacy has been demonstrated in other studies in which toxicity is mediated, ultimately, by free radicals (e.g., ischemia) (Mahadik, Murthy et al. , 1990; Karpiak, Mahadik and Wakade, 1990). Methodological considerations may explain the failure to observe a protective effect of GM1 in this study. Possible explanations for GM1's lack of efficacy include the following:

a. Acute exposure to hydrogen peroxide may have caused a degree of cell injury exceeding GM1's ability to repair. Gangliosides may be effective against free radicals when the amount of cell damage inflicted is within low to moderate limits. In a study using dopaminergic neurons, GM1 was able to repair damage inflicted by a low concentration of MPP^+ , but unable to repair damage caused by higher concentrations (Stull, Schneider and Iacovitti, 1994). Neurons were treated with MPP^+ for 1 day, followed by a 3-day exposure to 100 μM GM1. 2.5 μM MPP^+ treatment caused a 30% loss of tyrosine hydroxylase immunoreactive neurons which was prevented by GM1. The latter investigation suggests that GM1 may be effective against hydrogen peroxide toxicity if cells are exposed chronically to a low concentration of toxin. In the current study, the hydrogen peroxide concentrations chosen often caused more than 50% cell death. This may be because hydrogen peroxide-

induced injury was exacerbated by 1.) a lack of serum in cell culture media during hydrogen peroxide exposure and 2) the use of NGF-naive PC12 cells. It is possible that a protective effect of GM1 against hydrogen peroxide might have been observed if cells had been exposed chronically to low concentrations of hydrogen peroxide. In future studies, the glucose-glucose oxidase system could be used to expose cells chronically to low concentrations of hydrogen peroxide.

b. GM1 cytoprotection against hydrogen peroxide toxicity may require the presence of other neurotrophic factors, not present in the serum-free model (RPMI media containing 3 μM insulin) used in this study. GM1 is able to prevent the death of PC12 cells in serum-free media due to trophic factor deprivation (Ferrari, Batistatou and Greene, 1993). Recently, dimerization of Trk receptors by GM1 has been identified as a mechanism which, in part, is responsible for GM1-promoted survival in serum-free media (Ferrari, Anderson et al. , 1995). However, it is clear that one or more other mechanisms must also operate to permit the latter effect of GM1.

c. PC12 cells might not possess the signal transduction machinery necessary for GM1 to exert a positive effect on cell repair. PC12 cells, while possessing other endogenous gangliosides, do not contain GM1 (Yamamoto, Tsuji and Nagai, 1990). Given the variety of ganglioside species within cell membranes,

it is reasonable to assume that ganglioside actions are effected by multiple signal transduction pathways, some of which may not be available to GM1.

d. The means used to inflict cellular injury has a important bearing on the results of any study seeking to elucidate mechanisms of ganglioside cytoprotection. As noted in the Introduction, the primary theories regarding the mechanism(s) of ganglioside cytoprotection are: 1) attenuation of the glutamate-evoked translocation of PKC from the cytoplasm to the plasma membrane 2) protection of the plasma membrane and 3) inhibition of nitric oxide synthase and 4) stimulation of receptor kinases for trophic factors. However, there is also evidence to suggest that gangliosides provide cytoprotection by inhibiting glutamate-induced glutamate release (Nicoletti, Cavallaro et al. , 1989). Obviously, if the latter is an important mechanism for ganglioside action, cytoprotection would be observed in studies using ischemia to inflict injury, but not in studies using more direct means of free radical-induced cell damage (e.g., hydrogen peroxide).

The data collected using the present paradigm suggest that GM1 is unable to *repair* hydrogen peroxide-induced damage, but do not address whether GM1 is able to prevent such damage. The reason for this is that, although PC12 cells were exposed to hydrogen peroxide and GM1 "concurrently" for 24 hours, the stability of hydrogen peroxide in the presence of PC12 cells is very limited. The $t_{1/2}$ of hydrogen peroxide in PC12 cell suspensions containing 0.7 mg protein has been

reported to be 42 seconds (Halleck, Richburg and Kauffman, 1992). GM1 requires a substantial amount of time to become incorporated into cell membranes, where it can exert an effect (Saqr, Pearl and Yates, 1993).

V. Conclusions

This study demonstrates that expression of APP C-105 induces resistance to hydrogen peroxide. It is in agreement with earlier studies showing that Aß destabilizes calcium homeostasis, and shows that overexpression of APP C-105 induces a similar effect. In this study, GM1 protected PC12 cells from A23187 toxicity, but not from hydrogen peroxide toxicity.

The finding that APP C-105 overexpression increases cellular vulnerability to calcium and confers resistance to hydrogen peroxide toxicity, suggests that cells can not simultaneously maintain optimal calcium homeostasis and optimal operation of hydroxyl radical defense mechanisms. Other free radical species, NO and CO, have been shown to act as neurotransmitters (Dawson and Snyder, 1994). Although neither hydrogen peroxide nor hydroxyl radical have been identified as neurotransmitters, future studies may show this to be the case. In time, it may become reasonable to speak of "free radical homeostasis". Cells may seek to maintain balanced defenses against calcium and free radicals until actually faced with a toxic insult. Then, defense systems may be altered to combat the most

pressing threat. Various APP sequences have been shown to: lower intracellular calcium (APP_s), limit the ability of cells to maintain low concentrations of intracellular calcium (Aß), release hydrogen peroxide (Aß), induce gap junctions (APP C-97) and now, confer resistance to hydrogen peroxide (APP C-105). These facts strongly suggest that APP is an important regulator of cellular homeostasis, maintaining influence over subordinate defense mechanisms designed to protect cells against calcium and hydrogen peroxide. If this is the case, dysfunctions in APP processing over time may lead to manifestation of Alzheimer's disease.

An important implication of the finding that APP C-105 overexpression can confer resistance to hydrogen peroxide is that it permits a straightforward test of the hypothesis that free radical protection mechanisms are compromised in Alzheimer's disease. The balance existing between prooxidants and defense mechanisms could be threatened by mutations in the amyloid precursor protein which cause familial Alzheimer's disease. Multiple FAD-transfected clones could be tested to determine how PC12 vulnerability to hydrogen peroxide is affected.

Finally, it would be interesting to learn whether there is a connection between clonal susceptibility to NGF-induced death, and altered vulnerability to A23187 and hydrogen peroxide. Other APP C-100-transfected clones have been created which do not die in response to NGF (Sandhu, Kim et al. , 1996). The latter could

be tested to see whether they exhibit altered responses to A23187 and hydrogen peroxide.

Bibliography

Anonymous. (1995) *Current Protocols in Molecular Biology*. John Wiley & Sons.

Abraham, C.R., Selkoe, D.J., and Potter, H. , 1988. Immunochemical identification of the serine protease inhibitor, α1-antichymotrypsin in the brain amyloid deposits of Alzheimer's disease. *Cell, 52,* 487-501.

Adunsky, A., Baram, D., Hershkowitz, M., and Mekori, Y.A. , 1991. Increased cytosolic free calcium in lymphocytes of Alzheimer patients. *Journal of Neuroimmunology, 33,* 167-172.

Anderson, J.P., Chen, Y., Kim, K.S., and Robakis, N.K. , 1992. An alternative secretase cleavage produces soluble Alzheimer amyloid precursor protein containing a potentially amyloidogenic sequence. *Journal of Neurochemistry, 59,* 2328-2331.

Araki, W., Kitaguchi, N., Tokushima, Y., Ishii, K., Aratake, H., Shimohama, S., Nakamura, S., and Kimura, J. , 1991. Trophic effect of β-amyloid precursor protein on cerebral cortical neurons in culture. *Biochemical and Biophysical Research Communications, 181,* 265-271.

Araujo, D.M. and Cotman, C.W. , 1992. β-Amyloid stimulates glial cells in vitro to produce growth factors that accumulate in senile plaques in Alzheimer's disease. *Brain Research, 569,* 141-145.

Arispe, N., Rojas, E., and Pollard, H.B. , 1993. Alzheimer disease amyloid β protein forms calcium channels in bilayer membranes: blockade by tromethamine and aluminum. *Proceedings of the National Academy of Sciences of the United States of America, 90,* 567-571.

Balasubramanian, S.V., Sikdar, S.K., and Easwaran, K.R.K. , 1992. Bilayers containing calcium ionophore A23187 form channels. *Biochemical and Biophysical Research Communications, 189,* 1038-1042.

Bast, A. and Goris, R.J.A. , 1989. Oxidative stress, biochemistry and human disease. *Pharmaceutisch Weekblad Scientific Edition, 11,* 199-206.

Behl, C., Davis, J., Cole, G.M., and Schubert, D. , 1992. Vitamin E protects nerve cells from amyloid toxicity. *Biochemical and Biophysical Research Communications, 186 (2),* 944-950.

Behl, C., Davis, J.B., Klier, F.G., and Schubert, D. , 1994. Amyloid β peptide induces necrosis rather than apoptosis. *Brain Research, 645,* 253-264.

Behl, C., Davis, J.B., Lesley, R., and Schubert, D. , 1994. Hydrogen peroxide mediates amyloid β protein toxicity. *Cell, 77,* 817-827.

Berridge, M.J. , 1987. Inositol triphosphate and diacylglycerol: two interacting second messengers. *Annual Review of Biochemistry, 56,* 159-193.

Berridge, M.J. and Irvine, R.F. , 1989. Inositol phosphates and cell signalling. *Nature, 341,* 197-204.

Berridge, M.V. and Tan, A.S. , 1993. Characterization of the cellular reduction of 3-(4,5-dimethylthiazole-2-yl)-2,5-diphenyltetrazolium bromide (MTT): subcellular localization, substrate dependence, and involvement of mitochondrial electron transport in MTT reduction. *Archives of Biochemistry and Biophysics, 303,* 474-482.

Bertolino, M. and Llinas, R.R. , 1992. The central role of voltage-activated and receptor-operated calcium channels in neuronal cells. *Annual Review of Pharmacology and Toxicology, 32,* 399-421.

Braune, S. , 1991. Is ganglioside GM1 effective in the treatment of stroke? *Drugs and Aging, 1,* 57-66.

Bredt, D.S. and Snyder, S.H. , 1990. Isolation of nitric oxide synthetase, a calmodulin-requiring enzyme. *Proceedings of the National Academy of Sciences of the United States of America, 87,* 682-685.

Breen, K.C., Bruce, M., and Anderton, B.H. , 1991. Beta amyloid precursor protein mediates neuronal cell-cell and cell-surface adhesion. *Journal of Neuroscience Research, 28,* 90-100.

Busciglio, J., Gabuzda, D.H., Matsudaira, P., and Yankner, B.A. , 1993. Generation of β-amyloid in the secretory pathway in neuronal and nonneuronal cells. *Proceedings of the National Academy of Sciences of the United States of America, 90,* 2092-2096.

Busciglio, J., Lorenzo, A., and Yankner, B.A. , 1992. Methodological variables in the assessment of beta amyloid neurotoxicity. *Neurobiology of Aging, 13,* 609-612.

Busciglio, J., Yeh, J., and Yankner, B.A. , 1993. β-amyloid neurotoxicity in human cortical culture is not mediated by excitotoxins. *Journal of Neurochemistry, 61,* 1565-1568.

Bush, A.I., Multhaup, G., Moir, R.D., Williamson, T.G., Small, D.H., Rumble, B., Pollwein, P., Beyreuther, K., and Masters, C.L. , 1993. A novel zinc(II) binding site modulates the function of the βA4 amyloid protein precursor of Alzheimer's disease. *Journal of Biological Chemistry, 268,* 16109-16112.

Cai, X., Golde, T.E., and Younkin, S.G. , 1993. Release of excess amyloid β protein from a mutant amyloid β protein precursor. *Science, 259,* 514-516.

Chakraborti, S., Michael, J.R., and Patra, S.K. , 1991. Protein kinase C dependent and independent activation of phospholipase A_2 under calcium ionophore (A23187) exposure in rabbit pulmonary arterial smooth muscle cells. *FEBS Letters, 285,* 104-107.

Chartier-Harlin, M., Crawford, F., and Houlden, H. , 1991. Early-onset Alzheimer's disease caused by mutations at codon 717 of the beta-amyloid precursor protein gene. *Nature, 353,* 844-846.

Chen, M. and Yankner, B.A. , 1991. An antibody to the β amyloid and the amyloid precursor protein inhibits cell-substratum adhesion in many mammalian cell types. *Neuroscience Letters, 125,* 223-226.

Chen, W.-J., Goldstein, J.L., and Brown, M.S. , 1990. NPXY, a sequence often found in cytoplasmic tails, is required for coated-pit mediated internalization of the low density lipoprotein receptor. *Journal of Biological Chemistry, 265,* 3116-3123.

Chiueh, C.C. , 1994. Neurobiology of $NO^{\cdot}$ and $^{\cdot}OH$: Basic research and clinical relevance. *Annals of the New York Academy of Sciences, 738,* 279-281.

Choi, D.W. , 1985. Glutamate neurotoxicity in cortical cell culture is calcium dependent. *Neuroscience Letters, 58,* 293-297.

Choi, D.W. , 1988. Calcium-mediated neurotoxicity: relationship to specific channel types and role in ischemic damage. *Trends in Neurosciences, 11 (10),* 465-469.

Choi, D.W. , 1992. Excitotoxic cell death. *Journal of Neurobiology, 23,* 1261-1276.

Chuang, D.M. , 1989. Neurotransmitter receptors and phosphoinositide turnover. *Annual Review of Pharmacology and Toxicology, 29,* 71-110.

Citron, M., Oltersdorf, T., Haass, C., McConlogue, L., Yung, A.Y., Seubert, P., Vigo-Pelfrey, C., Lieberburg, I., and Selkoe, D.J. , 1992. Mutation of the β-amyloid precursor protein in familial Alzheimer's disease increases β-protein production. *Nature, 360,* 672-674.

Clark, M.A., Littlejohn, D., Mong, L., and Crooke, S.T. , 1986. Effect of leukotrienes, bradykinin and calcium ionophore (A23187) on bovine endothelial cells: release of prostacyclin. *Prostaglandins, 31,* 157-166.

Clemens, J.A. and Stephenson, D.T. , 1992. Implants containing β-amyloid protein are not neurotoxic to young and old rat brain. *Neurobiology of Aging, 13,* 581-586.

Cohen, G. , 1994. Enzymatic/nonenzymatic sources of oxyradicals and regulation of antioxidant defenses. *Annals of the New York Academy of Sciences, 738,* 8-14.

Contestabile, A., Virgili, M., Migani, P., and Barnabei, O. , 1990. Effects of short and long term ganglioside treatment on the recovery of neurochemical markers in the ibotenic acid-lesioned rat striatum. *Journal of Neuroscience Research, 26,* 483-487.

Corder, E.H., Saunders, A.M., and Strittmatter, W.J. , 1993. Gene dose of apolipoprotein E type 4 allele and the risk of Alzheimer's disease in late onset families. *Science, 261,* 921-923.

Coria, F., Castano, E., Larrondo-Lillo, M., Van Duinen, S., Shelanski, M.L., and Frangione, B. , 1988. Isolation and characterization of amyloid P component from Alzheimer's disease and other types of cerebral amyloidosis. *Laboratory Investigation, 58,* 454-458.

Cotgreave, I.A., Moldeus, P., and Orrenius, S. , 1988. Host biochemical defense mechanisms against prooxidants. *Annual Review of Pharmacology and Toxicology, 28,* 189-212.

Coyle, J.T. and Puttfarcken, P. , 1993. Oxidative stress, glutamate and neurodegenerative disorders. *Science, 262,* 689-694.

Cuello, A.C., Garofalo, L., Kenigsberg, R.L., and Maysinger, D. , 1989. Gangliosides potentiate in vivo and in vitro effects of nerve growth factor on central cholinergic neurons. *Proceedings of the National Academy of Sciences of the United States of America, 86,* 2056-2060.

Date, I., Felten, S.Y., and Felten, D.L. , 1989. Exogenous GM1 gangliosides induce partial recovery of the nigrostriatal dopaminergic system in MPTP-treated young mice, but not in aging mice. *Neuroscience Letters, 106,* 282-286.

Dawson, T.M., Hung, K., Dawson, V.L., Steiner, J.P., and Snyder, S.H. , 1995. Neuroprotective effects of gangliosides may involve inhibition of nitric oxide synthase. *Annals of Neurology, 37,* 115-118.

Dawson, T.M. and Snyder, S.H. , 1994. Gases as biological messengers: nitric oxide and carbon monoxide in the brain. *Journal of Neuroscience, 14,* 5147-5159.

Dawson, V.L., Dawson, T.M., and London, E.D. , 1991. Nitric oxide mediates glutamate neurotoxicity in primary cortical culture. *Proceedings of the National Academy of Sciences of the United States of America, 88,* 6368-6371.

De Erausquin, G.A., Manev, H., Guidotti, A., Costa, E., and Brooker, G. , 1990. Gangliosides normalize distorted single-cell intracellular free Ca^{+2} dynamics after toxic doses of glutamate in cerebellar granule cells. *Proceedings of the National Academy of Sciences of the United States of America, 87,* 8017-8021.

de Sauvage, F., Kruys, V., Marinx, O., Huez, G., and Octave, J.N. , 1992. Alternative polyadenylation of the amyloid protein precursor mRNA regulates translation. *The EMBO Journal, 11,* 3099-3103.

Drapier, J.-C. and Hibbs, J.B., Jr. , 1986. Murine cytotoxic activated macrophages inhibit aconitase in tumor cells. Inhibition involves the iron-sulfur prosthetic group and is reversible. *Journal of Clinical Investigation, 78,* 790-797.

Dyrks, T., Dyrks, E., Hartmann, T., Masters, C.L., and Beyreuther, K. , 1992. Amyloidogenicity of β/A4 and β/A4-bearing APP fragments by metal catalyzed oxidation. *Journal of Biological Chemistry, 267,* 18210-18217.

Dyrks, T., Dyrks, E., Monning, U., Urmoneit, B., Turner, J., and Beyreuther, K. , 1993. Generation of βA4 from the amyloid protein precursor and fragments thereof. *FEBS Letters, 335,* 89-93.

Emerich, D.F. and Walsh, T.J. , 1990. Ganglioside AGF2 promotes task-specific recovery and attenuates the cholinergic hypofunction induced by AF64A. *Brain Research, 527,* 299-307.

Emerich, D.F. and Walsh, T.J. , 1991. Ganglioside AGF2 prevents the cognitive impairments and cholinergic cell loss following intraventricular colchicine. *Experimental Neurology, 112,* 328-337.

Emre, M., Geula, C., Ransil, B.J., and Mesulam, M.-M. , 1992. The acute neurotoxicity and effects upon cholinergic axons of intracerebrally injected β-amyloid in the rat brain. *Neurobiology of Aging, 13,* 553-559.

Engstrom, I., Walsenstrom, A., and Ronquist, G. , 1993. Ionophore A23187 reduces energy charge by enhanced ion pumping in suspended human erythrocytes. *Scandinavian Journal of Clinical Laboratory Investigation, 53,* 239-246.

Ernst, R.L. and Hay, J.W. , 1994. The US economic and social costs of Alzheimer's disease revisited. *American Journal of Public Health, 84,* 1261-1264.

Esch, F.S., Keim, P.S., Beattie, E.C., Blacher, R.W., Culwell, A.R., Oltersdorf, T., McClure, D., and Ward, P.J. , 1990. Cleavage of amyloid β peptide during constitutive processing of its precursor. *Science, 248,* 1122-1124.

Facci, L., Leon, A., and Skaper, S.D. , 1990. Hypoglycemic neurotoxicity in vitro: involvement of excitatory amino acid receptors and attenuation by monosialoganglioside GM1. *Neuroscience, 37,* 709-716.

Favaron, M., Manev, H., Alho, H., Bertolino, M., Ferret, B., Guidotti, A., and Costa, E. , 1988. Gangliosides prevent glutamate and kainate neurotoxicity in primary neuronal cultures of neonatal rat cerebellum and cortex. *Proceedings of the National Academy of Sciences of the United States of America, 85,* 7351-7355.

Ferrari, G., Anderson, B.L., Stephens, R.M., Kaplan, D.R., and Greene, L.A. , 1995. Prevention of apoptotic neuronal death by GM1 ganglioside. *Journal of Biological Chemistry, 270,* 3074-3080.

Ferrari, G., Batistatou, A., and Greene, L.A. , 1993. Gangliosides rescue neuronal cells from death after trophic factor deprivation. *Journal of Neuroscience, 13 (5),* 1879-1887.

Ferrari, G., Fabris, M., and Gorio, A. , 1983. Gangliosides enhance neurite outgrowth in PC12 cells. *Developmental Brain Research, 8,* 215-221.

Figliomeni, B., Bacci, B., Panozzo, C., Fogarolo, F., Triban, C., and Fiori, M.G. , 1992. Effect of ganglioside treatment on axonal transport of cytoskeletal proteins. *Diabetes, 41,* 866-871.

Floyd, R.A. , 1990. Role of oxygen free redicals in carcinogenesis and brain ischemia. *FASEB Journal, 4,* 2587-2597.

Forloni, G., Chiesa, R., Smiroldo, S., Verga, L., Salmona, M., Tagliavini, F., and Angeretti, N. , 1993. Apoptosis mediated neurotoxicity induced by chronic application of β amyloid fragment 25-35. *NeuroReport, 4,* 523-526.

Fujita, K., Lazarovici, P., and Guroff, G. , 1989. Regulation of the differentiation of PC12 pheochromocytoma cells. *Environmental Health Perspectives, 80,* 127-142.

Fukuchi, K., Kamino, K., Deeb, S.S., Smith, A.C., Dang, T., and Martin, G.M. , 1992. Overexpression of amyloid precursor protein alters its normal processing and is associated

with neurotoxicity. *Biochemical and Biophysical Research Communications, 182 (1),* 165-173.

Games, D., Khan, K.M., Soriano, F.G., Keim, P.S., Davis, D.L., Bryant, K., and Lieberburg, I. , 1992. Lack of Alzheimer pathology after β-amyloid injections in rat brain. *Neurobiology of Aging, 13,* 569-576.

Ghiso, J., Gardella, J.E., Liem, L., Gorevic, P.D., and Frangione, B. , 1994. Characterization of a novel processing pathway for Alzheimer's amyloid β precursor protein. *Neuroscience Letters, 171,* 213-216.

Ghiso, J., Rostagno, A., Gardella, J.E., Liem, L., Gorevic, P.D., and Frangione, B. , 1992. A 109-amino-acid C-terminal fragment of Alzheimer's-disease amyloid precursor protein contains a sequence, -RHDS-, that promotes cell adhesion. *Biochemical Journal, 288,* 1053-1059.

Goate, A., Chartier-Harlin, M., Mullan, M., Brown, J., Crawford, F., Fidani, L., Giuffra, L., Haynes, A., Irving, N., James, L., Mant, R., Newton, P., Rooke, K., Roques, P., Talbot, C., Pericak-Vance, M., Roses, A.D., Williamson, R., Rossor, M., Owen, M., and Hardy, J. , 1991. Segregation of a missense mutation in the amyloid precursor protein gene with familial Alzheimer's disease. *Nature, 349,* 704-706.

Golconda, M.S., Ueda, N., and Shah, S.V. , 1993. Evidence suggesting that iron and calcium are interrelated in oxidant-induced DNA damage. *Kidney International, 44,* 1228-1234.

Golde, T.E., Estus, S., Younkin, L.H., Selkoe, D.J., and Younkin, S.G. , 1992. Processing of the amyloid protein precursor to potentially amyloidogenic derivatives. *Science, 255,* 728-730.

Gomez-Pinilla, F., Cummings, B.J., and Cotman, C.W. , 1990. Induction of basic fibroblast growth factor in Alzheimer's disease pathology. *NeuroReport, 1,* 211-214.

Greene, L.A. , 1978. Nerve growth factor prevents the death and stimulates neuronal differentiation of clonal PC12 pheochromocytoma cells in serum-free medium. *Journal of Cell Biology, 78,* 747-755.

Greene, L.A. and Tischler, A.S. , 1976. Establishment of a noradrenergic clonal line of rat adrenal pheochromocytoma cells which respond to nerve growth factor. *Proceedings of the National Academy of Sciences of the United States of America, 73,* 2424-2428.

Greene, L.A. and Tischler, A.S. , 1982. PC12 pheochromocytoma cultures in neurobiological research. *Advances in Cellular Neurobiology, 3,* 373-414.

Griffin, W.S.T., Stanley, L.C., Ling, C., White, L., MacLeod, V., Perrot, L.J., White, C.L., III, and Araoz, C. , 1989. Brain interleukin-1 and the S-100 immunoreactivity are elevated in Down sydrome and Alzheimer's disease. *Proceedings of the National Academy of Sciences of the United States of America, 86,* 7611-7615.

Grundke-Iqbal, I., Iqbal, K., Tung, Y., Quinlan, M., Wisniewski, H., and Binder, L. , 1986. Abnormal phosphorylation of the microtubule-associated protein τ (tau) in Alzheimer cytoskeletal pathology. *Proceedings of the National Academy of Sciences of the United States of America, 83,* 4913-4917.

Gutteridge, J.M.C. , 1994. Hydroxyl radicals, iron, oxidative stress and neurodegeneration. *Annals of the New York Academy of Sciences, 738,* 201-213.

Haass, C., Hung, A.Y., Schlossmacher, M.G., Oltersdorf, T., Teplow, D.B., and Selkoe, D.J. , 1993. Normal cellular processing of the β-amyloid precursor protein results in the secretion of the amyloid β peptide and related molecules. *Annals of the New York Academy of Sciences, 695,* 109-116.

Haass, C., Hung, A.Y., Schlossmacher, M.G., Teplow, D.B., and Selkoe, D.J. , 1993. β-Amyloid peptide and a 3-kDa fragment are derived by distinct cellular mechanisms. *Journal of Biological Chemistry, 268 (5),* 3021-3024.

Haass, C., Schlossmacher, M.G., Hung, A.Y., Vigo-Pelfrey, C., Mellon, A., Ostaszewski, B.L., Lieberburg, I., Koo, E.H., Schenk, D.B., Teplow, D.B., and Selkoe, D.J. , 1992. Amyloid β-peptide is produced by cultured cells during normal metabolism. *Nature, 359,* 322-325.

Halleck, M.M., Richburg, J.H., and Kauffman, F.C. , 1992. Reversible and irreversible oxidant injury to PC12 cells by hydrogen peroxide. *Free Radical Biology and Medicine, 12,* 137-144.

Hansen, M.B. , 1989. Re-examination and further development of a precise and rapid dye method for measuring cell growth/cell kill. *Journal of Immunological Methods, 119,* 203-210.

Harman, D. , 1992. Role of free radicals in aging and disease. *Annals of the New York Academy of Sciences, 673,* 126-141.

Hendricks, L., van Duijn, C.M., Cras, P., Cruts, P., Cruts, M., Van Hul, W., van Harskamp, F., Warren, A., McInnis, M.G., Antonarakis, S.E., and Martin, J.J. , 1992.

Presenile dementia and cerebral haemorrhage linked to a mutation at codon 692 of the beta-amyloid precursor protein gene. *Nature Genetics, 1,* 218-221.

Higashi, H., Omori, A., and Yamagata, T. , 1992. Calmodulin, a ganglioside-binding protein. *Journal of Biological Chemistry, 267 (14),* 9831-9838.

Higashi, H. and Yamagata, T. , 1992. Mechanism for ganglioside-mediated modulation of a calmodulin-dependent enzyme. *Journal of Biological Chemistry, 267 (14),* 9839-9843.

Hinshaw, D.B., Sklar, L.A., Bohl, B., Schraufstatter, I.U., Hyslop, P.A., Rossi, M.W., Spragg, R.G., and Cochrane, C.G. , 1986. Cytoskeletal and morphologic impact of cellular oxidant injury. *American Journal of Pathology, 123,* 454-464.

Hokin, L.E. , 1985. Receptors and phosphoinositide-generated second messengers. *Annual Review of Biochemistry, 54,* 205-235.

Hong, S.L., McLaughin, N.J., Tzeng, C.Y., and Patton, G. , 1985. Prostacyclin synthesis and deacylation of phospholipids in human endothelial cells: comparison of thrombin, histamine and ionophore A23187. *Thrombosis Research, 38,* 1-10.

Hu, J. and El-Fakahany, E.E. , 1993. β-Amyloid 25-35 activates nitric oxide synthase in a neuronal clone. *NeuroReport, 4,* 760-762.

Hungund, B.L., Gokhale, V., Ortiz, A., Karpiak, S.E., and Mahadik, S.P. , 1990. Membrane fatty acids in primary and peri-ischemic cortical tissue following acute GM1 ganglioside treatment. *Society for Neuroscience, 16,* 942

Hungund, B.L., Reddy, M.V., Bharucha, V.A., and Mahadik, S.P. , 1990. Monosialogangliosides (GM1 and AGF2) reduce ethanol intoxication: sleep time, mortality, and cerebral Na^+/K^+ ATPase. *Drug Development Research, 19,* 443-451.

Hyslop, P.A., Hinshaw, D.B., Halsey, W.A., Jr., Schraufstatter, I.U., Sauerheber, R.D., Spragg, R.G., Jackson, J.H., and Cochrane, C.G. , 1988. Mechanisms of oxidant-mediated cell injury. The glycolytic and mitochondrial pathways of ADP phosphorylation are major intracellular targets inactivated by hydrogen peroxide. *Journal of Biological Chemistry, 263,* 1665-1675.

Itoh, T., Kanmura, Y., and Kuriyama, H. , 1985. A23187 increases calcium permeability of store sites more than of surface membranes in the rabbit mesenteric artery. *Journal of Physiology, 359,* 467-484.

Jackson, G.R., Sampath, D., Werrbach-Perez, K., and Perez-Polo, J.R. , 1994. Effects of nerve growth factor on catalase and glutathione peroxidase in a hydrogen peroxide-resistant pheochromocytoma subclone. *Brain Research, 634,* 69-76.

Jesberger, J.A. and Richardson, J.S. , 1991. Oxygen free radicals and brain dysfunction. *International Journal of Neuroscience, 57,* 1-17.

Jornot, L., Petersen, H., and Junod, A.F. , 1991. Differential protective effects of O-phenanthroline and catalase on H_2O_2-induced DNA damage and inhibition of protein synthesis in endothelial cells. *Journal of Cellular Physiology, 149,* 408-413.

Joseph, R. and Han, E. , 1992. Amyloid β-protein fragment 25-35 causes activation of cytoplasmic calcium in neurons. *Biochemical and Biophysical Research Communications, 184 (3),* 1441-1447.

Kang, J., Lemaire, H.G., and Unterbeck, A. , 1987. The precursor of Alzheimer's disease amyloid A4 protein resembles a cell-surface receptor. *Nature, 325,* 733-736.

Karpiak, S.E., Li, Y.S., and Mahadik, S.P. , 1986. Gangliosides (GM1 and AGF2) reduce mortality due to ischemia: protection of membrane function. *Stroke, 18,* 184-187.

Karpiak, S.E., Mahadik, S.P., and Wakade, C.G. , 1990. Ganglioside reduction of ischemic injury. *Critical Reviews in Neurobiology, 5,* 221-237.

Katzmann, R. , 1986. Alzheimer's disease. *New England Journal of Medicine, 314,* 964-973.

Kimura, M., Maeda, K., and Hayashi, S. , 1992. Cytosolic calcium increase in coronary endothelial cells after H_2O_2 exposure and the inhibitory effect of U78517F. *British Journal of Pharmacology, 107,* 488-493.

Kitaguchi, N., Takahashi, Y., and Tokushima, Y. , 1988. Novel precursor of Alzheimer's disease amyloid protein shows protease inhibitory activity. *Nature, 331,* 530-532.

Koh, J., Yang, L.L., and Cotman, C.W. , 1990. β-amyloid protein increases the vulnerability of cultured cortical neurons to excitotoxic damage. *Brain Research, 533,* 315-320.

Kojima, H., Gorio, A., Janigro, D., and Jonsson, G. , 1984. GM1 ganglioside enhanced regrowth of noradrenaline terminals in rat cerebral cortex lesioned by the neurotoxin 6-OHDA. *Neuroscience, 13,* 1011-1022.

Kolber, M.A. and Haynes, D.H. , 1981. Fluorescence study of the divalent cation-transport mechanism of ionophore A23187 in phospholipid membranes. *Biophysical Journal, 36,* 369-390.

Kowall, N.W., McKee, A.C., Yankner, B.A., and Beal, M.F. , 1992. In vivo neurotoxicity of beta amyloid [β(1-40)] and the β(25-35) fragment. *Neurobiology of Aging, 13,* 537-542.

Kozlowski, M.R., Spanoyannis, A., Manly, S.P., Fidel, S.A., and Neve, R.L. , 1992. The neurotoxic carboxy-terminal fragment of the Alzheimer amyloid precursor binds specifically to a neuronal cell surface molecule: pH dependence of the neurotoxicity and the binding. *Journal of Neuroscience, 12 (5),* 1679-1687.

Kumar, U., Dunlop, D., and Richardson, J.S. , 1994. Mitochondria from Alzheimer's fibroblasts show decreased uptake of calcium and increased sensitivity to free radicals. *Life Sciences, 54,* 1855-1860.

Le Quan Sang, K.H., Mignot, E., Gilbert, J.C., Huguet, R., Aquino, J.P., Regnier, O., and Devynck, M.A. , 1993. Platelet cytosolic free-calcium concentration is increased in aging and Alzheimer's disease. *Biological Psychiatry, 33,* 391-393.

LeBlanc, A.C. and Gambetti, P. , 1994. Production of Alzheimer 4kDa β-amyloid peptide requires the C-terminal cytosolic domain of the amyloid precursor protein. *Biochemical and Biophysical Research Communications, 204,* 1371-1380.

Lemaire, H.G., Salbaum, J.M., Multhaup, G., Kang, J., Bayney, R.M., Unterbeck, A., Beyreuther, K., and Muller-Hill, B. , 1989. The PreA4 695 precursor protein of Alzheimer's disease A4 amyloid is encoded by 16 exons. *Nucleic Acids Research, 17,* 517-522.

Lepoivre, M., Chenais, B., Yapo, A., Lemaire, G., Thelander, L., and Tenu, J.P. , 1990. Alterations of ribonucleotide reductase activity following induction of the nitrite-generating pathway in adenocarcinoma cells. *Journal of Biological Chemistry, 265,* 14143-14149.

Levy, E., Carman, M.D., Fernandez-Madrid, I.J., Power, M.D., Lieberburg, I., van Duinen, S.G., Bots, G.T.A.M., Luyendijk, W., and Frangione, B. , 1990. Mutation of the Alzheimer's disease amyloid gene in hereditary cerebral hemorrhage, Dutch-type. *Science, 248,* 1124-1126.

Levy-Lahad, E., Wasco, W., Poorkaj, P., Romano, D.M., Oshima, J., Pettingell, W.H., Yu, C., Jondro, P.D., Schmidt, S.D., Wang, K., Crowley, A.C., Fu, Y.-H., Guenette, S.Y., Galas, D., Nemens, E., Wijsman, E.M., Bird, T.D., Schellenberg, G.D., and Tanzi,

R.E. , 1995. Candidate gene for the chromosome 1 familial Alzheimer's disease locus. *Science, 269,* 973-977.

Levy-Lahad, E., Wijsman, E.M., Nemens, E., Anderson, L., Goddard, K.A.B., Weber, J., Bird, T.D., and Schellenberg, G.D. , 1995. A familial Alzheimer's disease locus on chromosome 1. *Science, 269,* 970-973.

Lipartiti, M., Lazzaro, A., Zanoni, R., Mazzari, S., Toffano, G., and Leon, A. , 1991. Monosialoganglioside GM1 reduces NMDA neurotoxicity in neonatal rat brain. *Experimental Neurology, 113,* 301-305.

Loveland, B.E., Johns, T.G., Mackay, I.R., Vaillant, F., Wang, Z.-X., and Hertzog, P.J. , 1992. Validation of the MTT assay for enumeration of cells in proliferative and antiproliferative assays. *Biochemistry International, 27,* 501-510.

Lukas, W. and Jones, K.A. , 1994. Cortical neurons containing calretinin are selectively resistant to calcium overload and excitotoxicity in vitro. *Neuroscience, 61,* 307-316.

Lynn, B.D., Marotta, C.A., and Nagy, J.I. , 1995. Propagation of intercellular calcium waves in PC12 cells overexpressing a carboxy-terminal fragment of amyloid precursor protein. *Neuroscience Letters, 199,* 21-24.

Mackenzie, I.R.A. , 1994. Senile plaques do not progressively accumulate with normal aging. *Acta Neuropathology, 87,* 520-525.

Macq, A.-F., Philippe, B., and Octave, J.N. , 1994. The amyloid peptide of Alzheimer's disease is not produced by internal initiation of translation generating C-terminal amyloidogenic fragments of its precursor. *Neuroscience Letters, 182,* 227-230.

Mahadik, S.P. (1992). Gangliosides: New generation of neuroprotective agents. In P.J. Marangos & H. Lal (Eds.), *Emerging Strategies in Neuroprotection.* (pp. 187-223). Boston: Birkhauser.

Mahadik, S.P., Hawver, D.B., Hungund, B.L., Li, Y.S., and Karpiak, S.E. , 1989. GM1 ganglioside treatment protects changes in membrane fatty acids and properties of Na^{+}, K^{+}-ATPase and Mg^{+2}-ATPase. *Journal of Neuroscience Research, 24,* 402-412.

Mahadik, S.P., Murthy, J., Ortiz, A., and Karpiak, S.E. , 1990. GM1 ganglioside treatment maintains capacity of ischemic tissue to defend against free radical damage. *Society for Neuroscience, 16,* 942

Mahley, R.W. , 1988. Apolipoprotein E: Cholesterol transport protein with expanding role in cell biology. *Science, 240,* 622-628.

Majerus, P.W., Ross, T.S., Cunningham, T.W., Caldwell, K.K., and Jefferson, A.B. , 1990. Recent insights in phosphatidylinositol signalling. *Cell, 63,* 459-465.

Manev, H., Favaron, M., Guidotti, A., and Costa, E. , 1989. Delayed increase of Ca^{+2} influx elicited by glutamate: Role in neuronal death. *Molecular Pharmacology, 36,* 106-112.

Manev, H., Favaron, M., Vicini, S., and Guidotti, A. , 1990. Ganglioside-mediated protection from glutamate-induced neuronal death. *Acta Neurobiol Exp, 50,* 475-488.

Manev, H., Favaron, M., Vicini, S., Guidotti, A., and Costa, E. , 1990. Glutamate-induced neuronal death in primary cultures of cerebellar granule cells: Protection by synthetic derivatives of endogenous sphingolipids. *Journal of Pharmacology and Experimental Therapeutics, 252,* 419-427.

Marini, M., Frabetti, F., Brunelli, M.A., and Raggi, M.A. , 1993. Inhibition of poly(ADP-ribose) polymerization preserves the glutathione pool and reverses cytotoxicity in hydrogen peroxide-treated lymphocytes. *Biochemical Pharmacology, 46,* 2139-2144.

Matsuda, S. , 1995. Protective effects of calcium antagonist (nitrendipine) on calcium ionophore A23187-induced liver cell injury. *Bulletin of Tokyo Medical and Dental University, 38,* 35-44.

Mattson, M.P. , 1994. Secreted forms of β-amyloid precursor protein modulate dendrite outgrowth and calcium responses to glutamate in cultured embryonic hippocampal neurons. *Journal of Neurobiology, 25,* 439-450.

Mattson, M.P., Cheng, B., Culwell, A.R., Esch, F.S., Lieberburg, I., and Rydel, R.E. , 1993. Evidence for excitoprotective and intraneuronal calcium-regulating roles for secreted forms of the β-amyloid precursor protein. *Neuron, 10,* 243-254.

Mattson, M.P., Cheng, B., Davis, D., Bryant, K., Lieberburg, I., and Rydel, R.E. , 1992. β-amyloid peptides destabilize calcium homeostasis and render human cortical neurons vulnerable to excitotoxicity. *Journal of Neuroscience, 12 (2),* 376-389.

Mattson, M.P., Engle, M.G., and Rychlik, B. , 1991. Effects of elevated intracellular calcium levels on the cytoskeleton and tau in cultured human cortical neurons. *Molecular and Chemical Neuropathology, 15,* 117-142.

McCoy, K., Mullins, R., Newcomb, T., Ng, G., Pavlinkova, G., Polinsky, R., Nee, L., and Sisken, J. , 1993. Serum- and bradykinin-induced calcium transients in familial Alzheimer's fibroblasts. *Neurobiology of Aging, 14,* 447-455.

McDonald, L.J. and Moss, J. , 1993. Stimulation by nitric oxide of an NAD linkage to glyceraldehyde-3-phosphate dehydrogenase. *Proceedings of the National Academy of Sciences of the United States of America, 90,* 6238-6241.

Meister, A. and Anderson, M.E. , 1996. Glutathione. *Annual Review of Biochemistry, 52,* 711-760.

Michel, P.P., Vyas, S., Anglade, P., Ruberg, M., and Agid, Y. , 1994. Morphological and molecular characterization of the response of differentiated PC12 cells to calcium stress. *European Journal of Neuroscience, 6,* 577-186.

Milward, E.A., Papadopoulos, R., Fuller, S.J., Moir, R.D., Small, D., Beyreuther, K., and Masters, C.L. , 1992. The amyloid protein precursor of Alzheimer's disease is a mediator of the effects of nerve growth factor on neurite outgrowth. *Neuron, 9,* 129-137.

Mishra, O.P., Delivoria-Papadopoulos, M., Cahillane, G., and Wagerle, L.C. , 1989. Lipid peroxidation as the mechanism of modification of the afffinity of Na^+, K^+, -ATPase active sites for ATP, K^+, Na^+ and strophanthidin in vitro. *Neurochemical Research, 14,* 845-851.

Miyazaki, K., Hasegawa, M., Funahashi, K., and Umeda, M. , 1993. A metalloproteinase inhibitor domain in Alzheimer amyloid protein precursor. *Nature, 362,* 839-841.

Moolten, F. and Wells, J.M. , 1993. Curability of tumors bearing herpes thymidine kinase genes transferred by retroviral vectors. *Journal of the National Cancer Institute, 82,* 297-300.

Moslen, M.T. (1992). Protection against free radical-mediated tissue injury. In M.T. Moslen & C.V. Smith (Eds.), *Free Radical Mechanisms of Tissue Injury.* (pp. 203-215). Boca Raton: CRC Press.

Mosmann, T. , 1983. Rapid colorimetric assay for cellular growth and survival: application to proliferation and cytotoxicity assays. *Journal of Immunological Methods, 65,* 55-63.

Mullan, M., Crawford, F., Axelman, K., Houlden, H., Lilius, L., Winblad, B., and Lannfelt, L. , 1992. A pathogenic mutation for probable Alzheimer's disease in the APP gene at the N-terminus of β-amyloid. *Nature Genetics, 1,* 345-347.

Mullan, M., Houlden, H., Windelspecht, M., Fidani, L., Lombardi, C., Diaz, P., Rossor, M., Crook, R., Hardy, J., Duff, K., and Crawford, F. , 1992. A locus for familial early onset Alzheimer's disease on the long arm of chromosome 14, proximal to α1-antichymotrypsin. *Nature Genetics, 1,* 340-342.

Murrell, J., Farlow, M., and Ghetti, B. , 1991. A mutation in the amyloid precursor protein associated with hereditary Alzheimer's disease. *Science, 254,* 97-98.

Mutoh, T., Tokuda, A., Miyadai, T., Hamaguchi, M., and Fujiki, N. , 1995. Ganglioside GM1 binds to the Trk protein and regulates receptor function. *Proceedings of the National Academy of Sciences of the United States of America, 92,* 5087-5091.

Nakamura, K., Wu, G., and Ledeen, R.W. , 1992. Protection of Neuro-2A cells against calcium ionophore cytotoxicity by gangliosides. *Journal of Neuroscience Research, 31,* 245-253.

Namba, Y., Tomonaga, M., Kawasaki, H., Otomo, E., and Ikeda, K. , 1991. Apolipoprotein E immunoreactivity in cerebral deposits and neurofibrillary tangles in Alzheimer's disease and kuru plaque amyloid in Creutzfeldt-Jakob disease. *Brain Research, 541,* 163-166.

Nath, K.A., Enright, H., Nutter, L., Fischereder, M., Zou, J.N., and Hebbel, R.P. , 1994. Effect of pyruvate on oxidant injury to isolated and cellular DNA. *Kidney International, 45,* 166-176.

Nathan, C.F. and Hibbs, J.B., Jr. , 1991. Role of nitric oxide synthesis in macrophage antimicrobial activity. *Current Opinion in Immunology, 3,* 65-70.

Nicoletti, F., Cavallaro, S., Bruno, V., Virgili, M., Catania, M.V., Contestabile, A., and Canonico, P.L. , 1989. Gangliosides attenuate NMDA receptor-mediated excitatory amino acid release in cultured cerebellar neurons. *Neuropharmacology, 28,* 1283-1286.

Nicotera, P., Bellomo, G., and Orrenius, S. , 1992. Calcium-mediated mechanisms in chemically induced cell death. *Annual Review of Pharmacology and Toxicology, 32,* 449-470.

Ninomiya, H., Roch, J., Sundsmo, M.P., Otero, D.A.C., and Saitoh, T. , 1993. Amino acid sequence RERMS represents the active domain of amyloid β/A4 protein precursor that promotes fibroblast growth. *Journal of Cell Biology, 121 (4),* 879-886.

Nishimoto, I., Okamoto, T., Matsuura, Y., Takahashi, S., Murayama, Y., and Ogata, E. , 1993. Alzheimer amyloid protein precursor complexes with brain GTP-binding protein G_o. *Nature, 362,* 75-79.

Olanow, C.W. , 1993. A radical hypothesis for neurodegeneration. *Trends in Neurosciences, 16,* 439-443.

Olney, J.W. , 1990. Excitotoxic amino acids and neuropsychiatric disorders. *Annual Review of Pharmacology and Toxicology, 30,* 47-71.

Oltersdorf, T., Ward, P.J., and Henriksson, T. , 1990. The Alzheimer amyloid precursor protein. Identification of a stable intermediate in the biosynthetic/degradative pathway. *Journal of Biological Chemistry, 265,* 4492-4497.

Orrenius, S., Burkitt, M.J., Kass, G.E.N., Dypbukt, J.M., and Nicotera, P. , 1992. Calcium ions and oxidative cell injury. *Annals of Neurology, 32,* S33-S42.

Orrenius, S., McConkey, D.J., Bellomo, G., and Nicotera, P. , 1989. Role of Ca^{2+} in toxic cell killing. *TIPS, 10,* 281-285.

Pahlsson, P., Shakin-Eshleman, S.H., and Spitalnik, S.L. , 1992. N-linked glycosylation of β-amyloid precursor protein. *Biochemical and Biophysical Research Communications, 189,* 1667-1673.

Pericak-Vance, M., Bebout, J.L., and Gaskell, P.C. , 1991. Linkage studies in familial Alzheimer's disease: Evidence for chromosome 19 linkage. *American Journal of Human Genetics, 48,* 1034-1050.

Petroni, A., Bertazzo, A., Sarti, S., and Galli, C. , 1989. Accumulation of arachidonic acid cyclo- and lipoxygenase metabolites products in rat brain during ischemia and reperfusion: effects of treatment with GM1-lactone. *Journal of Neurochemistry, 53,* 747-752.

Phoenix, J., Edwards, R.H.T., and Jackson, M.J. , 1991. The effect of vitamin E analogues and long hydrocarbon chain compounds on calcium-induced muscle damage. A novel role for α -tocopherol? *Biochimica et Biophysica Acta, 1097,* 212-218.

Pike, C.J., Burdick, D., Walencewicz, A.J., Glabe, C.G., and Cotman, C.W. , 1993. Neurodegeneration induced by β-amyloid peptides in vitro: The role of peptide assembly state. *Journal of Neuroscience, 13(4),* 1676-1687.

Pike, C.J. and Cotman, C.W. , 1995. Calretinin-immunoreactive neurons are resistant to β-amyloid toxicity in vitro. *Brain Research, 671,* 293-298.

Podlisny, M.B., Stephenson, D.T., Frosch, M.P., Lieberburg, I., Clemens, J.A., and Selkoe, D.J. , 1992. Synthetic amyloid β-protein fails to produce specific neurotoxicity in monkey cerebral cortex. *Neurobiology of Aging, 13,* 561-567.

Ponte, P., Gonzalez-DeWhitt, P., and Schilling, J. , 1988. A new A4 amyloid mRNA contains a domain homologous to serine proteinase inhibitors. *Nature, 331,* 525-527.

Pressman, B.C. , 1976. Biological applications of ionophores. *Annual Review of Biochemistry, 45,* 501-530.

Puskin, J.S., Visties, M.I., and Wene, M.T. , 1981. A fluorecence study of A23187 interaction with phospholipid vesicles. *Archives of Biochemistry and Biophysics, 206,* 164-172.

Querfurth, H.W. and Selkoe, D.J. , 1994. Calcium ionophore increases amyloid β production by cultured cells. *Biochemistry, 33,* 4550-4561.

Rengasamy, A. and Johns, R.A. , 1994. Effect of hydrogen peroxide and catalase on rat cerebellum nitric oxide synthase. *Biochemical Pharmacology, 48,* 423-425.

Richter, C. and Kass, G.E.N. , 1991. Oxidative stress in mitochondria: its relationship to cellular Ca^{+2} homeostasis, cell death, proliferation and differentiation. *Chem -Biol Interactions, 77,* 1-23.

Roberts, G.W., Gentleman, S.M., Lynch, A., Murray, L., Landon, M., and Graham, D.I. , 1994. β amyloid protein deposition in the brain after severe head injury: implications for the pathogenesis of Alzheimer's disease. *Journal of Neurology, Neurosurgery and Psychiatry, 57,* 419-425.

Rogaev, E.I., Sherrington, R., Rogaeva, E.A., Levesque, G., Ikeda, M., Liang, Y., Chi, H., Lin, C., Holman, K., and Tsuda, T. , 1995. Familial Alzheimer's disease in kindreds with missense mutations in a gene on chromosome 1 related to the Alzheimer's disease type 3 gene. *Nature, 376,* 775-778.

Rosen, D.R., Martin-Morris, L., Luo, L., and White, K. , 1989. A Drosophila gene encoding the human β-amyloid protein precursor. *Proceedings of the National Academy of Sciences of the United States of America, 89,* 2478-2482.

Ross, A.H. , 1991. Identification of tyrosine kinase Trk as a nerve growth factor receptor. *Cell Regulation, 2,* 685-690.

Rothman, S. , 1984. Synaptic release of excitatory amino acid neurotransmitter mediates anoxic neuronal death. *Journal of Neuroscience, 4,* 1884-1891.

Rukenstein, A., Rydel, R.E., and Greene, L.A. , 1993. Multiple agents rescue PC12 cells from serum-free cell death by translation- and transcription-independent mechanisms. *Journal of Neuroscience, 11 (8),* 2552-2563.

Rush, D.K., Aschimies, S., and Merriman, M.C. , 1992. Intracerebral β-amyloid(25-35) produces tissue damage: Is it neurotoxic? *Neurobiology of Aging, 13,* 591-594.

Sagara, Y., Dargusch, R., Klier, F.G., Schubert, D., and Behl, C. , 1996. Increased antioxidant enzyme activity in amyloid β protein-resistant cells. *Journal of Neuroscience, 16,* 497-505.

Saitoh, T., Sundsmo, M.P., Roch, J., Kimura, N., Cole, G., Schubert, D., Oltersdorf, T., and Schenk, D.B. , 1989. Secreted form of amyloid β protein precursor is involved in the growth regulation of fibroblasts. *Cell, 58,* 615-622.

Salbaum, J.M., Weidemann, A., Lemaire, H.G., Masters, C.L., and Beyreuther, K. , 1988. The promoter of Alzheimer's disease amyloid A4 precursor gene. *The EMBO Journal, 7,* 2807-2813.

Sandhu, F.A., Kim, Y., Lapan, K.A., Salim, M., and Aliuddin, V. , 1996. Expression of the C-terminus of the amyloid precursor protein alters growth factor responsiveness in stably transfected PC12 cells. *Proceedings of the National Academy of Sciences of the United States of America, 93,* 2180-2185.

Saqr, H.E., Pearl, D.K., and Yates, A.J. , 1993. A review and predictive models of ganglioside uptake by biological membranes. *Journal of Neurochemistry, 61,* 1-17.

Saunders, A.M., Strittmatter, W.J., Schmechel, D.E., St.George-Hyslop, P., Pericak-Vance, M., Joo, S.H., Rosi, B.L., Gusella, J.F., Crapper-MacLachlan, D.R., Alberts, M.J., Hulette, C., Crain, B.J., Goldgaber, D., and Roses, A.D. , 1993. Association of apolipoprotein E allele E4 with late-onset familial and sporadic Alzheimer's disease. *Neurology, 43,* 1467-1472.

Schellenberg, G.D., Bird, T.D., Wijsman, E.M., Orr, H.T., Anderson, L., Nemens, E., White, J.A., Bonnycastle, L., Weber, J.L., Alonso, M.E., Potter, H., Heston, L.L., and Martin, G.M. , 1992. Genetic linkage evidence for a familial Alzheimer's disease locus on chromosome 14. *Science, 258,* 668-671.

Schraufstatter, I.U., Hinshaw, D.B., Hyslop, P.A., Spragg, R.G., and Cochrane, C.G. , 1985. Glutathione cycle activity and pyridine nucleotide levels in oxidant-induced injury of cells. *Journal of Clinical Investigation, 9,* 1131-1139.

Schraufstatter, I.U., Hinshaw, D.B., Hyslop, P.A., Spragg, R.G., and Cochrane, C.G. , 1986. Oxidant injury of cells. *Journal of Clinical Investigation, 77,* 1312-1320.

Schubert, D., Jin, L., Saitoh, T., and Cole, G. , 1989. The regulation of amyloid β protein precursor secretion and its modulatory role in cell adhesion. *Neuron, 3,* 689-694.

Selkoe, D.J. , 1991. The molecular pathology of Alzheimer's disease. *Neuron, 6,* 487-498.

Selkoe, D.J. , 1994. Normal and abnormal biology of the β-amyloid precursor protein. *Annual Review of Neuroscience, 17,* 489-517.

Seren, M.S., Rubini, R., Lazzaro, A., Zanoni, R., Fiori, M.G., and Leon, A. , 1990. Protective effects of a monosialoganglioside derivative following transitory forebrain ischemia in rats. *Stroke, 21,* 1607-1612.

Seubert, P., Oltersdorf, T., Lee, M.G., Barbour, R., Blomquist, C., Davis, D.L., Bryant, K., Fritz, L.C., Galasko, D., Thal, L.J., Lieberburg, I., and Schenk, D.B. , 1993. Secretion of β-amyloid precursor protein cleaved at the amino terminus of the β-amyloid peptide. *Nature, 361,* 260-263.

Seubert, P., Vigo-Pelfrey, C., and Esch, F.S. , 1992. Isolation and quantitation of soluble Alzheimer's β-peptide from biological fluids. *Nature, 359,* 325-327.

Shearman, M.S., Ragan, C.I., and Iversen, L.L. , 1994. Inhibition of PC12 cell redox activity is a specific, early indicator of the mechanism of β-amyloid-mediated cell death. *Proceedings of the National Academy of Sciences of the United States of America, 91,* 1470-1474.

Sherrington, R., Rogaev, E.I., Liang, Y., Rogaeva, E.A., Levesque, G., Ikeda, M., Chi, H., Lin, C., Li, G., Holman, K., Tsuda, T., Mar, L., Foncin, J.-F., Bruni, A.C., Montesi, M.P., Sorbi, S., Rainero, I., Pinessi, L., Nee, L., Chumakov, I., Pollen, D., Brookes, A., Sanseau, P., Polinsky, R.J., Wasco, W., Da Silva, H.A.R., Haines, J.L., Pericak-Vance, M.A., Tanzi, R.E., Roses, A.D., Fraser, P.E., Rommens, J.M., and St.George-Hyslop, P.H. , 1995. Cloning of a gene bearing missense mutations in early-onset familial Alzheimer's disease. *Nature, 375,* 754-760.

Shier, W.T., DuBourdieu, D.J., and Wang, H.L. , 1991. Role of lipid metabolism in cell killing by calcium plus ionophore A23187. *J Biochem Toxicology, 6,* 7-17.

Shifman, M. , 1991. The effect of gangliosides upon the recovery of aspartate/glutaminergic synapses in the striatum after lesions of the rat sensorimotor cortex. *Brain Research, 568,* 323-324.

Shoji, M., Golde, T., Ghiso, J., Cheung, T.T., Estus, S., Shaffer, L.M., Cai, X., McKay, D.M., Tintner, R., Frangione, B., and Younkin, S.G. , 1992. Production of the Alzheimer amyloid β protein by normal proteolytic processing. *Science, 258,* 126-129.

Sisodia, S.S. , 1992. Beta amyloid precursor protein cleavage by a membrane-bound protease. *Proceedings of the National Academy of Sciences of the United States of America, 89,* 6075-6079.

Sisodia, S.S., Koo, E.H., Beyreuther, K., Unterbeck, A., and Price, D.L. , 1990. Evidence that β-amyloid is not derived by normal processing. *Science, 248,* 492-495.

Skaper, S.D., Facci, L., and Leon, A. , 1990. Gangliosides attenuate the delayed neurotoxicity of aspartic acid in vitro. *Neuroscience Letters, 117,* 154-159.

Skaper, S.D., Facci, L., Milani, D., and Leon, A. , 1989. Monosialoganglioside GM1 protects against anoxia-induced neuronal death in vitro. *Experimental Neurology, 106,* 297-305.

Skaper, S.D., Leon, A., and Facci, L. , 1991. Death of cultured hippocampal pyramidal neurons induced by pathological activation of N-Methyl-D-Aspartate receptors is reduced by monosialogangliosides. *Journal of Pharmacology and Experimental Therapeutics, 259,* 452-457.

Slater, T.F., Sawyer, B., and Strauli, U. , 1963. Studies on succinate-tetrazolium reductase systems III. Points of coupling of four different tetrazolium salts. *Biochimica et Biophysica Acta, 77,* 383-393.

Small, D.H. , 1994. A heparin binding domain in the amyloid protein precursor of Alzheimer's disease is involved in the regulation of neurite outgrowth. *Journal of Neuroscience, 14,* 2117-2127.

Smith, C.V. (1992). Free radical mechanisms of tissue injury. In M.T. Moslen & C.V. Smith (Eds.), *Free radical mechanisms of tissue injury.* (pp. 1-22). Boca Raton: CRC Press.

Smith, R.P., Higuchi, D.A., and Broze, G.J. , 1990. Platelet coagulation factor XIa-inhibitor, a form of Alzheimer amyloid precursor protein. *Science, 248,* 1126-1128.

Smith-Swintosky, V.L., Pettigrew, L.C., Craddock, S.D., Culwell, A.R., Rydel, R.E., and Mattson, M.P. , 1994. Secreted forms of β-amyloid precursor protein protect against ischemic brain injury. *Journal of Neurochemistry, 63,* 781-784.

Snow, A.D., Nochlin, D., Sumi, S., Bird, T.D., and Wight, T.N. , 1988. Immunolocalization of heparan sulfate proteoglycans to "primitive plaques" and multi-core prion positive plaques in familial dementia. *Alzheimer's Disease and Associated Disorders, 2,* 232-240.

Sola, C., Mengod, G., Probst, A., and Palacios, J.M. , 1993. Differential regional and cellular distribution of β-amyloid precursor protein messenger RNAs containing and lacking the kunitz protease inhibitor domain in the brain of the human, rat and mouse. *Neuroscience, 53,* 267

Sprecher, C.A., Grant, F.J., Grimm, G., O'Hara, P.J., Norris, F., Norris, K., and Foster, D.C. , 1993. Molecular cloning of the cDNA for a human amyloid precursor protein homolog: Evidence for a multigene family. *Biochemistry, 32,* 4481-4486.

St.George-Hyslop, P., Haines, J., Rogaev, E., Mortilla, M., Vaula, G., Pericak-Vance, M., Foncin, J., Montesi, M., Bruni, A., Sorbi, S., Rainero, I., Pinessi, L., Pollen, D., Polinsky, R., Nee, L., Kennedy, J., Macciardi, F., Rogaeva, E., and Liang, Y. , 1992. Genetic evidence for a novel familial Alzheimer's disease locus on chromosome 14. *Nature Genetics, 2,* 330-334.

Strittmatter, W.J., Saunders, A.M., Schmechel, D.E., Pericak-Vance, M., Enghild, J., Salvesen, G.S., and Roses, A.D. , 1993. Apolipoprotein E: High-avidity binding to β-amyloid and increased frequency of type 4 allele in late-onset familial Alzheimer disease. *Proceedings of the National Academy of Sciences of the United States of America, 90,* 1977-1981.

Strittmatter, W.J., Weisgraber, K.H., Huang, D.Y., Dong, L.-M., Salvesen, G.S., Pericak-Vance, M., Schmechel, D.E., Saunders, A.M., Goldgaber, D., and Roses, A.D. , 1993. Binding of human apolipoprotein E to synthetic amyloid β peptide: Isoform-specific effects and implications for late-onset Alzheimer disease. *Proceedings of the National Academy of Sciences of the United States of America, 90,* 8098-8102.

Struble, R.G., Powers, R.E., Casanova, M.F., Kitt, C.A., Brown, E.C., and Price, D.L. , 1987. Neuropeptidergic systems in plaques of Alzheimer's disease. *Journal of Neuropathology and Experimental Neurology, 46,* 567-584.

Stryer, L. (1988). *Biochemistry.* New York: W. H. Freeman and Company.

Stull, N.D., Schneider, J.S., and Iacovitti, L. , 1994. GM1 ganglioside partially rescues cultured dopaminergic neurons from MPP^+ -induced damage: dependence on initial damage and time of treatment. *Brain Research, 640,* 308-315.

Takashima, A., Noguchi, K., Sato, K., Hoshino, T., and Imahori, K. , 1993. Tau protein kinase I is essential for amyloid β-protein-induced neurotoxicity. *Proceedings of the National Academy of Sciences of the United States of America, 90,* 7789-7793.

Tanzi, R.E., McClatchey, A.I., Lamperti, E.D., Villa-Komaroff, L., Gusella, J.F., and Neve, R.L. , 1988. Protease inhibitor domain encoded by an amyloid protein precursor mRNA associtated with Alzheimer disease. *Nature, 331,* 528-530.

Thomas, J.M.F., Chap, H., and Douse-Blazy, L. , 1981. Calcium ionophore A23187 induces arachidonic acid release from phosphatidylcholine in cultured human endothelial cells. *Biochemical and Biophysical Research Communications, 103,* 819-824.

Vaccarino, F.M., Guidotti, A., and Costa, E. , 1987. Ganglioside inhibition of glutamate-mediated protein kinase C translocation in primary cultures of cerebellar neurons. *Proceedings of the National Academy of Sciences of the United States of America, 84,* 8707-8711.

van Broeckhoven, C. , 1995. Presenilins and Alzheimer's disease. *Nature Genetics, 11,* 230-232.

van Broeckhoven, C., Backhovens, H., Cruts, M., De Winter, G., Bruyland, M., Cras, P., and Martin, J. , 1992. Mapping of a gene predisposing to early-onset Alzheimer's disease to chromosome 14q24.3. *Nature Genetics, 2,* 335-339.

Van Nostrand, W.E., Schmaier, A.H., Farrow, J.S., and Cunningham, D.D. , 1990. Protease Nexin-II (Amyloid β-Protein Precursor): A platelet α-granule protein. *Science, 248,* 745-748.

Wasco, W., Bupp, K., Magendantz, M., Gusella, J.F., Tanzi, R.E., and Solomon, F. , 1992. Identification of a mouse cDNA that encodes a protein related to the Alzheimer disease-associated amyloid β protein precursor. *Proceedings of the National Academy of Sciences of the United States of America, 89,* 10758-10762.

Wasco, W., Gurubhagavatula, S., Paradis, M.D., Romano, D., Sisodia, S.S., Hyman, B., Neve, R.L., and Tanzi, R.E. , 1993. Isolation and characterization of the human APLP2 gene, encoding a homologue of the Alzheimer's associated β protein precursor. *Nature Genetics, 5,* 95-100.

Watson, A.J.M., Askew, J.N., and Sandle, G.I. , 1994. Characterization of oxidative injury to an intestinal cell line (HT-29) by hydrogen peroxide. *Gut, 35,* 1575-1581.

Weidemann, A., Konig, G., Bunke, D., Fischer, P., Salbaum, J.M., Masters, C.L., and Beyreuther, K. , 1989. Identification, biogenesis, and localization of precursors of Alzheimer's disease A4 protein. *Cell, 57,* 115-126.

Weiss, J.H., Pike, C.J., and Cotman, C.W. , 1994. Ca^{+2} channel blockers attenuate β-amyloid peptide toxicity to cortical neurons in culture. *Journal of Neurochemistry, 62,* 372-375.

Whitson, J.S., Mims, M.P., Strittmatter, W.J., Yamaki, T., Morrisett, J.D., and Appel, S.H. , 1994. Attenuation of the neurotoxic effect of Aβ amyloid peptide by apolipoprotein E. *Biochemical and Biophysical Research Communications, 199,* 163-170.

Whitson, J.S., Selkoe, D.J., and Cotman, C.W. , 1989. Amyloid β protein enhances the survival of hippocampal neurons in vitro. *Science, 243,* 1488-1490.

Whittemore, E.R., Loo, D.T., and Cotman, C.W. , 1995. A detailed analysis of hydrogen peroxide-induced cell death in primary neuronal culture. *Neuroscience, 67,* 921-932.

Wink, D.A., Kasprzak, K.S., Maragos, C., Elespuru, R.K., Misra, M., Dunams, T.M., Cebula, T.A., Koch, W.H., Andrews, A.W., and Allen, J.S. , 1991. DNA deaminating ability and genotoxicity of nitric oxide and its progenitors. *Science, 254,* 1001-1003.

Wisniewski, T., Ghiso, J., and Frangione, B. , 1994. Alzheimer's disease and soluble Aβ. *Neurobiology of Aging, 15,* 143-152.

Wolozin, B., Bacic, M., Merrill, M.J., Lesch, K.P., Chen, C., Lebovics, R.S., and Sunderland, T. , 1992. Differential expression of carboxyl terminal derivatives of amyloid precursor protein among cell lines. *Journal of Neuroscience Research, 33,* 163-169.

Wood, K. and Youle, R.J. , 1994. Apoptosis and free radicals. *Annals of the New York Academy of Sciences, 738,* 400-407.

Yamamoto, H., Tsuji, S., and Nagai, Y. , 1990. Tetrasialoganglioside GQ1b reactive monoclonal antibodies: their characterization and application for quantification of GQ1b in some cell lines of neuronal and adrenal origin. *Journal of Neurochemistry, 54,* 513-517.

Yamamoto, K., Miyoshi, T., Yae, T., Kawashima, K., Araki, H., Hanada, K., Otero, D.A.C., Roch, J.-M., and Saitoh, T. , 1994. The survival of rat cerebral cortical neurons in the presence of trophic APP peptides. *Journal of Neurobiology, 25,* 585-594.

Yankner, B.A. , 1992. Commentary and perspective on studies of beta amyloid neurotoxicity. *Neurobiology of Aging, 13,* 615-616.

Yankner, B.A., Dawes, L.R., Fisher, S., Villa-Komaroff, L., Oster-Granite, M.L., and Neve, R.L. , 1989. Neurotoxicity of a fragment of the amyloid precursor associated with Alzheimer's disease. *Science, 245,* 417-420.

Yankner, B.A., Duffy, L.K., and Kirschner, D.A. , 1990. Neurotrophic and neurotoxic effects of amyloid β protein: reversal by tachykinin neuropeptides. *Science, 250,* 279-282.

Yu, R.K., & Saito, M. (1989). R.U. Margolis & R.K. Margolis (Eds.), *Neurobiology of Glycoconjugates.* New York: Plenum Press.

Zhang, J., Dawson, V.L., Dawson, T.M., and Snyder, S.H. , 1994. Nitric oxide activation of poly(ADP-ribose) synthetase in neurotoxicity. *Science, 263,* 687-689.

Zhang, J., Pieper, A., and Snyder, S.H. , 1995. Poly (ADP-ribose) synthetase activation: an early indicator of neurotoxic DNA damage. *Journal of Neurochemistry, 65,* 1411-1414.

Curriculum Vitae